ALMA MATER STUDIORUM
UNIVERSITÀ DI BOLOGNA

DOTTORATO DI RICERCA IN

SCIENZE BIOMEDICHE E NEUROMOTORIE

Ciclo 38

Settore Concorsuale: 06/F4 - MALATTIE APPARATO LOCOMOTORE E MEDICINA FISICA E RIABILITATIVA

Settore Scientifico Disciplinare: MED/33 - MALATTIE APPARATO LOCOMOTORE

RADIOLOGIC CHANGES AFFECTING ANKLE JOINT AFTER TOTAL KNEE ARTHROPLASTY: RETROSPECTIVE STUDY AIMED AT COMPARING IN FRONTAL ANKLE ALIGNMENT IN PATIENTS UNDERGOING TOTAL KNEE ARTHROPLASTY USING NAVIGATION-ASSISTED FUNCTIONAL ALIGNMENT VERSUS CONVENTIONAL JIG-BASED MECHANICAL ALIGNMENT TECHNIQUES.

Presentata da: Bartlomiej Dobromir Bulzacki Bogucki

Coordinatore Dottorato

Matilde Yung Follo

Supervisore

Cesare Faldini

Co-supervisore

Alberto Corrado Di Martino

Esame finale anno 2026

INDEX

ABSTRACT	**3**
PREFACE	**4**
ANATOMY OF THE KNEE	**5**
BIOMECHANICS OF THE KNEE JOINT	**20**
INSTRUMENTAL ASSESSMENT OF THE KNEE JOINT	**25**
KNEE OSTEOARTHRITIS	**33**
KNEE REPLACEMENT	**37**
PRINCIPLES AND TECHNIQUES OF ALIGNMENT IN TOTAL KNEE ARTHROPLASTY	**48**
ANATOMY AND BIOMECHANICS OF THE ANKLE AND FOOT	**50**
TKA ALIGNMENT STRATEGIES AND THEIR IMPACT ON ANKLE AND HINDFOOT: A SYSTEMATIC REVIEW	**58**
ANKLE AND HINDFOOT ALIGNMENT CHANGES FOLLOWING TOTAL KNEE ARTHROPLASTY: INFLUENCE OF ALIGNMENT STRATEGY	**83**
EXPERIMENTAL STUDY	**86**
INTRODUCTION	**86**
MATERIALS AND METHODS	**88**
RESULTS	**93**
DISCUSSION	**99**
CONCLUSIONS	**103**
REFERENCES	**104**

ABSTRACT

Objectives

This doctoral thesis aims to evaluate how different alignment philosophies in total knee arthroplasty (mechanical vs functional) affect frontal ankle alignment. Using a retrospective comparative design, it will analyse radiographic parameters, clinical findings, and patient-reported outcomes to identify distal biomechanical adaptations and their clinical relevance. The goal is to generate evidence that supports more personalized surgical planning and optimizes both functional and biomechanical results for patients.

Materials and methods

All patients who underwent total knee arthroplasty (TKA) for primary osteoarthritis were included in the study. They were divided into two cohorts according to the alignment strategy used: mechanical alignment or functional alignment. Preoperative evaluation consisted of a detailed clinical assessment of knee and ankle range of motion, joint stability, and functional disability, combined with standardized long-leg weight-bearing radiographs including the hip, knee, and ankle. Radiographic analysis included measurement of hip–knee–ankle (HKA) angle, ground–plafond angle, ground–talus angle, plafond–talus angle, mechanical plafond axis, mechanical talus axis, and lateral distal tibial angle (LDTA).
All surgeries were performed at the Rizzoli Orthopaedic Institute using either conventional jig-based instrumentation (mechanical alignment group) or computer-assisted navigation (ExatechGPS) implementing a functional alignment strategy (functional alignment group).
Postoperative follow-up at a minimum of 12 months included repeat long-leg radiographs and clinical reassessment with the same preoperative protocol, as well as patient-reported outcome measures (KSS, Oxford Knee Score, WOMAC, SF-36 PCS/MCS, EuroQoL-5D). All preoperative and postoperative data were analysed to compare changes in ankle and hindfoot alignment between the two alignment strategies, and to evaluate the relationship between these changes, ankle osteoarthritis symptoms, and functional outcomes.

Results

A total of 105 patients were included (52 FA, 53 MA), with no significant differences in baseline demographics or comorbidities. Both groups achieved marked improvements in knee and ankle range of motion, joint stability, and PROMs at one year. Radiographically, significant correction of the hip–knee–ankle angle was observed in both groups, whereas changes at the ankle and hindfoot were modest. Directional trends suggested that MA was associated with greater lateral talar displacement, while FA showed a tendency toward medial plafond adaptation, though between-group differences did not reach statistical significance and effect sizes were small. Multivariable regression revealed a significant association between ΔHKA and medial plafond angle. Preoperative ankle pain emerged as the strongest predictor of persistent postoperative ankle symptoms, independent of alignment strategy or correction magnitude.

Conclusions

This study demonstrates that while both mechanical and functional alignment strategies provide comparable improvements in function and patient satisfaction at one-year, subtle biomechanical differences can be detected at the ankle and hindfoot. Functional alignment appears to better preserve physiological load distribution, whereas mechanical alignment may predispose to lateral talar shift. However, the small effect sizes and low explanatory power suggest that these trends should be interpreted with caution. Importantly, preoperative ankle pain proved to be the dominant determinant of postoperative symptoms, underscoring the need for thorough preoperative assessment of the ankle–hindfoot complex. These findings support the adoption of individualized alignment strategies in TKA, with future research needed to clarify the long-term clinical impact of these biomechanical adaptations.

PREFACE

Knee osteoarthritis (OA) is a condition that causes pain, stiffness, and functional impairment, significantly reducing patients' quality of life. Epidemiological studies report that 37.4% of adults aged 60 years and older present radiographic signs of knee OA, and 12.1% have symptomatic radiographic OA[1]. The knee is a complex joint composed of three compartments—medial, lateral, and patellofemoral[2–4].

Surgical management is indicated when conservative measures fail, with unicompartmental knee arthroplasty (UKA) and total knee arthroplasty (TKA) being effective treatments for symptomatic OA[5–7].

Mechanical alignment (MA) has been the gold standard in TKA: prosthetic components are positioned at 90° to the femoral and tibial mechanical axes to achieve a neutral limb axis[8–10].

This approach aims to evenly distribute loads across the implant to reduce wear and loosening risk[11].

Long-term survivorship for MA-TKA is excellent[8,12,13]; however, functional outcomes are more controversial. Patient satisfaction rates range from 71% to 92%, yet only about 22% of patients describe their result as "excellent," indicating that optimal biomechanics may not be fully restored in many cases[14,15].

Recent research has highlighted variability in natural lower limb alignment among healthy individuals. Moser et al.[16], reported a mean hip–knee angle (HKA) between 176.7° and 180.7° in non-arthritic knees[17,18]. Bellemans et al.[19] defined neutral alignment as 180° ± 3° and introduced the concept of constitutional varus (<177°) and valgus (>183°).

Moreover, studies have shown that postoperative static frontal alignment is a poor predictor of in vivo implant loading, knee function, and implant survivorship during gait, suggesting that alternative philosophies might better replicate native biomechanics[20–22].

Functional alignment (FA), derived from kinematic alignment principles, represents one such approach. FA aims to restore native joint line height and obliquity, achieving balanced flexion and extension gaps with symmetric soft tissue tension, through individualized bone resections and fine-tuning of component position[23].

While FA has theoretical advantages, its superiority over MA in terms of natural knee kinematics and patient-reported outcomes remains debated[24–28].

Importantly, changes in knee alignment after TKA can propagate biomechanical adaptations distally along the kinetic chain, influencing ankle and hindfoot alignment[29]. Radiographic studies have demonstrated that coronal realignment of the knee can induce measurable distal changes, especially in patients with severe preoperative varus deformity. The most frequent pattern observed after MA-TKA is a shift of the hindfoot from compensatory valgus toward neutral alignment. However, ankle-specific parameters—such as talar tilt, tibial plafond inclination, and tibiotalar alignment—often show variable or minimal change, suggesting partial mechanical dissociation between ankle and hindfoot and a significant role for the subtalar joint in compensating proximal correction.

Clinically, this variability is relevant: in some patients, especially those with pre-existing ankle OA, severe deformities, or rigid hindfoot architecture, correction of knee alignment may exacerbate ankle symptoms, accelerate degenerative changes, or fail to restore optimal load distribution. Conversely, others may experience complete biomechanical recovery along the limb[30–32].

To date, only one study[30] has directly compared the effects of kinematic alignment and mechanical alignment on ankle alignment, and no standardized investigations have been conducted to evaluate the impact of FA versus MA. Therefore, further research with consistent methodology, adequate sample size, and standardized outcome measures is needed to clarify the distal biomechanical consequences of different TKA alignment philosophies.

The hypothesis of this doctoral project is that mechanical and functional alignment strategies in TKA produce distinct effects on the frontal ankle axis. The objective is to compare pre- and postoperative ankle alignment in two cohorts undergoing MA- or FA-TKA, using radiographic measurements, clinical evaluation, and patient-reported outcomes, in order to understand the nature and clinical significance of distal adaptations and guide more personalized surgical planning.

ANATOMY OF THE KNEE

ANATOMY OF THE KNEE JOINT

The knee is the largest and most complex joint in the human body, allowing reciprocal motion between the thigh and the leg. It is formed by three bones—the femur, tibia, and patella—stabilized by surrounding soft tissues. The joint can be subdivided into the femorotibial and femoropatellar articulations. The articulation between distal femur and proximal tibia is a condylar joint, while that between the patella and the femoral trochlea resembles a gliding joint. Functionally, the knee is primarily a hinge joint, enabling flexion and extension of the leg relative to the thigh. Within different degrees of flexion, additional limited movements occur, including internal and external tibial rotation, varus–valgus deviation, and minor translational motions. Clinically and radiographically, the knee can be described in terms of three compartments: medial (between the medial femoral condyle and tibial plateau), lateral (between the lateral condyle and plateau), and anterior or patellofemoral (between the patella and femoral trochlea).

Femur

The femur is the largest and strongest bone of the human skeleton, designed to sustain body weight and transmit forces from the pelvis to the tibia through the knee joint. Its shaft is slightly curved with an anterior convexity, a configuration that allows it to better absorb mechanical stresses during locomotion. The diaphysis presents three distinct surfaces—anterior, medial, and lateral—and three borders, to which intermuscular septa attach, separating the anterior, medial, and posterior compartments of the thigh. This structural arrangement reflects the dual role of the femur as both a supporting pillar and a lever arm for muscular forces.

The morphology of the femoral canal varies significantly among individuals. In the early 1990s, classifications based on cortical thickness were proposed, distinguishing three morphotypes: type A, characterized by a narrow canal with thick cortices, typical of young individuals with robust bone; type B, an intermediate form, common in middle-aged adults; and type C, with a wide canal and thin cortices, typical of elderly subjects and often associated with osteoporosis. These morphotypes are not only an anatomical curiosity but also have biomechanical implications: they influence how loads are distributed along the shaft, how the femur resists bending forces, and ultimately how stresses are transmitted to the distal epiphysis and to the knee joint.

In the frontal plane, the femoral shaft aligns with the knee joint through the cervico-diaphyseal angle and the orientation of the condyles. The angle of declination, or anteversion, measures the torsion between the axis of the femoral neck and the axis of the condyles, averaging around 10–20°. Although this angle is traditionally measured proximally, its biomechanical consequences are distal: it dictates the rotational alignment of the knee, affecting tibiofemoral tracking, patellofemoral congruence, and overall lower limb kinematics. Variations in anteversion or retroversion influence the distribution of forces across the condyles and can predispose to maltracking, instability, or degenerative changes at the knee.

The distal femur broadens into two large condyles, medial and lateral, which articulate with the tibial plateau and the patella. The medial condyle is larger and longer in the anteroposterior dimension, with a nearly constant sagittal curvature, providing stability throughout the flexion–extension arc. In contrast, the lateral condyle is smaller, with a variable radius of curvature, designed to allow more translation and facilitate the screw-home mechanism of the knee. In the axial plane, the lateral condyle is oriented almost parallel to the sagittal axis, while the medial condyle is oblique, forming an angle of about 20° directed from posterior to anterior and from medial to lateral. This asymmetry between the condyles is crucial, as it enables coupled motion: flexion–extension is accompanied by automatic rotation, a key element of normal gait.

Anteriorly, the condylar surfaces merge to form the trochlear groove, which is deepest at its medial aspect and progressively shallower laterally. This configuration stabilizes the patella, guiding it during knee flexion and extension. The intercondylar fossa, located posteriorly, separates the two condyles and houses the cruciate ligaments, essential stabilizers that control anterior–posterior translation and rotation of the tibia relative to the femur. On the medial and lateral margins of the condyles lie the epicondyles, which serve as attachment sites for the medial and lateral collateral ligaments. Proximal and posterior to the medial epicondyle lies the adductor tubercle, insertion site of the adductor magnus tendon, while superior to the epicondyles originate the medial and lateral heads of the gastrocnemius muscle. Additionally, the popliteus tendon originates near the lateral epicondyle, playing an essential role in unlocking the knee from full extension.

This detailed architecture reflects the balance between stability and mobility that characterizes the knee joint. The medial compartment is designed for stability, with a larger condyle, stronger ligamentous support, and more constrained motion, while the lateral compartment favors mobility and rotation, thanks to its smaller condyle and less restrictive geometry. The interaction of these asymmetrical structures allows the knee to perform not only flexion and extension but also subtle rotational and varus–valgus adjustments, essential during gait, running, and changes of direction.

The morphology of the distal femur also plays a critical role in load distribution across the knee. During stance phase of gait, the medial condyle bears greater loads, consistent with its larger surface and more uniform curvature, while the lateral condyle participates more actively in guiding motion and accommodating rotational adjustments. This distribution of roles explains why degenerative changes in osteoarthritis often initiate medially and why malalignment can profoundly alter the mechanical environment of the tibiofemoral joint[33–35].

Tibia

The tibia is the main weight-bearing bone of the leg and forms, together with the femur and fibula, the complex architecture of the knee joint proximally and the ankle joint distally. It is a long bone with a straight shaft and two enlarged extremities, proximal and distal, adapted for articulation and load transmission. Unlike the fibula, which mainly serves as a stabilizer and muscle attachment site, the tibia supports the majority of axial forces from the femur to the talus, making it a critical element in lower limb biomechanics.

The proximal epiphysis is expanded to form the tibial plateau, composed of two articular surfaces for the femoral condyles. The medial plateau is broader and almost flat, reflecting its function as the main load-bearing surface of the knee, while the lateral plateau is smaller, more circular, and slightly convex, designed to facilitate rotational adjustments and dynamic stability. Together, these surfaces are inclined posteriorly by 5–12° relative to the tibial axis, forming the tibial slope. This slope is not only a fundamental anatomical parameter but also a determinant of anterior–posterior stability, as it directly influences the biomechanics of the cruciate ligaments.

Between the two plateaus rises the intercondylar eminence, consisting of medial and lateral tubercles, which provide anchoring points for the anterior and posterior cruciate ligaments, as well as the horns of the medial and lateral menisci. This region functions as the "keystone" of knee stability, translating the forces transmitted by the femoral condyles into tibial support while guiding rotational kinematics.

On the anterior surface of the proximal tibia lies the tibial tuberosity, a robust prominence where the patellar tendon inserts. This insertion is part of the extensor mechanism of the knee, transmitting the contraction of the quadriceps to the tibia. Laterally, just below the joint line, the Gerdy's tubercle serves as the insertion site for the iliotibial band, a structure that contributes to lateral stabilization of the knee and dynamic control during gait.

The proximal tibia is also a key site of soft tissue insertions. Laterally, the fibular head articulates with the tibia at the proximal tibiofibular joint, a plane synovial joint allowing only slight sliding movements. The fibular head itself serves as the anchoring site for the biceps femoris tendon, the lateral collateral ligament, and the arcuate ligament, which together provide important posterolateral stability. Medially, just below the joint line, the semimembranosus tendon and the deep layer of the medial collateral ligament insert, reinforcing medial stability. More distally, the pes anserinus tendons (sartorius, gracilis, semitendinosus) insert onto the anteromedial surface, forming a conjoined tendinous expansion with significant clinical importance in reconstructive surgery. Posteriorly, the proximal tibia gives attachment to the superficial medial collateral ligament, the posterior cruciate ligament, and muscular structures such as the popliteus and the soleus, emphasizing the dense network of stabilizers converging at this level.

The diaphysis of the tibia is triangular in cross-section, with three surfaces (medial, lateral, and posterior) and three borders (anterior, medial, and interosseous). The anterior border, sharp and palpable, extends from the tibial tuberosity to the medial malleolus. The medial surface is subcutaneous throughout most of its length, while the lateral surface faces the fibula and is connected to it by the interosseous membrane. The posterior surface presents the oblique soleal line, the origin of the soleus muscle, which also serves as an anatomical landmark dividing the vascular territories of the tibia. The shaft of the tibia has thick cortical bone, particularly in its anterior and medial aspects, which are subject to compressive loads, whereas the posterior region, relatively thinner, is more exposed to tensile forces.

The distal epiphysis expands again to participate in the ankle joint. It terminates medially in the medial malleolus, a palpable landmark that stabilizes the talus medially. The articular surface of the distal tibia, also called the plafond, is concave anteroposteriorly and convex mediolaterally, fitting the talar dome. This surface is adapted to transmit vertical loads while permitting dorsiflexion and plantarflexion. Laterally, the distal tibia forms a notch that articulates with the fibula, stabilized by the distal tibiofibular syndesmosis, which includes the anterior and posterior tibiofibular ligaments and the interosseous ligament. This articulation, though allowing minimal motion, is essential for the integrity and stability of the ankle mortise.

The tibia bears approximately 85–90% of the load transmitted through the leg, while the fibula carries the remainder. The medial plateau, larger and more stable, sustains the majority of knee joint forces, which explains the greater susceptibility of the medial compartment to degenerative changes. The lateral plateau, though smaller, plays a key role in controlling rotation and dynamic adjustment, particularly during gait and pivoting movements. The posterior tibial slope is a critical determinant of cruciate ligament function: increased slope tends to increase anterior tibial translation and stress on the anterior cruciate ligament, while reduced slope affects posterior tibial translation and posterior cruciate ligament loading.

The tibia's shaft, with its triangular cross-section and thick cortices, resists bending and torsional forces during locomotion. Variations in morphology, such as tibial torsion or differences in plateau inclination, significantly affect knee kinematics, lower limb alignment, and susceptibility to injury. The distal tibia, through its plafond and malleoli, ensures both weight transmission and multiplanar stability of the ankle joint, completing the functional chain from the femur to the ground[36–39].

Fibula

The fibula is the slender lateral bone of the leg. Unlike the tibia, it does not directly participate in weight-bearing to a significant degree but plays an essential role in lateral stability, muscle attachment, and ankle joint integrity. Together with the tibia, it contributes to the architecture of the leg and the transmission of forces from the knee to the foot.

The proximal epiphysis expands to form the fibular head, which articulates with the lateral aspect of

the tibia at the proximal tibiofibular joint. This articulation is a plane synovial joint, permitting slight gliding motions that accommodate tibial torsion during knee and ankle movement.
The fibular head is a crucial site for ligamentous and tendinous attachments: the lateral collateral ligament of the knee inserts here, providing resistance against varus stresses, while the biceps femoris tendon also anchors to the fibular head, contributing to posterolateral knee stability. Additionally, the arcuate ligament complex inserts here, reinforcing the posterolateral corner of the knee.
Just below the fibular head lies the fibular neck, a narrow region of clinical importance because it is crossed by the common peroneal nerve, which winds around it before dividing into the deep and superficial peroneal nerves. This anatomical relationship makes the fibular neck a vulnerable site in traumatic injuries, such as fractures or compressive lesions, often associated with foot drop.
The fibular shaft is long, thin, and slightly curved, running parallel to the tibia. In cross-section, it is more rounded than the tibia and presents four surfaces (anterior, posterior, medial, and lateral) and four borders (anterior, posterior, interosseous, and lateral). The medial surface provides attachment for the interosseous membrane, which firmly connects the fibula to the tibia, ensuring additional stability while permitting limited relative motion between the two bones.
Despite transmitting only a small proportion of axial load, the fibular shaft plays a crucial role as a site of muscular origin and insertion. The lateral surface anchors the peroneus longus and peroneus brevis, the primary evertors of the foot, essential for maintaining lateral stability during gait. The anterior surface gives origin to the extensor digitorum longus and extensor hallucis longus, while the posterior surface provides attachment for the tibialis posterior and the flexor hallucis longus. This arrangement distributes muscular leverage across all compartments of the leg, allowing the fibula to act as a structural "column" that supports complex foot and ankle motions, including dorsiflexion, plantarflexion, inversion, and eversion.
The distal epiphysis forms the lateral malleolus, a prominent and palpable bony landmark that extends more distally than the medial malleolus of the tibia. This anatomical feature contributes to the stability of the ankle mortise, particularly in resisting excessive eversion. The articular surface of the lateral malleolus articulates with the talus, while its medial surface forms part of the ankle mortise.
Ligamentous insertions in this region are fundamental for ankle stability. The lateral malleolus anchors the three components of the lateral collateral ligament complex of the ankle: the anterior talofibular ligament, the calcaneofibular ligament, and the posterior talofibular ligament. Together, these ligaments counteract excessive inversion and rotational forces, which are common mechanisms of ankle sprain. The distal fibula is also stabilized by the syndesmotic ligaments, which bind it to the distal tibia and maintain the congruency of the ankle mortise during load transmission.
Although the fibula transmits only about 10–15% of the axial load through the leg, it has a crucial role in lower limb biomechanics. The proximal fibula contributes to posterolateral knee stability through its ligamentous and tendinous insertions, while the shaft provides leverage for ankle and foot muscles across all compartments of the leg. The distal fibula, with the lateral malleolus, is indispensable for the stability of the ankle joint, ensuring proper articulation of the talus within the tibiofibular mortise.
The fibula's limited weight-bearing role makes it particularly suited for bone graft harvesting in reconstructive surgery, where vascularized or non-vascularized fibular grafts can be used without severely compromising limb function. Its anatomical relationship with the common peroneal nerve, however, underscores the importance of caution during surgical approaches to the proximal fibula[40–46].

Patella

The patella is the largest sesamoid bone of the human body and is embedded within the quadriceps tendon. Its shape is roughly triangular, with a broad base oriented superiorly and an apex directed inferiorly, which serves as the proximal attachment of the patellar tendon. The anterior surface is

convex and subcutaneous, easily palpable beneath the skin, and often marked by vertical striations due to the overlying tendon fibers.
The posterior surface is divided by a vertical ridge into medial and lateral articular facets, both of which articulate with the femoral trochlea. The articular surface is covered by hyaline cartilage, reaching up to 6–7 mm, reflecting the high mechanical demands placed on the patellofemoral joint. Superior to the ridge lies a smooth area, while the inferior part is rough and corresponds to the insertion of the infrapatellar fat pad (Hoffa's fat pad). The ridge ensures congruence with the trochlear groove, improving stability during knee flexion and extension.
Functionally, the patella acts as a fulcrum, increasing the lever arm of the quadriceps muscle during extension of the knee. By displacing the line of action of the quadriceps tendon anteriorly, it enhances the efficiency of the extensor apparatus, reducing the amount of force required for knee extension, walking, running, or maintaining an upright posture. In addition, the patella distributes compressive loads over a wider area of the femoral trochlea, protecting articular cartilage from localized stress peaks.
The morphology of the patella is variable, and several classifications describe differences in facet size and orientation, which can influence patellofemoral biomechanics and predispose to instability. The lateral facet is generally larger and steeper, acting as a stabilizer against lateral displacement, whereas the medial facet is smaller and flatter. The odd facet, located medially and contacting the femur only in deep flexion, further contributes to joint congruity at high flexion angles.
Clinically, the patella is central to the stability and function of the knee joint. Alterations in its position, such as patella alta (high-riding patella) or patella baja (low-riding patella), can significantly modify the biomechanics of the extensor mechanism and predispose to anterior knee pain or instability. Moreover, given its subcutaneous location, the patella is particularly prone to direct trauma, fractures, and repetitive stress syndromes. The articulation between the patella and trochlea is also frequently affected in degenerative conditions, leading to isolated patellofemoral osteoarthritis[47–50].

SOFT TISSUES OF THE KNEE

Joint capsule and synovial membrane

The capsule of the knee is a strong yet flexible fibrous membrane that completely envelops the joint, playing a central role in maintaining stability while allowing the knee to perform its wide range of movements. It is not uniform in thickness, as certain areas are reinforced by fibrous expansions that are functionally recognized as ligaments, ensuring that the capsule is not only a passive envelope but also an active stabilizer of the joint. Distally, the capsule attaches circumferentially to the margin of the tibia, except in the posterolateral region at the popliteal hiatus, where the popliteus tendon passes through to enter the joint. In this area, the capsule is specialized to form two important reinforcing structures: the oblique popliteal ligament and the arcuate popliteal ligament. The oblique popliteal ligament originates from the insertion of the semimembranosus tendon and extends obliquely across the posterior joint capsule to the lateral femoral condyle. This broad, flat ligament strengthens the posterior aspect of the capsule, contributes to the floor of the popliteal fossa, and lies in close anatomical relationship to the popliteal artery, highlighting its relevance in both clinical assessment and surgical procedures. The arcuate popliteal ligament, in contrast, runs in an arch-like fashion between the lateral meniscus and the fibular head, reinforcing the posterolateral corner of the knee and contributing significantly to the overall stability of this complex region.
On the inner surface of the capsule lies the synovial membrane, a delicate, highly vascularized tissue that is essential to joint homeostasis. It extends proximally into the suprapatellar recess, which communicates with the main joint cavity and is separated from the femur by a pad of adipose tissue that acts as both cushioning and structural support. In its normal condition, synovium appears pink,

translucent, and smooth, reflecting its healthy state. Microscopically, it is composed of two main cell types. Type I synoviocytes resemble macrophages and are primarily responsible for immune surveillance and the phagocytosis of debris within the joint cavity. Type II synoviocytes, in contrast, are secretory cells that produce the components of synovial fluid. This viscous fluid, rich in hyaluronic acid and lubricin, has a dual function: it lubricates the articular surfaces, reducing friction during motion, and provides essential nutrients and waste removal for the avascular articular cartilage. The constant interaction between the fibrous capsule, the synovium, and the synovial fluid ensures that the knee remains a well-lubricated, shock-absorbing, and resilient articulation capable of withstanding high mechanical loads[51–58].

Joint Bursae

Surrounding the knee capsule are multiple bursae, which are fluid-filled sacs that further reduce friction between moving structures. The prepatellar bursa, located just anterior to the patella beneath the skin, cushions the patella from direct pressure and is frequently involved in inflammatory conditions such as prepatellar bursitis following repeated kneeling. The suprapatellar bursa lies superior to the patella and beneath the quadriceps tendon; it communicates with the joint cavity and minimizes friction between the tendon and the anterior femur. The infrapatellar bursa, found deep to the patellar tendon, protects the tendon from excessive compression against the anterior tibia during movement. Medially, the anserine bursa lies between the conjoined tendons of the pes anserinus and the tibia, while an additional bursal sac is interposed between the superficial medial collateral ligament and these tendons, ensuring smooth gliding during flexion and extension. Posteriorly, the synovial cavity communicates with the popliteal bursa, which is interposed between the semimembranosus tendon and the medial head of the gastrocnemius muscle. When this bursa becomes distended due to intra-articular effusion or chronic inflammation, it may give rise to a Baker's cyst, which manifests as a palpable swelling in the popliteal fossa and may be symptomatic if large enough to compress surrounding structures[51,59–61].

LIGAMENTS OF THE KNEE

Cruciate ligaments

The cruciate ligaments are robust bands of dense connective tissue connecting the femur to the tibia. They are located within the joint capsule but remain extrasynovial, since the synovial membrane folds posteriorly around them. Their principal role is to stabilize the knee in the sagittal plane, limiting anterior or posterior displacement of the tibia relative to the femur, while also contributing secondarily to rotational control.

The anterior cruciate ligament (ACL) arises from the medial surface of the lateral femoral condyle and inserts onto the anterior intercondylar area of the tibia, just anterior to the tibial eminence. It measures approximately 30–35 mm in length and is classically described as having two functional bundles: the anteromedial bundle, which becomes taut in flexion and relaxes in extension, and the posterolateral bundle, which behaves in the opposite manner, tightening in extension and relaxing in flexion. This reciprocal tensioning ensures that the acl is active throughout the full range of motion, providing both anterior restraint and rotational stability, particularly against excessive internal tibial rotation and valgus stress[62–64].

The posterior cruciate ligament (PCL) is thicker and stronger than the acl and is regarded as the main stabilizer of the knee. It originates from the anterolateral surface of the medial femoral condyle and inserts on the posterior aspect of the tibial plateau, approximately one centimeter below the articular surface. Functionally, the pcl is composed of an anterolateral bundle, taut during flexion, and a posteromedial bundle, which becomes taut in extension. It prevents posterior translation of the tibia and also plays an important role in restraining external rotation and varus stresses at higher flexion angles.

Together, the cruciate ligaments not only guide the rolling and gliding motion of the femoral condyles during flexion and extension but also provide proprioceptive input to the neuromuscular system, as they are richly innervated with mechanoreceptors[65–68].

Anterolateral ligament (ALL)

The anterolateral ligament is a distinct structure of the lateral knee compartment. It originates from the lateral femoral epicondyle, anterior and distal to the origin of the lateral collateral ligament and inserts on the proximal anterolateral tibia between gerdy's tubercle and the fibular head, maintaining a close relationship with the lateral meniscus. Its biomechanical role is particularly relevant in controlling excessive internal tibial rotation, acting synergistically with the acl and lateral collateral ligament. The all has also been associated with segond fractures, small avulsion fractures occurring at its tibial insertion, often linked to acl injuries[69–71].

Collateral ligaments

The collateral ligaments are the principal stabilizers of the knee in the coronal plane, counteracting varus and valgus stresses.

The medial collateral ligament (MCL) is a broad, flat band that originates from the medial femoral epicondyle and inserts onto the medial aspect of the proximal tibia. With a length of about 10–12 cm, it is the largest structure on the medial side of the knee and the primary restraint against valgus forces across the entire arc of motion. The mcl comprises two components: a superficial vertical portion and a deeper oblique portion. The superficial fibers remain taut throughout flexion and extension, whereas the oblique fibers contribute to the formation of the posterior oblique ligament at the posteromedial corner. This posterior component is lax in flexion and thus contributes mainly to stability in extension. The mcl acts in concert with other medial stabilizers—including the pes anserinus tendons, the semimembranosus tendon, the posteromedial capsule, and the medial gastrocnemius tendon—to limit medial joint opening, restrain anteroposterior translation, and provide overall stability to the medial compartment[71–73].

The lateral collateral ligament (LCL) is a cord-like structure and the primary static restraint to varus stress. It arises from the lateral femoral epicondyle, posterior and superior to the popliteus tendon insertion, and attaches distally to the fibular head. At its distal end, the lcl blends with the biceps femoris tendon, while lying superficial to the popliteus tendon and deep to the lateral retinaculum. Unlike the mcl, the lcl is extracapsular, separated from the joint capsule by a thin fat pad and the inferolateral genicular vessels. Together with the pcl and the popliteo-arcuate complex, the lcl is fundamental for stabilizing the posterolateral corner of the knee, particularly against combined forces of varus stress, external tibial rotation, and posterior tibial translation. Injury to these structures results in posterolateral instability, which often manifests as both coronal and rotational laxity[74–77].

Other capsular and ligamentous reinforcements

Beyond the cruciate, collateral, and anterolateral ligaments, the knee capsule is reinforced by several additional structures. Posteriorly, the oblique popliteal ligament, derived from the semimembranosus tendon, and the arcuate popliteal ligament, spanning from the fibular head to the posterior capsule, provide significant resistance against hyperextension and posterior displacement. Anteriorly, the patellar tendon and medial and lateral retinacula contribute to anterior stabilization, transmitting forces from the quadriceps to the tibia while anchoring the patella within the trochlear groove. These retinacular structures are essential in patellofemoral mechanics, maintaining patellar alignment during motion. Together, these secondary stabilizers complement the function of the major ligaments, ensuring overall knee stability under the complex multi-planar stresses encountered in daily activities[65].

MENISCI

The menisci are fibrocartilaginous structures interposed between the femoral condyles and the tibial plateaus. They are primarily composed of collagen, with type I collagen being the predominant form, which provides resistance to tensile forces. Morphologically, the medial meniscus has a C-shaped configuration, while the lateral meniscus is almost circular, resembling an O-shape. Each meniscus can be divided into three main regions: the anterior horn, the body, and the posterior horn. From the periphery to the center, three distinct zones are recognizable: an outer capsular region that anchors to the joint capsule, an intermediate zone, and an inner free edge facing the articular surface.

The lateral meniscus has additional stabilizing connections through the meniscofemoral ligaments, which arise from its posterior horn and extend toward the lateral aspect of the medial femoral condyle. Two separate bands are typically described: the posterior meniscofemoral ligament (Wrisberg ligament), which runs posterior and superficial to the posterior cruciate ligament, and the anterior meniscofemoral ligament (Humphrey ligament), which courses anterior and deep to the posterior cruciate ligament. These accessory ligaments contribute to the stability of the lateral meniscus and the overall coordination of posterior knee structures.

Meniscal vascularization is limited and is provided by small vessels that penetrate only the outermost region of the menisci, leaving the inner portion essentially avascular. These vessels originate primarily from the genicular arteries. Based on vascular supply, Arnoczky and Warren classified the menisci into three concentric zones: a peripheral red-red zone, which is well vascularized; a transitional red-white zone with scarce vascularization; and a central white-white zone, which is completely avascular. Because of this poor blood supply, meniscal healing capacity is limited, and tears involving the inner avascular region rarely heal spontaneously.

Functionally, the menisci are indispensable to normal knee joint mechanics. They contribute to stability across all planes of motion, enhance the congruence between the femoral condyles and the tibial plateau, and play a key role in load distribution by absorbing and dissipating axial forces. By increasing the contact surface between the femur and tibia, they reduce stress on the articular cartilage, thereby providing a protective effect against degenerative changes. Furthermore, they act as shock absorbers during gait and dynamic activities, protect the synovial and capsular tissues from impingement, and assist in guiding knee kinematics during flexion, extension, and rotation.

In addition to these mechanical roles, the menisci also contribute to proprioception through mechanoreceptors located predominantly in the anterior and posterior horns. These receptors provide sensory feedback about joint position and movement, which is essential for coordinated neuromuscular control. Consequently, the loss or removal of meniscal tissue, as occurs in meniscectomy, has long-term implications, including increased articular cartilage stress, higher risk of osteoarthritis, and potential compromise of joint stability[74,78–85].

MUSCLES OF THE KNEE

The muscular structures acting on the knee joint are arranged in different compartments of the thigh and leg, enclosed by fascial layers that provide support and separation. These muscles contribute to knee flexion, extension, rotation, and joint stabilization during movement. The organization of these muscles reflects both their anatomical location and functional role in gait and posture.

The muscles influencing knee biomechanics can be grouped into distinct compartments:

1. anterior knee region
2. posterior knee region
3. medial knee region
4. lateral knee region
5. leg muscles crossing the knee

These muscles act in synergy to maintain stability, absorb loads, and guide movement. The quadriceps group ensures powerful extension and controls deceleration of flexion during gait, while the hamstrings counterbalance by providing flexion and posterior stability. The pes anserinus muscles reinforce the medial side, working with the medial collateral ligament to resist valgus forces. The lateral structures, including the iliotibial band and biceps femoris, protect against varus stresses and external tibial rotation. The gastrocnemius and plantaris integrate knee and ankle function, coupling flexion with plantarflexion. The popliteus serves as a central stabilizer in the initiation of flexion and in fine-tuning rotational alignment.
Altogether, these muscular systems ensure both static and dynamic stability of the knee joint, allowing efficient motion while protecting against injury during high-demand activities such as running, pivoting, and jumping.

Muscles of the anterior knee region
Within the anterior knee region, the sartorius and quadriceps femoris represent the main muscular structures, coordinating complex motions of the knee joint. The sartorius contributes to hip flexion, abduction, and external rotation, and maintains a close anatomical relationship with the tensor fasciae latae, positioned anteriorly and medially.
The quadriceps femoris consists of four muscular heads: rectus femoris, vastus lateralis, vastus medialis, and vastus intermedius. As a group, they constitute the primary extensor mechanism of the leg at the knee. Among them, the rectus femoris arises from the pelvis and also plays a role in flexion of the hip. While the tensor fasciae latae, sartorius, and rectus femoris act on both hip and knee joints, the vastus lateralis, medialis, and intermedius are confined in action to the knee. The tensor fasciae latae is a flat, narrow muscle located in the upper lateral portion of the thigh. Its origins include the anterior margin of the lateral lip of the iliac crest, the lateral surface of the anterior superior iliac spine, and the adjoining notch. It inserts into the iliotibial tract within its upper and middle thirds. This muscle is supplied by the superior and inferior gluteal arteries and innervated by the superior gluteal nerve (L4, L5). Through its attachment to the iliotibial band, it contributes to extension and external rotation of the leg, while also assisting in thigh abduction and medial rotation. When standing, it plays an important role in maintaining pelvic stability. The sartorius, a long and slender ribbon-shaped muscle, arises from the anterior superior iliac spine and the upper half of the adjacent notch. It runs obliquely across the anterior thigh and descends vertically on the medial side of the knee. The muscle fibers continue into a broad aponeurosis through a flat tendon, which inserts on the superior part of the medial tibial surface, anterior to the gracilis and semitendinosus, thus forming part of the pes anserinus. Its actions include flexion of both the thigh at the hip and the leg at the knee, as well as abduction and external rotation of the hip. It is innervated by the femoral nerve (L2, L3) and vascularized by branches of the femoral artery. The quadriceps femoris extends over the anterior, medial, and lateral portions of the femoral shaft. Its four muscular heads merge distally to form the quadriceps tendon, which attaches to the patella and continues as the patellar ligament to insert on the tibial tuberosity. The rectus femoris, unique among the quadriceps for crossing both hip and knee, originates by two tendons: a direct one from the anterior inferior iliac spine and a reflected one from the acetabular margin. It terminates in a broad aponeurosis that becomes a tendon inserting into the base of the patella. The vastus lateralis, the largest component of the group, arises from the intertrochanteric line and adjacent femoral structures through an extended aponeurosis, descending to form a thick tendon attached to the base and lateral border of the patella. The vastus medialis begins from the lower part of the intertrochanteric line, the spiral line, and the medial lip of the linea aspera, inserting predominantly into the medial edge of the patella. The vastus intermedius takes origin from the anterior and lateral surfaces of the proximal two-thirds of the femoral shaft. Its fibers end in an aponeurosis inserting into the lateral border of the patella and the lateral tibial condyle. The articularis genus muscle may appear as an independent structure or

fused with the vastus intermedius; its fibers originate on the distal anterior femur and insert into the synovial membrane of the knee, helping to elevate the suprapatellar bursa. The quadriceps femoris and the articularis genus share innervation from the femoral nerve (L3, L4) and a vascular supply from the profunda femoris, perforating branches, and the genicular arteries. Their primary role is extension of the leg at the knee, with the rectus femoris also flexing the hip or, if the thigh is fixed, tilting the pelvis anteriorly[86–89].

Muscles of the posterior knee region

In the posterior compartment of the knee, the main muscles involved in knee flexion are the biceps femoris, semitendinosus, and semimembranosus, commonly referred to together as the hamstring group. These muscles arise from the ischial tuberosity and extend distally to insert onto the tibia and fibula through their tendinous and ligamentous structures, including the pes anserinus. Their functional importance lies in ensuring dynamic protection and stabilization of the hip and knee joints during locomotion. The biceps femoris occupies the posterolateral aspect of the thigh. It presents two distinct heads: the long head begins at the ischial tuberosity, sharing a tendon of origin with the semitendinosus, whereas the short head originates from the lateral margin of the linea aspera and the lateral supracondylar ridge. The long head develops into a fusiform belly that descends laterally, crossing over the sciatic nerve, before blending into an aponeurosis that also receives fibers from the short head. Distally, the muscle continues as a tendon that divides into two branches, one curving around the lateral collateral ligament to insert on the fibular head, and the other attaching to the lateral condyle of the tibia. Its innervation comes from the sciatic nerve (L5, S1), while its vascularization is provided by branches of the ischiatic, internal pudendal, circumflex femoral, and perforating arteries. The semitendinosus is found in the posteromedial thigh and shares its common point of origin at the ischial tuberosity with the long head of the biceps femoris. Its fusiform muscle belly ends a little below the mid-thigh, transitioning into a long tendon. This tendon courses superficially over the semimembranosus, curves around the medial tibial condyle, and inserts onto the proximal medial surface of the tibia, situated behind the sartorius and just below the gracilis. The muscle receives innervation from the sciatic nerve (L5, S1) and blood supply from the ischiatic, internal pudendal, circumflex femoral, and perforating arteries. The semimembranosus, which also belongs to the posteromedial group, originates from a broad flat tendon attached to the ischial tuberosity, positioned laterally with respect to the biceps femoris and semitendinosus tendons. The proximal tendon travels medially beside the adductor magnus, widening into an aponeurosis that continues deep to the semitendinosus. Around mid-thigh, muscular fibers emerge from this aponeurotic sheet, converging toward a distal aponeurosis that narrows into a tendon inserting on the posterior surface of the medial tibial condyle. It is innervated by the sciatic nerve (L5, S1) and nourished by the same vascular sources as the other hamstring muscles. Functionally, the muscles of the posterior thigh extend the hip when the pelvis is stable and flex the knee when the femur is fixed, acting as fundamental antigravity elements. When the knee is semiflexed, the biceps femoris produces external rotation, whereas the semitendinosus and semimembranosus act as internal rotators[90–96].

Muscles of the medial knee region

The medial knee region muscles include the adductor group—pectineus, adductor longus, adductor brevis, and adductor magnus—along with the gracilis. All of them cross the hip joint, but the gracilis alone continues past the knee. The gracilis, a slender and superficial muscle of this region, arises from a narrow aponeurosis attached to the medial portion of the pubic body and the ascending ramus of the ischium. Its vertically oriented fibers converge into a cylindrical tendon that travels across the medial femoral condyle and tibial plateau before spreading at its insertion on the medial surface of the proximal tibia. The gracilis is innervated by the obturator nerve (L2) and supplied by the obturator

artery. Its action includes adduction of the thigh, flexion of the knee, and internal rotation of the leg. The pectineus, a flat quadrangular muscle located in the femoral triangle, originates from the pectineal line of the pubis and extends posterolaterally to insert on the pectineal line of the femur between the lesser trochanter and linea aspera. It is innervated by the femoral nerve (L2, L3) and receives arterial branches from both the obturator and femoral circumflex arteries. Its functions are adduction and flexion of the hip. The adductor longus, fan-shaped and most anterior among the adductors, begins from the pubic body near the pubic crest and symphysis, forming a broad muscular belly that inserts by aponeurosis on the middle third of the linea aspera. It is supplied by the femoral artery and innervated by the anterior branch of the obturator nerve (L2, L3). The adductor brevis, triangular in shape, originates from the external surface of the pubis and extends backward and downward to insert on the femur between the lesser trochanter and linea aspera. Its vascularization is derived from the femoral artery, and its innervation is provided by the obturator nerve (L2, L3). The adductor magnus, the most voluminous muscle of the medial thigh, has a broad triangular form. It arises from the inferior pubic and ischial rami as well as the ischial tuberosity. The portion originating from the pubic ramus courses horizontally to the gluteal tuberosity of the femur, while fibers from the ischial ramus fan out to the linea aspera and medial supracondylar ridge. The vertical fibers from the ischial tuberosity continue into a cylindrical tendon inserting into the medial femoral condyle, interrupted by fibrous arches fixed to the bone. The muscle is innervated by both the obturator nerve and the tibial division of the sciatic nerve (L2–L4) and receives blood supply from the femoral artery. Collectively, the adductors primarily adduct the thigh, thereby supporting locomotion and posture, while the adductor longus and magnus also participate in internal rotation of the thigh[91,97–100].

Muscles of the lateral knee region

The lateral aspect of the knee is primarily supported by the iliotibial band, a dense longitudinal condensation of the fascia lata. This fibrous reinforcement originates proximally from the insertions of the tensor fasciae latae and the gluteus maximus, descending along the lateral thigh to terminate at Gerdy's tubercle on the anterolateral surface of the tibia. Functionally, the iliotibial band is essential in resisting excessive varus stresses, distributing mechanical load across the joint, and contributing to lateral stability. It also exerts a key influence on patellofemoral biomechanics by providing lateral restraint, thereby controlling patellar tracking. Clinically, it is frequently involved in overuse conditions, particularly the iliotibial band friction syndrome, one of the most common causes of lateral knee pain in athletes and long-distance runners. The iliotibial band, being a specialization of the fascia lata, does not possess direct muscular innervation; its vascularization is mainly derived from perforating branches of the lateral circumflex femoral artery and the superior lateral genicular artery. Additional reinforcement of the lateral knee is provided by the distal insertion of the biceps femoris tendon, which attaches to the fibular head. Together with the iliotibial band, it significantly enhances posterolateral stability of the joint and counters excessive external rotational forces. The biceps femoris is innervated by the sciatic nerve, specifically the tibial division for the long head and the common fibular division for the short head (L5, S1). Its vascular supply arises from perforating branches of the profunda femoris artery, as well as contributions from the inferior gluteal and circumflex femoral arteries.

Deep to these superficial layers lies the popliteus, a small but functionally crucial muscle of the posterolateral corner. It originates from the lateral femoral condyle and the posterior horn of the lateral meniscus, inserting on the posterior tibial surface above the soleal line. The popliteus plays a pivotal role as a dynamic stabilizer: it initiates knee flexion by "unlocking" the joint, internally rotates the tibia relative to the femur in non-weightbearing conditions, externally rotates the femur on the tibia during stance, and retracts the lateral meniscus posteriorly to prevent entrapment during movement. In addition, it protects against excessive posterior tibial translation during flexion. The popliteus receives

its innervation from the tibial nerve (L4–S1), and its vascularization is provided by branches of the popliteal artery, in particular the medial inferior genicular artery[101–106].

Leg muscles crossing the knee

Among the muscles of the leg that cross the knee joint, the gastrocnemius is the most prominent and superficial structure of the posterior compartment. It consists of two heads, medial and lateral, which originate respectively from the posterior surfaces of the medial and lateral femoral condyles. These muscular bellies merge distally into a strong common tendon that contributes to the Achilles tendon, inserting on the posterior surface of the calcaneus. In addition to being the most powerful plantarflexor of the ankle, the gastrocnemius assists knee flexion, particularly when the limb is extended, and provides significant contribution to propulsion during walking, running, and jumping. The gastrocnemius is innervated by the tibial nerve (S1, S2) and vascularized by the sural branches of the popliteal artery and by the posterior tibial artery.

Lying deep to the gastrocnemius is the plantaris, a small and often variable muscle, traditionally referred to as the "freshman's nerve" due to its slender, elongated tendon. It arises from the lateral supracondylar ridge of the femur and descends obliquely between the gastrocnemius and soleus muscles, with its long tendon running parallel to the Achilles tendon and inserting on the calcaneus. Although its mechanical role is minimal compared to the gastrocnemius and soleus, the plantaris provides weak assistance in knee flexion and ankle plantarflexion. Its tendon, however, is thought to have a proprioceptive function because of its abundance of muscle spindles. The plantaris receives innervation from the tibial nerve (S1, S2) and is vascularized by branches of the popliteal artery.

The popliteus, a deeper muscle located in the posterior knee, plays a fundamental stabilizing role. It originates from the lateral femoral condyle and the posterior horn of the lateral meniscus, inserting onto the posterior surface of the tibia just above the soleal line. The popliteus is essential in initiating knee flexion by "unlocking" the joint: in non-weightbearing conditions it internally rotates the tibia on the femur, while in weightbearing conditions it externally rotates the femur on the tibia. Moreover, it retracts the lateral meniscus posteriorly during knee flexion, preventing its entrapment, and acts as a dynamic stabilizer of the posterolateral corner by controlling external rotation and resisting excessive posterior tibial translation. The popliteus is innervated by the tibial nerve (L4–S1) and vascularized by the medial inferior genicular branch of the popliteal artery[106–114].

BLOOD SUPPLY TO THE KNEE

The arterial blood supply to the knee joint is largely ensured by the genicular arteries, branches of the popliteal artery. These vessels form an extensive anastomotic network that surrounds the articulation and guarantees vascular supply to all its structures.

The popliteal artery is the distal continuation of the superficial femoral artery. It exits Hunter's canal and enters the popliteal fossa at the junction between the middle and distal thirds of the femur. Proximally, it is separated from the femur by a thick fat pad, while at the level of the posterior joint line it lies in direct contact with the oblique popliteal ligament. Distally, it courses superficial to the popliteal fascia and terminates at the lower border of the popliteus muscle, dividing into the anterior and posterior tibial arteries. Along its course, it gives rise to several muscular branches and five main articular branches:

Middle genicular artery arises from the anterior surface of the popliteal artery and passes through the oblique popliteal ligament. It supplies the posterior capsule and intra-articular structures, including the posterior horns of the menisci. Its ligamentous branches cross the synovium and form a vascular plexus that provides blood supply to both the anterior and posterior cruciate ligaments.

Superior genicular arteries originate from the posterior surface of the popliteal artery and pass around the distal femur just above the condyles. The superior lateral genicular artery runs deep to the tendon of the biceps femoris before anastomosing with the descending branch of the lateral femoral circumflex artery. The superior medial genicular artery courses anteriorly, deep to the semimembranosus and semitendinosus, and proximally toward the origin of the medial head of the gastrocnemius.
Inferior genicular arteries arise distal to the joint line, below the condyles, on either side of the popliteal artery. The inferior lateral genicular artery lies adjacent to the lateral joint line, passing deep to the lateral collateral ligament, just proximal to the fibular head, and runs anterolaterally to join the anterior anastomosis. The inferior medial genicular artery passes approximately two fingerbreadths below the medial joint line, deep to the medial collateral ligament, and also contributes to the anterior anastomosis.
Branches of the inferior genicular arteries form a capillary network within the anterior fat pad, providing abundant blood supply to the fat pad itself, the synovial cavity, and the patellar tendon.
The terminal branches of the four superior and inferior genicular arteries extend also to the menisci. It has been shown that the lateral genicular arteries contribute more significantly to meniscal vascularization than the medial ones.
The anterior anastomotic network of the knee is established by the four superior and inferior genicular arteries, by branches of the descending genicular artery, by the descending branch of the lateral femoral circumflex artery, and by recurrent branches of the anterior tibial artery. This creates a connection between the femoral artery at the origin of its deep branch, the popliteal artery, and the anterior tibial artery.
Anteriorly, the anastomosis forms a vascular ring around the patella. From this network, a variable number of nine to twelve nutrient arteries arise at the inferior pole and ascend along the anterior surface of the patella through a series of grooves to penetrate into its middle third.
The skin covering the anterior aspect of the knee is supplied by perforating vessels derived from the terminal branches of the anterior anastomosis, together with musculocutaneous branches from the rectus femoris and vastus muscles. An additional and important contribution to the cutaneous vascularization comes medially from the saphenous artery, which originates from a common trunk with the descending genicular artery from the superficial femoral artery.
Surgical exposure of the knee inevitably interrupts arterial flow in parts of this terminal perforating network. However, a single midline anterior incision usually causes little impairment of wound healing. In cases of reoperation on multiple previous scars, it is preferable to choose a more lateral incision along the median line, since the arterial inflow to the skin derives predominantly from medial contributions[115–121]

NEUROANATOMY OF THE KNEE
The innervation of the knee includes both motor and sensory components.
Motor innervation controls the mechanical action of the muscles responsible for joint movements, while sensory innervation provides cutaneous and articular supply from multiple nerve branches.
The sciatic nerve innervates the flexor musculature of the thigh, including the biceps femoris, semimembranosus, semitendinosus, and part of the adductor magnus. Its terminal branches continue distally to innervate the muscles of the leg and foot.
The femoral nerve supplies the extensor musculature, represented by the quadriceps femoris—rectus femoris, vastus medialis, vastus lateralis, and vastus intermedius—as well as the sartorius muscle.
The sensory innervation of the knee is provided by several distinct nerve trunks depending on the region considered. The anterior aspect of the knee is predominantly supplied by branches of the femoral nerve, with a small contribution distally in the anterolateral region from the common fibular nerve, and proximally in the anterolateral region from the lateral femoral cutaneous nerve of the thigh.

The posterior aspect of the knee is innervated by the posterior femoral cutaneous nerve of the thigh, the lateral femoral cutaneous nerve of the thigh, the tibial nerve, and the common fibular nerve.
The tibial nerve, also referred to as the medial or internal popliteal nerve, arises from the sciatic nerve approximately halfway along the thigh. It runs distally through the popliteal fossa, initially lying within the adipose tissue beneath the deep fascia. Further distally, it passes deeper, situated between the two proximal heads of the gastrocnemius. A cutaneous branch, the sural nerve, descends along the surface of the lateral gastrocnemius. Terminal branches of the tibial nerve extend to the two heads of the gastrocnemius, the plantaris, the soleus, and the popliteus muscles. In addition, numerous articular branches originate here and provide innervation to the joint. The largest and most consistent of these, the posterior articular nerve, usually arises within the popliteal fossa but may occasionally originate from the tibial division of the sciatic nerve in the thigh. It courses laterally, winding around the popliteal vessels, before passing deeper to join the popliteal plexus. Fibers from this plexus penetrate the oblique popliteal ligament to innervate the posterior capsule, the perimeniscal capsule, and the synovium covering the cruciate ligaments.
The common fibular nerve, also known as the external popliteal sciatic nerve, enters the popliteal fossa lateral to the tibial nerve and descends along the medial surface of the biceps tendon. It then passes between the tendon of the biceps femoris and the lateral head of the gastrocnemius, continuing distally behind the fibular head. It subsequently curves superficially around the lateral aspect of the fibular neck before piercing the peroneus longus muscle through a fibrous tunnel, where it divides into the superficial fibular (musculocutaneous) nerve and the deep fibular (anterior tibial) nerve. Its cutaneous branches include the communicating sural nerve, which accompanies the sural nerve, and a small branch directed to the skin over the superior anterolateral aspect of the leg. Two articular branches also arise from the common fibular nerve: the lateral articular nerve, which originates at the level of the joint line and supplies the inferolateral capsule and the lateral collateral ligament, and the recurrent fibular nerve, which ascends along the anterior surface of the tibia within the peroneus longus and enters the joint anterolaterally.
The capsule and the anteromedial and anterolateral regions of the knee are innervated by the anterior afferent nerve group, which also supplies the quadriceps muscle through its articular branches[122–125]

BIOMECHANICS OF THE KNEE JOINT

The biomechanics of the knee are defined by the intricate relationship between its axes, alignment, kinematics, and stabilizing structures. Understanding these elements is essential to explain how the joint combines stability and mobility, distributes loads efficiently, and adapts to both static and dynamic activities.

AXES AND ALIGNMENT OF THE KNEE

At the femoral level, two distinct axes can be identified: the anatomical axis and the mechanical axis. The anatomical axis of the femur is defined as the mid-diaphyseal line equidistant from the femoral cortices. The mechanical axis of the femur is described as the line connecting the center of hip rotation, corresponding to the femoral head, and the center of knee rotation, corresponding to the tibial spines. Between the anatomical and mechanical axes of the femur there is an angle of approximately 6°, corresponding to the physiological valgus of the femur, which is due to the femoral neck introducing a lateralizing component. The mechanical axis runs proximo-distally and is almost perpendicular to the ground, forming an angle with the vertical between 0° and 3°. This value is greater in females due to the wider pelvis compared to males.

At the tibial level, both an anatomical and a mechanical axis can also be defined. The anatomical axis is the mid-diaphyseal line equidistant from the tibial cortices, while the mechanical axis connects the center of knee rotation with the center of ankle rotation, corresponding to the tibial plafond. Unlike the femur, in the tibia the anatomical and mechanical axes are considered almost coincident, since the angle between them is virtually null in physiological conditions, ranging between 0° and 3°.

In the biomechanical study of the knee, it is fundamental to consider the mechanical angles of epiphyseal deformity of the distal femur and proximal tibia, known as the lateral distal femoral angle (LDFA) and medial proximal tibial angle (MPTA), both ranging physiologically between 85° and 90°. The LDFA is defined as the laterally open angle between the femoral mechanical axis and the tangent line to the distal condylar surface. Values above 90° indicate a varus deformity, while values below 85° indicate valgus. The MPTA is the medially open angle between the tibial mechanical axis and the tangent line to the proximal tibial plateau. Values below 85° define a varus deformity, while values above 90° indicate valgus. In most knees, physiological mean values are around 88° for the LDFA and 87° for the MPTA, corresponding to a slightly valgus distal femur combined with a slightly varus proximal tibia. The angle between the distal femoral condyles and the tibial plateau is referred to as the joint line convergence angle (JLCA), which in physiological conditions averages 0° to 2°.

To describe frontal plane alignment of the knee, the entire lower limb must be considered. The mechanical axis of the lower limb is defined as the line passing through the hip center and ankle center. If this axis passes through the center of the knee within a margin of about 3°, the knee is considered neutral. If the axis passes medial to the center, the alignment is varus, if lateral, valgus. For an angular description of knee alignment, the mechanical hip–knee–ankle angle (mHKA) is defined as the angle subtended by the hip, knee, and ankle centers. Positive values represent valgus alignment when the angle opens outward, while negative values represent varus alignment when the angle opens inward. At birth, the knee presents an anatomical varus of approximately 15°, which persists until the onset of walking. With the beginning of ambulation, the axis progressively aligns toward neutral, then shifts to valgus, reaching by the age of 6 to 8 years the definitive alignment represented by an anatomical valgus of 5° to 7°, which corresponds to a mechanical axis within the normal range[126].

For a long time, the literature debated what should be considered physiological mechanical alignment of the knee. Recent studies have demonstrated significant variability in constitutional alignment within the population, beyond the classical frontal neutrality, especially following the introduction of the

coronal plane alignment of the knee (CPAK) classification by MacDessi in 2021[127]. This system introduced two additional angular parameters: the arithmetic hip–knee–ankle angle (aHKA) and the joint line obliquity (JLO). The aHKA is calculated by subtracting the LDFA from the MPTA and reflects constitutional coronal alignment. A negative value (MPTA greater than LDFA) corresponds to constitutional varus, while a positive value (LDFA greater than MPTA) corresponds to constitutional valgus. When LDFA and MPTA are equal within a margin of confidence, the aHKA approximates 0°, corresponding to neutral alignment. The JLO is calculated by summing MPTA and LDFA and represents joint line obliquity on the coronal plane. A value below 180° indicates distal apex obliquity, a value equal to 180° corresponds to neutral, and a value greater than 180° represents proximal apex obliquity.
The CPAK classification, based on a large sample of asymptomatic healthy knees, identified nine constitutional alignment types, expanding the definition of physiological alignment beyond neutral. The most common patterns observed in the healthy population are neutral alignment with distal apex joint line (39.2%) and varus alignment with distal apex joint line (26.4%). Other patterns occur at lower frequencies. According to these data, within valgus types of deviations up to 6° may still be considered physiological, while in varus types of deviations up to 8°–10° may remain within physiological range. The introduction of these new concepts has led to questioning the indication for corrective osteotomy in young patients with valgus or varus deviations. Increasingly, surgical correction is limited to cases with pathological deviations beyond safe ranges, symptomatic patients, or those with known secondary etiologies such as post-traumatic deformity, Blount's disease, or femoropatellar dysplasia[18,128–131].

KNEE MOVEMENTS

The tibiofemoral joint, defined as a condylarthrosis, presents six degrees of freedom: flexion–extension, tibial internal and external rotation, varus–valgus, anteroposterior translation, compression–distraction, and mediolateral translation. The primary movement of the knee joint is flexion–extension of the leg relative to the thigh, with the other movements acting as functional adaptations to optimize this motion.

Flexion-extension

Flexion–extension occurs in the sagittal plane and depends on the relative orientation of the femoral and tibial axes. The reference position is full extension, in which the femoral and tibial axes are parallel and coplanar in the sagittal plane. In the physiological knee, passive extension of about 5°–10° beyond this reference is possible, which must be distinguished from hyperextension, a pathological condition observed in neurological or post-traumatic disorders known as genu recurvatum.
The arc of active flexion varies depending on hip position. With the hip flexed, active knee flexion normally reaches 140°, while with the hip extended, flexion is limited to about 120°. This variability reflects the action of biarticular muscles, particularly the hamstrings and rectus femoris, whose tension depends on the position of both joints. Passive knee flexion can reach approximately 160°.
The axis of flexion–extension is essentially horizontal, opening an angle of about 81° with the femoral shaft laterally, reflecting the combined deviation of 3° between the vertical and the femoral mechanical axis and 6° between the femoral mechanical and anatomical axes. For this reason, in full flexion the leg axis does not lie directly posterior to the femoral axis but slightly medially, bringing the heel into contact with the ischial tuberosity.
Biomechanical studies have investigated the transverse axes of flexion–extension. The primary axis is not considered fixed but shifts with knee flexion, drawing a theoretical helical path along the condyles. With increasing flexion, the femoral contact area shifts posteriorly. The rotation axis describes a J-shaped path, termed the J-curve. This occurs because of posterior rolling of the femur relative to the

tibia, known as femoral rollback, which is controlled by the posterior cruciate ligament. This phenomenon allows the knee to flex beyond 90° without bone impingement.
Recent kinematic studies using three-dimensional reconstructions have revised these concepts, showing that the articular surfaces of the femoral condyles along which flexion–extension occurs can be described as cylindrical, with the medial condyle having a slightly larger radius than the lateral condyle but sharing the same axis of rotation.
On this basis, three axes of reference have been described for knee kinematics: the transverse axis of tibiofemoral flexion–extension, also referred to as the primary axis; the transverse axis of patellar flexion–extension, or secondary axis; and the longitudinal axis of tibial internal and external rotation. The two transverse axes are both involved in flexion–extension. Unlike older models, these axes are now considered fixed and constant throughout the motion. The primary transverse axis passes through the femoral condyles and represents the axis around which the tibia flexes and extends relative to the femur. The secondary transverse axis represents the axis of patellofemoral flexion–extension and runs parallel to the primary one, located anterior and proximal to it.
The extensor apparatus of the knee functions over the femoral trochlea as a pulley, facilitating extension of the leg. The patella alters the direction of the quadriceps force vector and increases the lever arm, enhancing the extensor moment by more than 50%. During a full flexion–extension cycle, the patella travels approximately 7–8 cm craniocaudally, nearly twice its own length. The contact relationship between the patella and femoral trochlea varies during this motion, with maximal contact surface occurring around 45° of flexion. Normally, patellar movement is restricted to the vertical plane; transverse displacements are considered pathological in flexion, while in full extension some lateral translation may occur due to reduced soft tissue restraints. The action of the extensor musculature is essential for its antigravity role in maintaining upright stance. When the knee is extended or slightly flexed during standing, the body weight vector lies posterior to the primary flexion–extension axis, creating a tendency toward further flexion, which is counterbalanced by quadriceps contraction. Conversely, in hyperextension the weight vector lies anterior to the axis. In this position, spontaneous hyperextension is immediately limited by tension of the posterior capsule and ligaments, allowing the position to be maintained passively without significant muscular activity, which explains the concept of paralytic knee[132–135].

Tibial rotation relative to the femur
The anatomical design of the joint allows tibial rotation on the femoral condyles, but this occurs only when the knee is flexed. The motion takes place around the longitudinal tibial axis and is best assessed with the knee at 90° of flexion, both actively and passively. Tibial rotation is closely related to flexion–extension. Full knee extension is invariably accompanied by tibial external rotation, while the initial degrees of flexion are associated with tibial internal rotation and femoral external rotation. This mechanism is known as the screw-home mechanism.
The medial tibial plateau is larger and more congruent than the lateral one. During the last 20° of extension, the less congruent lateral plateau undergoes external rotation to maintain joint congruity. This mechanism allows complete extension and stabilizes the knee in standing by tensioning the anterior cruciate ligament. Once full extension is achieved, unlocking the knee to initiate flexion requires the action of the popliteus muscle. Its function depends on the kinetic chain: in a closed chain, when the foot is fixed, the popliteus externally rotates the femoral condyles on the tibial plateau, while in an open chain, when the foot is free, it internally rotates the tibia on the femoral condyles.
If bone geometry alone were considered, femorotibial contact would occur on a very limited area, resulting in high contact stress. The menisci serve to redistribute these forces across a larger surface, reducing stress on the articular cartilage. They also stabilize the rolling and sliding motion of the curved femoral condyles on the irregular tibial plateau. During flexion–extension, the menisci move

accordingly: in extension they translate anteriorly, pulled by the femoral condyles and meniscopatellar ligaments, while in flexion they shift posteriorly under the influence of the femoral condyles and the semimembranosus and popliteus insertions. This movement is not symmetrical: the lateral meniscus is approximately twice as mobile as the medial meniscus, with displacements of about 12 mm and 6 mm, respectively.
In summary, during extension the patella translates proximally, the tibia shifts posteriorly, and the femur rotates internally relative to the tibia, producing relative tibial external rotation. During flexion, initiated by the popliteus tendon unlocking the screw-home mechanism, the patella translates distally, the tibia shifts anteriorly due to femoral rollback, and the femur rotates externally relative to the tibia, producing relative tibial internal rotation[114,136–140].

ARTICULAR STABILITY

A joint is defined as stable if contact between the articular surfaces is maintained throughout its entire range of motion. The knee, due to the poor congruence of its bony surfaces, requires both passive and active stabilizers to ensure adequate stability. Passive stabilizers include ligaments and the capsule, while active stabilizers are represented by muscles and tendons.
In simplified terms, the collateral ligaments resist varus and valgus stress, while the cruciate ligaments oppose tibial translation relative to the femur and control rotational movements. It is important to note, however, that the cruciate ligaments also contribute to coronal plane stability. Additional key stabilizers of the knee include the tendons of the pes anserinus (sartorius, gracilis, semitendinosus) and the semimembranosus on the medial side, as well as the iliotibial band, the biceps femoris tendon, and the popliteus tendon on the lateral side.
The knee is fully stable in the coronal plane when in complete extension. This stability is provided by the cruciate ligaments, particularly the anterior cruciate ligament, together with the collateral ligaments and the degree of congruence offered by the menisci. When the knee is flexed, the anterior cruciate ligament decreases its contribution to coronal plane stability, with only its anteromedial bundle remaining under tension, while the posterior cruciate ligament becomes the key stabilizer. During flexion, coronal stability is primarily ensured by the medial and lateral collateral ligaments. However, the collateral ligaments are more relaxed in flexion compared to extension, which explains why most knee instabilities are revealed in flexion, whereas instabilities in extension are extremely rare. This change in tension during flexion is due to the femoral insertions of the collateral ligaments, which move proximally in extension, tightening the ligaments.
Anteroposterior stability of the knee is provided mainly by the cruciate ligaments and, secondarily, by the posterior capsule and the surrounding flexor and extensor musculature. The cruciate ligaments play a crucial role in allowing a hinge-like flexion-extension movement of the knee, while limiting translational displacements in the anteroposterior direction[141–143].

RELATIONS WITH HIP AND ANKLE IN THE KINETIC CHAIN AND COMPENSATORY MECHANISMS

The knee joint represents the central link of the lower limb kinetic chain, transmitting forces between the hip and the ankle during both static postural control and dynamic activities such as walking, running, and jumping. Biomechanically, the knee functions as a modified hinge joint, allowing flexion-extension with accessory rotational movements, while being heavily influenced by the alignment and function of adjacent joints. Alterations at the hip or ankle inevitably modify knee kinematics and loading patterns. Excessive femoral anteversion, acetabular dysplasia, or hip abductor weakness can increase dynamic valgus forces transmitted to the knee, thereby predisposing to lateral patellar maltracking and overloading of the medial tibiofemoral compartment. Similarly, restricted dorsiflexion at the ankle leads to compensatory knee hyperflexion during gait and may accentuate sagittal plane

loading. The knee itself participates in compensatory strategies: in the presence of hip contractures, it increases flexion to maintain upright posture, whereas in cases of ankle deformity it adapts by altering tibial rotation and varus-valgus angulation. These compensatory mechanisms, both proximally and distally, underline the integrative role of the knee in the kinetic chain and explain why pathology at one level often produces secondary dysfunctions at others[144–147].

INSTRUMENTAL ASSESSMENT OF THE KNEE JOINT

The knee joint can be affected by a wide spectrum of pathologies such as congenital deformities, degenerative, inflammatory, metabolic conditions, traumatic injuries, and oncological diseases. For this reason, once a diagnostic suspicion has been formulated based on an accurate medical history and physical examination, it is often necessary to proceed with confirmatory instrumental tests.
Radiography represents the first-level diagnostic examination. If radiography is not sufficient for a correct diagnosis, or if further diagnostic work-up is required, second-level instrumental examinations must be performed such as computed tomography (CT), magnetic resonance imaging (MRI), and ultrasound. These latter techniques make it possible to identify lesions in structures that are not normally visualized by conventional radiography.
Second-level examinations have very specific indications; in particular, CT is indicated in the study of intra-articular fractures and in the assessment of severe deformities. MRI represents the primary examination for evaluating periarticular soft tissues, oncologic diseases, ischemic conditions, and finally stress-related injuries. Ultrasound allows a detailed assessment of periarticular musculo-tendinous structures, with limited capability for evaluating intra-articular anatomical structures.

STANDARD RADIOGRAPHY

A complete radiographic examination of the knee classically consists of three projections: anteroposterior (AP), lateral, and axial. However, numerous other projections can and should be selected based on the clinician's diagnostic suspicion (panoramic radiograph of the lower limbs, Rosenberg view, oblique projections, etc.).
In trauma settings, the radiographic examination usually consists only of the anteroposterior and lateral projections; other projections should be requested solely for additional diagnostic investigation. For example, to exclude fractures, the standard anteroposterior and lateral projections, if not diagnostic, can be supplemented with oblique projections, which are usually performed in the supine position, without weight bearing on the affected limb. Conversely, in the absence of clinical suspicion of fracture, it is advisable, if possible, to perform radiographic projections with the patient in the upright position, that is, under load. Finally, so-called "dynamic" projections can be performed: in cases of suspected knee instability or ligament injuries, stress radiographs allow the demonstration of joint laxity, although the use of these projections has been significantly reduced with the introduction of magnetic resonance imaging.

Radiographic projections

The evaluation of the x-ray by the orthopaedic surgeon must follow a rational and systematic approach, highly repeatable, allowing diagnostic errors to be minimized. Each projection provides specific information or allows the assessment of angular parameters distinct from those assessable in other projections.
The evaluation of the radiographic series must always begin with the anteroposterior (AP) projection[148]. It is performed with the knee extended and the feet parallel, the radiographic cassette placed posteriorly to the knee, and the X-ray beam perpendicular to the cassette; in this setup the patella often appears projected on the lateral side of the knee: this is not a pathological sign; specific projections are used to evaluate patellar alterations. The structures that can be assessed on an anteroposterior projection of the knee are the medial and lateral femoral condyles, the medial and lateral compartments of the joint, the tibial spines, the tibial plateau, and the proximal third of the tibia and fibula.
The evaluation of the joint space represents a step of fundamental importance; it should be considered, however, that its assessment for degenerative and non-traumatic pathology requires weight-bearing

projections with the patient standing. Its width is closely related to the condition of the articular cartilage: a reduction in width correlates with its wear, in one or more compartments. In the physiological knee, the joint space in the lateral compartment is slightly wider than that of the medial compartment, in consideration of the articular geometry specific to the knee (the lateral femoral condyle is smaller than the medial condyle).
The anteroposterior projection, if performed in the standing position, also provides a rough assessment of alignment between the tibia and femur; nevertheless, when axial alterations of the knee are suspected, it is always necessary to perform a full-length standing radiograph of the lower limbs and pelvis, from the pelvis to the tibiotalar joint.
The parameters that can be evaluated on the anteroposterior projection, preferably on a full-length standing radiograph of the lower limbs and pelvis in orthostasis, are numerous.
● Mechanical axis of the lower limb, and anatomical and mechanical axes of the femur and tibia[149].
● Epiphyseal axis of the tibia: represented by the line drawn between the midpoint of the tibial spines and the midpoint of the growth plate.
● Cartier angle: represents the angle between the perpendicular to the tangent line to the lateral tibial plateau and the mechanical axis of the tibia. This angle is important in preoperative planning to decide the correct indication between unicompartmental prosthesis and total knee arthroplasty. In the presence of a Cartier angle greater than 5° there is an indication for total prosthetic replacement, whereas for lower angles a unicompartmental prosthetic replacement is possible. With values greater than 5°, tibial varus is excessive to guarantee satisfactory long-term survivorship with a partial prosthetic implant[150].
A parameter that can be evaluated on the AP projection of a full-length panoramic radiograph of the lower limbs is the Q angle. This represents the angle formed by the line connecting the anterior superior iliac spine and the center of the patella, which corresponds to the direction of the force vector that the quadriceps muscle exerts at the patella, and by the line drawn between the center of the patella and the anterior tibial tuberosity. Values between 10° and 20° are usually considered physiological; its alterations (particularly increases) are associated with lateral overload of the patella up to true dislocations. It is important to note a significant variability of this parameter based on sex, being greater in women[151]. Unlike the angles mentioned previously, this angle must be measured on a projection performed in the supine position.
A variant of the normal anteroposterior projection is the Rosenberg projection[152], which is a posteroanterior (PA) projection. The patient is placed standing with bipodal support, with the feet parallel and the knee under examination flexed 40°–45°; the patella is placed against the radiographic cassette; the beam is angled on the sagittal plane in a craniocaudal direction to make it tangential to the surface of the tibial plateau. This projection is useful for the evaluation of osteoarthritic conditions; in particular, it allows appreciation of joint space narrowing in the weight-bearing zones due to cartilage loss; this aspect is often underestimated or misinterpreted in a standing anteroposterior projection. Comparison of intraoperative and radiographic results demonstrates that the flexed posteroanterior projection has greater accuracy, sensitivity, and specificity than the traditional one. The radiographic evaluation then proceeds with the lateral projection, where the patella, the distal femur, the proximal tibia, and the proximal fibula can be assessed.
This projection is obtained with the patient in lateral decubitus on the side of the affected limb, with the knee flexed to about 30°. The radiographic cassette is positioned beneath the outer side of the knee, and the X-ray beam is directed perpendicular to the cassette. This projection can also be performed in the standing position: in this case the radiograph is taken with the knee maintained at 30° of flexion and the longitudinal axis of the tibia perpendicular to the floor. Nonetheless, there are variants of the projection in which the knee is fully extended. In any case, in a correctly performed radiograph, the femoral condyles must be superimposed, to avoid artifacts secondary to improper rotations. The medial femoral condyle is slightly larger than the lateral condyle and therefore appears to “encompass” the lateral

condyle completely on the lateral projection. The lateral projection assumes great importance in the evaluation of the patellofemoral joint, both regarding the width of the joint space and the height of the patella (patella alta or baja). On the lateral projection the tibial plateaus slope posteriorly downward, giving rise to the anatomical characteristic known as the tibial slope. The tibial plateaus differ in certain features: the higher of the two tibial spines belongs to the medial tibial plateau. In its posterior portion, the medial tibial plateau tilts dorsally and is square. Conversely, the posterior margin of the lateral tibial plateau gently projects downward with a rounded contour[144–146].

The parameters that can be evaluated on the lateral projection are:
● Tibial slope: represents the angle of inclination of the tibial plateau on the sagittal plane. There is no universal method for calculating the tibial slope, as the angle can be subtended by four distinct lines. The primary line that remains constant in all measurements is the line connecting the most anterior and posterior high points of the medial tibial plateau; the second line can be represented by the tangent to the anterior cortical of the tibia, by the proximal diaphyseal axis of the tibia, by the tangent to the posterior cortical of the tibia, or by the diaphyseal axis of the fibula. The tibial slope represents a fundamental parameter for the entire biomechanics of the knee, from ligament function to joint kinematics: an increase in slope increases the tension of the posterior cruciate ligament and reduces the extensor capacity of the knee; conversely, a reduction in slope increases the tension of the anterior cruciate ligament with a reduction in flexion capacity of the knee and an increase in joint instability, particularly in so-called mid-range flexion (30°–60°)[153,154].
● Posterior offset of the femoral condyles represents the distance between the tangent line to the posterior cortical of the femoral diaphysis and the posterior extremity of the femoral condyles. This parameter is directly correlated with the ability to obtain knee flexion without impingement between femur and tibia. A reduction of this parameter by about 3 mm correlates with a reduction of maximum flexion by 10°. For this reason, this parameter is of particular importance in knee arthroplasty to ensure preservation of joint function. An evolution of it is represented by the posterior condylar offset ratio, which is a dimensionless parameter that removes the confounding factor represented by radiographic magnification. The normal ratio is 0.44 for both males and females, 0.47 if the cartilage of the posterior condyles is considered, a parameter useful for postoperative evaluation of knee prosthesis[155]
● Insall–Salvati index (ISI): represents the ratio between the length of the patellar tendon and the length of the patella from the superior pole to the inferior pole. These two lengths are usually similar and their ratio ranges between 0.8 and 1.2. If the ratio is greater than 1.2 the patella is defined as alta, whereas if the ratio is less than 0.8 it is defined as baja[156].
● Modified Insall–Salvati index (MISI): represents the ratio between the distance from the insertion of the patellar tendon to the inferior apex of the patellar articular surface and the length of the patellar articular surface. Normal values range between 1 and 2; values greater than 2 define a high-riding patella, while values less than 1 indicate a low-riding patella. This index has better reproducibility than the classic Insall–Salvati index[157].
● Caton–Deschamps index represents the ratio between the distance from the inferior pole of the patella to the anterosuperior border of the tibia and the length of the patellar articular surface. The normal value is 0.96 in men and 0.99 in women. This parameter is characterized by high reliability and reproducibility[156].
● Blackburne–Peel ratio: represents the ratio between the length of the line perpendicular to the tangent to the tibial plateau up to the inferior articular margin of the patella and the length of the patellar articular surface. Normal values are around 0.8; values greater than 1 are representative of a high-riding patella[158,159].
● Blummensaat's line represents the line tangent to the roof of the intercondylar notch that may or may not intersect the inferior border of the patella. If the patella is positioned superior to this line it is high;

conversely, it defines a picture of a low patella. Although used very frequently, it is a poorly reliable index that has therefore been progressively abandoned over the years. Another morphological assessment of the patella is that provided by Grelsamer. Three types of patellae have been described based on the ratio between the length of the patella and the length of the articular surface. Most patellae have a ratio between 1.2 and 1.5 and are classified as type I. Those of type II have a ratio greater than 1.5. Those with a ratio less than 1.2 are instead classified as type III[160].

Axial patellar projections allow visualization of the patellofemoral joint, both on the patellar side and on the femoral side. Numerous distinct axial projections have been described that allow highlighting the radiographic characteristics of the joint at different degrees of flexion–extension (Merchant, Sunrise, Ficat, Laurin)[160].

The most frequently used axial projection is the Merchant view. The patient is positioned supine on the radiographic table; the knees are flexed at 45° (using a rigid or adjustable platform) and the cassette is positioned at the level of the proximal third of the tibia (the radiographic cassette is oriented about 30° relative to the horizontal plane). Both knees are exposed simultaneously, with the X-ray beam directed toward the feet, inclined about 30° relative to the horizontal plane. This projection provides excellent evaluation of patellofemoral alignment. It is ideal for assessing the osseous patellofemoral articular surfaces, and therefore for highlighting any signs of extensor apparatus malalignment[161]. Another axial projection (Sunrise projection) can be obtained with the patient prone and the knee in maximum flexion (over 115°). This projection makes it possible to evaluate the posterior surface of the patella, whereas the femoral articular surface shown does not correspond to the femoral trochlea. The use of the Sunrise projection is limited since accurate evaluation of patellofemoral alignment is impossible when the knee is excessively flexed. Finally, some patients have difficulty tolerating this position[160].

The Merchant projection represents the gold standard in axial radiographic evaluation of the patellofemoral joint, allowing assessment of numerous parameters that characterize this joint:

● Trochlear morphology: the trochlea is classified using Dejour's scheme into four grades based on its depth and morphology, which are assessed both on the sagittal projection and on the axial projection. It is also possible to evaluate the sulcus angle, formed by the junction lines between the deepest point of the intercondylar sulcus and the highest points of the medial and lateral femoral condyles; normally this angle is 138° ± 6° but it can even reverse, exceeding 180°[162,163].

● Patellar morphology: the patella, like the femoral trochlea, can also present constitutional variants that can alter the normal V-shaped morphology the patella assumes on the axial projection. Wiberg's classification makes it possible to categorize patellar morphologies into four main variants based on the profile of the medial and lateral articular facets[164].

● Patellar lateralization (patellar shift): represents an assessment of patellar lateralization on the axial plane and is evaluated by the congruence angle (or Merchant angle). To measure this parameter, the sulcus angle is bisected to create a reference line represented by the bisector of the angle itself. An additional line is then drawn from the deepest part of the trochlear sulcus to the patellar apex. The angle formed between this line and the reference line is the congruence angle. If the patellar apex is located lateral to the reference line, then the value of the congruence angle is positive, whereas if the apex lies medial to the reference line, the value of the congruence angle is negative. The normal congruence angle is 6 degrees (± 11 degrees)[165].

● Patellar tilt: patellar tilt represents the angle formed by the patella with the posterior plane of the two femoral condyles. This parameter requires CT to be measured precisely. However, an estimate of patellar tilt can be made using the Laurin angle calculated on an axial patellar radiograph by the angle between the anterior tangent to the femoral condyles and the tangent to the lateral articular facet[166].

Supplementary projections

There are supplementary projections that are not performed routinely but must be known because they allow a specialized assessment in particular cases.

● Tunnel view: this is a projection on the coronal plane (posteroanterior). The patient is positioned prone on the table with the knee flexed 30°–45° and the patella resting on the radiographic cassette; the beam is angled craniocaudally by about 45° (perpendicular to the axis of the leg). This projection shows the posterior aspect of the intercondylar notch, the inner posterior profiles of the medial and lateral femoral condyles, the tibial spines and plateaus, making it ideal for the evaluation of patients with suspected osteochondritis dissecans, which tends to occur in the most posterior zone of the intercondylar notch.

● Lyon–Schuss projection: this is a projection very similar to the Rosenberg view. The patient, in the standing position with bipodal support, is positioned with the knees flexed at 30° with the patellae resting on the radiographic cassette. The beam is angled in a craniocaudal direction to make it parallel to the surface of the tibial plateau. As with the Rosenberg projection, it is required to evaluate the weight-bearing articular cartilage.

Oblique projections represent projections that are of particular importance in the trauma setting, allowing better identification of any fracture lines present. Oblique projections are obtained at 45° of internal and external rotation of the lower limb, with the patient in the supine position, the affected knee extended and the radiographic cassette behind the knee. The X-ray beam should be directed with a cranial inclination of about 5° to neutralize the physiological tibial slope. The projections should show the patella, femoral condyles, tibial plateaus, and fibula. In external rotation the tibia and fibula overlap, whereas in internal rotation the overlap is less pronounced. Occult fractures and tibiofibular osteoarthritis can be more easily detected with oblique projections than with routine anteroposterior projections.

Various stress projections have been described for the evaluation of instabilities, which include varus and valgus stress radiographs for the evaluation of the collateral ligaments and anteroposterior stress radiographs for the evaluation of the anterior cruciate ligament (ACL). These require the use of a mechanical stress device or lead gloves worn by the radiologic technologist to manually stress the knee joint. In current clinical practice these projections are rarely requested because MRI is considered the reference standard for the evaluation of intra-articular soft-tissue injuries. In addition, stress projections often must be performed under local anesthesia for pain control[167–172].

COMPUTED TOMOGRAPHY

Computed tomography (CT) provides detailed information on bone structures and generally serves as a second-level diagnostic examination. At the level of the knee, CT is indicated especially for certain particular clinical situations such as articular fractures, delayed fracture healing, and intra-articular loose bodies of bony nature. CT is increasingly used for preoperative planning of arthroplasty procedures (particularly in robotic surgery), in the evaluation of painful prostheses, and for planning revision arthroplasty. It is also possible to use CT for the evaluation of the extensor apparatus and the patellofemoral joint.

CT arthrography with iodinated contrast can be requested to evaluate the menisci and/or the articular cartilage when a patient cannot undergo an MRI examination: patients with claustrophobia or metallic devices that are a contraindication to MRI, such as older-generation pacemakers.

A CT scan of the knee can be interpreted in any of the three standard imaging planes: axial, sagittal, or coronal. In addition, 3D reconstructions and surface-rendered reconstructions can be created at an independent workstation. These are useful in the context of complex bony trauma to obtain a more complete view[173–175].

MAGNETIC RESONANCE IMAGING

Magnetic resonance imaging (MRI) is an instrumental technique that allows excellent assessment of internal structures of the knee and of the articular cartilage. MRI represents the gold-standard examination in the diagnosis of numerous pathological processes, such as soft-tissue pathologies (osteochondral lesions, meniscal tears, ligament injuries), neoplasms, infections, metabolic bone diseases, and suspected complications following knee arthroplasty[176].

Ligaments

The anterior cruciate ligament (ACL) is generally visualized on the sagittal plane on several images because of its oblique course. The ACL is also assessed on the coronal and axial planes. To produce images of the entire course of the ligament, dedicated imaging on an oblique sagittal plane can be performed, which allows it to be evaluated in its entirety in a single image. The normal appearance of the ACL consists of a low-signal (hypointense) band in all imaging sequences with a linear intrasubstance signal, from intermediate to bright, derived from the normal interposition of adipose tissue and synovial membrane.

The posterior cruciate ligament (PCL) is wider and more robust than the ACL. The PCL originates from the anterolateral surface of the medial femoral condyle and, with an oblique course, inserts inferiorly on the posterior intercondylar area of the tibial plateau. The normal representation of the PCL is that of a low-intensity structure in all sequences; it is usually visualized on one or two consecutive images on the sagittal plane. The PCL is taut in flexion and tends to be laxer in extension (the classic position in which the knee is found during an MRI). It should have a slightly curved configuration when viewed on the sagittal plane.

The medial collateral ligament (MCL) is a ligamentous complex composed of three layers. The MCL should appear as a uniformly hypointense structure in all sequences. It is best appreciated in coronal and axial sequences. MCL injuries range from sprains, in which the ligament appears normal in a context of surrounding edematous tissue, to partial- or full-thickness tears with disruption of the superficial and/or deep fibers.

The lateral collateral ligament (LCL) is also composed of three layers. The constituents of the LCL complex and of the posterolateral corner normally appear as homogeneous hypointense structures on MRI, clearly visible both on coronal and axial projections. Tears of any portion of the LCL complex present as hyperintense signals and as discontinuities of the ligamentous or tendinous fibers. True disruptions of the LCL are closely associated with lesions of the posterolateral corner and entail multiplanar instability[176–179].

Menisci

The menisci are semilunar wedge-shaped fibrocartilaginous structures that lie between the femoral condyles and the tibial plateau. Each meniscus is arbitrarily divided into an anterior horn, a body, and a posterior horn. The inner margin of the meniscus is called the free margin or apex, and on coronal MRI it should appear as a sharp point. The superior surface is concave and is shaped to accommodate the femoral condyles, while the inferior surface is flat and rests on the tibial plateau.

The menisci are homogeneous structures, hypointense on all sequences, and should be evaluated on the sagittal and coronal planes. On the sagittal plane, normal menisci should appear as black triangles with a pointed inner margin. The sagittal visualization of the two horns, anterior and posterior, with the meniscal body in between, normally appears as a butterfly shape. On the coronal plane, the appearance of the meniscal body and the insertions of the meniscal roots can be better visualized.

Meniscal tears present as clear linear abnormalities on T2-weighted sequences (fluid-sensitive) that reach the articular surface, or as alterations in normal meniscal morphology. The presence of a meniscal body on coronal section larger than 15 mm, broad or extending into the intercondylar notch, suggests the diagnosis of discoid meniscus. The anterior intermeniscal or transverse ligament connects

the anterior horns of the two menisci. It is present in 44–58% of individuals. On the sagittal plane, the interface of this structure with the anterior horn of the lateral meniscus often resembles a lesion. Following this pseudolesion in sequential images helps in recognizing the normal structure[180,181].

Tendons

The extensor apparatus of the knee includes the quadriceps tendon and the patellar tendon. The normal quadriceps tendon is hypointense on all sequences, with slightly more intense internal striations that represent the subdivision of the tendinous heads. The patellar tendon is composed primarily of fibers coming from the rectus femoris, which continues inferiorly from the patella to then insert on the tibial tuberosity. It normally appears as a homogeneous and hypointense structure on MRI. The extensor apparatus is best evaluated on the sagittal plane. Axial sequences allow visualization of the medial and lateral retinacula, which originate from the patella and insert respectively on the medial and lateral femoral condyles. The tendons of the semimembranosus muscle and of the pes anserinus run along the posteromedial surface of the knee. They appear as hypointense structures on MRI. The semimembranosus tendon has multiple expansions that insert both on the medial tibia and on the joint capsule. The pes anserinus tendon is formed by the union of three tendons: gracilis, sartorius, and semitendinosus. The three united tendons insert on the medial face of the anterior tibia at the level of the MCL insertion. They are well evident on the axial plane.

The popliteus tendon originates from the posteromedial aspect of the tibia, runs anterosuperiorly, and inserts on the lateral aspect of the lateral femoral condyle. The superior and inferior popliteomeniscal fascicles are points of anchorage between the lateral meniscus, the popliteus tendon, and the capsule to form the roof and floor of the popliteal hiatus. The fascicles control the movement of the lateral meniscus during flexion–extension and appear as faint hypointense signals extending from the posterolateral aspect of the lateral meniscus to the joint capsule[176].

Cartilage

Various techniques are used to evaluate the cartilage of the knee joint. Fat-suppression sequences provide images that highlight lesions, offering high resolution and clear differentiation between fluid and cartilage, and furthermore providing excellent cartilage detail. Other advanced but less frequently used techniques include T2 mapping, DWI (diffusion-weighted sequences), and dGEMRIC (sequences with gadolinium). The latter have today greater application in research rather than in clinical practice[182].

ULTRASOUND

Knee ultrasound allows dynamic evaluation of the soft tissues, certainly less defined than MRI but in some cases more specific, as for example for the evaluation of the popliteal fossa. Possible vascular pathologies, such as aneurysms of the popliteal artery, can be studied and analyzed with the characteristics of their flow. In addition, during the diagnostic phase interventional procedures can be performed (injections or aspirations); for example, popliteal cysts can be identified, with the aim of ultrasound-guided aspiration. Another application of ultrasound is the evaluation of the extensor apparatus. A series of conditions can be identified, such as patellar tendon tears and prepatellar bursitis. Ultrasound can also be used to evaluate patients with meniscal and parameniscal symptoms. The availability of high-frequency, high-resolution linear transducers allows the diagnosis and treatment of symptomatic parameniscal cysts[183–185].

NUCLEAR MEDICINE

Nuclear medicine has many applications, although its use is relatively limited in common practice. At the knee, nuclear medicine examinations can be requested for occult fractures, stress injuries, infections, complications of arthroplasty, arthritis, metabolic bone diseases, and tumor pathologies. Nuclear medicine examinations of the knee are complementary to anatomical studies, as well as to radiographs, CT scans, or MRI. It is useful to have correlated examinations available during the interpretation of a bone scan because they help localize abnormalities in radiotracer activity[186].

GAIT ANALYSIS

Gait analysis represents the most comprehensive method for studying knee biomechanics within the context of whole-body locomotion. The knee plays a crucial role in shock absorption, propulsion, and stability during walking and running, and instrumented evaluation allows these contributions to be quantified objectively. Modern gait laboratories employ three-dimensional motion capture systems, synchronized with force platforms and surface or fine-wire electromyography, to assess kinematics, kinetics, and muscle activation patterns throughout the gait cycle.

During normal gait, the knee demonstrates a highly coordinated pattern of motion. At initial contact and loading response, the knee flexes slightly to absorb impact forces, with quadriceps eccentric activity controlling flexion and preventing collapse. In mid-stance, the knee extends to allow efficient weight transfer, while ground reaction forces pass close to the joint center to minimize muscular demand. At terminal stance and pre-swing, rapid knee flexion contributes to limb clearance and facilitates forward propulsion, supported by plantarflexor push-off and hamstring activity. Any pathological alteration of this sequence leads to compensatory changes at proximal and distal joints, highlighting the interdependence of the kinetic chain.

In degenerative knee disease, gait analysis frequently reveals reduced knee flexion at loading response, a strategy that decreases quadriceps demand but increases shock transmission to articular cartilage. In advanced medial osteoarthritis, dynamic varus thrust may be observed, characterized by a sudden medial collapse of the knee during stance, which correlates strongly with compartmental overload and radiographic progression. Conversely, anterior cruciate ligament insufficiency produces increased anterior tibial translation and altered rotational kinematics, with patients often adopting a stiff-knee gait pattern to reduce instability.

Kinetic data further enrich understanding of these alterations. In medial compartment osteoarthritis, the external knee adduction moment is consistently elevated, reflecting increased medial load transmission; this parameter is now considered a biomechanical biomarker of disease severity and progression. Electromyography often reveals abnormal quadriceps–hamstring co-contraction, interpreted as a protective mechanism against instability, although it also increases joint compressive forces.

Although currently used primarily in research settings, gait analysis is increasingly recognized as a valuable adjunct in clinical decision-making. It provides objective documentation of functional limitations, allows comparison of pre- and postoperative outcomes, and may help to predict surgical prognosis. For example, persistent gait asymmetry after total knee arthroplasty has been linked to lower patient satisfaction and poorer functional recovery, even in the presence of satisfactory radiographic alignment. For this reason, integration of gait analysis into surgical planning and rehabilitation strategies has the potential to refine indications and improve individualized patient care[187–189].

KNEE OSTEOARTHRITIS

Definition

Knee osteoarthritis, also referred to as gonarthrosis, represents the combination of clinical symptoms and radiographic alterations characteristic of articular cartilage degeneration. It usually involves both the femoral and tibial components of the joint, although the patellofemoral joint is also commonly affected. The onset of symptoms is typically insidious, with a slowly progressive worsening of the clinical condition. Gonarthrosis can be classified as primary or secondary: primary osteoarthritis is defined only after a differential diagnosis excluding all secondary etiologies[190].

Primary osteoarthritis	Primary osteoarthritis	
	Outcomes of traumatic injuries	Articular fractures
		Meniscal injuries
		Ligament injuries
		Osteochondarl injuries
	Outcomes of osteonecrosis	
	Outocomes of systemic diseases	Rheumatic diseases
		Metabolic diseases
	Deformities	Axial and sagittal deformities

Table 1: possible causes of knee osteoarthritis are shown.

Epidemiology

The knee is the joint most frequently affected by osteoarthritis, followed by the lumbar spine and the hip. This high prevalence is mainly due to the elevated loads transmitted across the knee during daily activities and to the relatively low congruence of the articular surfaces, which makes the joint more vulnerable to mechanical imbalance. In a neutrally aligned knee, the medial compartment bears approximately 60–70% of load forces, which explains why it is most commonly involved in degenerative changes.

The prevalence of gonarthrosis is slightly higher in females and increases proportionally with age. Radiographic signs of knee osteoarthritis are observed in about 60% of individuals over 65 years old, even in those who may remain asymptomatic. Genetic background and ethnicity also appear to influence prevalence: higher rates have been reported in Caucasian populations compared to Asian or African groups, suggesting a multifactorial etiology that combines mechanical and genetic predispositions. Occupational exposure to repetitive stress, rural versus urban lifestyles, and a history of high-impact sports also affect incidence[190,191].

Pathogenesis

The development of primary gonarthrosis is influenced by genetic predisposition, hormonal environment, and lifestyle. Estrogens exert a protective effect, explaining the increased incidence of knee osteoarthritis in postmenopausal women, while an excess of growth hormone (GH) may favor early onset in both sexes. Other important predisposing factors include obesity, which increases joint loading, intense sports involving torsional stresses, and physically demanding occupations.

Secondary gonarthrosis can result from multiple pre-existing conditions affecting the knee. The main causes are post-traumatic (sequelae of intra-articular fractures, meniscal tears, or ligamentous injuries), post-inflammatory, or related to systemic diseases such as rheumatologic or metabolic disorders. Axial

deformities (varus or valgus) play a pivotal role in altering load distribution, leading to focal degenerative lesions. Overall, varus alignment is the single most important isolated risk factor for medial compartment osteoarthritis, while valgus deformity predisposes to lateral compartment degeneration. Patellofemoral osteoarthritis may also occur independently or in association, especially in patients with maltracking, trochlear dysplasia, or increased Q-angle[190,191].

Pathological Anatomy

The earliest structural damage occurs in the articular cartilage, which has a very limited capacity for repair. Progressive degeneration leads to fibrillation, fissuring, and eventual loss of cartilage with exposure of the subchondral bone. The medial tibial plateau is typically the first area to be involved, reflecting its role as the main load-bearing surface, followed by progressive extension to the entire medial femorotibial compartment and subsequently to the lateral and patellofemoral compartments.
In early stages, meniscal fibrocartilage undergoes degenerative calcification and extrusion, altering knee biomechanics and accelerating joint space narrowing. With disease progression, large marginal osteophytes form as a compensatory mechanism aimed at increasing the articular surface. Although initially adaptive, osteophyte formation ultimately worsens joint mechanics and contributes to pain and stiffness.
The degenerative process extends to the capsule and ligaments, which undergo thickening, fibrosis, and loss of elasticity. This capsular contracture, often associated with fibrosis of the flexor muscles, produces a persistent flexion attitude of the knee. Over time, flexion contracture reduces the functional load-bearing surface, accelerates joint wear, and predisposes to mid-flexion instability. Periarticular muscles atrophy, particularly the quadriceps, further compromising stability.
Histologically, cartilage shows loss of proteoglycans, increased water content, and fibrillation. Subchondral bone exhibits sclerosis, cystic degeneration (geodes), and angiogenesis, which contribute to pain. Synovial inflammation and hypertrophy may coexist, often correlating with acute painful exacerbations[192–194].

Clinical Presentation

The typical age of onset is after 55 years, although the degenerative process begins much earlier and remains silent for years. Secondary gonarthrosis may present earlier depending on the underlying cause. Onset is usually gradual, and patients often present to the clinician with advanced radiographic osteoarthritis but relatively mild or recent pain.
When symptomatic, pain is typically localized to the anteromedial region, sometimes radiating to the thigh or leg. The pain has the characteristic pattern of mechanical osteoarthritis: morning stiffness or pain after inactivity (start-up pain), improvement with moderate activity, and relief with rest. In advanced stages, pain becomes persistent throughout the day and is exacerbated by loading, posture changes, stair climbing, or walking on uneven ground.
Functional limitation is progressive, with reduced range of motion caused by joint deformity, capsular contracture, and reflex muscle spasm. Extension loss and flexion contracture are common, eventually leading to significant gait impairment. Patients may also report episodes of swelling due to synovitis, often resolving spontaneously or with rest, NSAIDs, or intra-articular injections. Crepitus and crackling may be palpable during motion.
On examination, the knee often appears moderately flexed at rest. Pain is elicited on movement, with marked tenderness and palpable crepitus. Gait abnormalities include antalgic limp, varus thrust, or lateral thrust depending on the compartment affected. Ligamentous instability may be unmasked during mid-flexion. Quadriceps wasting is frequently observed, worsening functional disability[190,191].

Radiologic Assessment

The first-line diagnostic tool, and often sufficient for diagnosis, is weight-bearing knee radiography in anteroposterior and lateral views. A full-length standing x-ray of the lower limbs and pelvis is recommended to assess overall limb alignment and deformities that influence disease severity. Axial patellofemoral views are also useful for evaluating involvement of this compartment.
Typical radiographic findings of osteoarthritis include joint space narrowing (usually asymmetric), subchondral sclerosis, subchondral cysts (geodes), tibial spine prominence, and marginal osteophytes. Bone deformities become apparent in advanced stages.
CT scanning may be employed in cases of severe deformity or bone loss, particularly for preoperative planning. MRI is considered a third-level investigation and is not routinely indicated but may be used to exclude alternative diagnoses (osteonecrosis, tumors, complex regional pain syndrome) or to assess cartilage, menisci, and ligaments in atypical presentations. Ultrasound may provide additional information on effusion, synovitis, or Baker's cysts.

Classification
Knee osteoarthritis can be classified based on radiographic severity. The most widely used system is the Kellgren–Lawrence classification (1957), which defines five grades from 0 to 4.[195] Other classifications, such as the Ahlbäck system, are sometimes employed to describe more advanced stages with joint space obliteration and bone attrition[196]. Clinical classifications may also consider functional limitation, deformity, and instability.

Kellgren-Lawrence Classification

- 0: No radiographic signs of osteoarthritis
- 1: Initial joint space narrowing (<2 mm) and possible osteophytes
- 2: Presence of osteophytes with initial joint space narrowing
- 3: Multiple osteophytes, joint space narrowing, subchondral sclerosis, and initial bone deformity
- 4: Large osteophytes, severe joint space narrowing, severe subchondral sclerosis, and marked bone deformities

Ahlbäck Classification

Grade 1: Joint space narrowing (<3 mm) compared to the contralateral knee
Grade 2: Joint space obliteration
Grade 3: Minor bone attrition (<5 mm)
Grade 4: Moderate bone attrition (5–10 mm)
Grade 5: Severe bone attrition (>10 mm)

Correlation between morphology, symptomatology, and surgical indications
Knee osteoarthritis (OA) represents the most common degenerative disorder of the lower limb, and its clinical presentation results from the interaction between morphological alterations, biomechanical load distribution, and patient-specific compensatory strategies. The disease is characterized by progressive articular cartilage loss, subchondral bone remodeling, osteophyte formation, and variable degrees of synovial inflammation, which together modify the structural environment of the joint.
From a biomechanical perspective, the knee is exposed to considerable cyclical loading during locomotion, and alterations in coronal and sagittal alignment strongly influence disease onset and progression. Medial compartment OA is particularly frequent, explained by the physiological varus moment during gait that directs greater loads medially. Conversely, valgus malalignment predisposes to lateral compartment involvement. Morphological parameters such as tibial slope, femoral condyle

geometry, and patellofemoral congruence also affect disease patterns and determine the extent of functional impairment.
Symptomatology does not always correlate linearly with radiographic severity. Some patients with advanced radiographic degeneration remain only mildly symptomatic, while others with moderate morphological changes report significant pain and disability. Pain mechanisms are multifactorial, including mechanical overload of subchondral bone, synovial inflammation, and altered neuromuscular control. Malalignment often accentuates pain by creating abnormal stress distribution, while secondary soft tissue changes, such as medial collateral ligament laxity or lateral retinacular tightness, further destabilize the joint and exacerbate symptoms.
Clinical evaluation focuses on the relationship between morphology and function. Dynamic assessment frequently reveals gait abnormalities, including reduced knee flexion during loading response and dynamic varus or valgus thrust. These findings not only reflect symptom severity but also provide prognostic information. For instance, patients with pronounced varus thrust tend to progress more rapidly to advanced medial OA and exhibit poorer outcomes after conservative management.
Surgical indication in knee OA derives from the integration of radiographic morphology, patient symptoms, and functional limitations. Joint-preserving procedures, such as high tibial osteotomy or distal femoral osteotomy, are generally reserved for younger patients with unicompartmental involvement and malalignment, aiming to redistribute load across the joint. In contrast, total knee arthroplasty is indicated in advanced, multicompartmental OA with disabling pain and functional restriction refractory to conservative measures. Importantly, the threshold for surgical intervention is not determined solely by morphological changes but also by the patient's quality of life, activity level, and responsiveness to non-operative treatments.
The biomechanical environment of the knee should be considered alongside imaging in surgical planning. Parameters such as the knee adduction moment, sagittal kinematics, and quadriceps strength have been correlated with postoperative outcomes. Persistent abnormal loading after arthroplasty may explain why some patients remain symptomatic despite optimal implant positioning. Therefore, aligning surgical indications with both structural and functional assessment represents a key step toward personalized management of knee osteoarthritis[190,191,197].

Treatment
Initial treatment is conservative, particularly in early stages. Core measures include weight management, quadriceps and hip muscle strengthening, low-impact aerobic exercises (cycling, swimming), and postural training. Pharmacological therapy involves analgesics (acetaminophen, opioids for severe pain), anti-inflammatories (NSAIDs, corticosteroids), and symptomatic slow-acting drugs for osteoarthritis (glucosamine, chondroitin, diacerein), although their efficacy is debated. Intra-articular injections with corticosteroids, hyaluronic acid, platelet-rich plasma, or stem cell-based products are employed to reduce symptoms in selected cases. Patients must be counseled about the progressive nature of the disease: conservative measures can relieve pain and improve function but cannot halt progression.
When conservative treatment fails and pain or functional limitation becomes intolerable, surgical intervention is indicated. Surgical options include corrective osteotomies (for younger patients with unicompartmental disease and malalignment), unicompartmental knee arthroplasty (UKA) in selected patients with isolated compartment involvement, and total knee arthroplasty (TKA) for advanced, multicompartmental disease. Each option requires evaluation of range of motion, ligament stability, deformity reducibility, and patient functional demands. In specific cases, cartilage repair techniques (microfracture, mosaicplasty, autologous chondrocyte implantation) or partial prostheses may be considered. Clear patient education and shared decision-making are crucial, as surgical choice impacts lifestyle, rehabilitation, and long-term outcomes[191].

KNEE REPLACEMENT

Knee arthroplasty represents one of the most successful surgical procedures in modern orthopedics, with excellent long-term survival rates and significant improvement in pain, mobility, and overall quality of life. It remains the treatment of choice for patients with advanced knee osteoarthritis or severe joint destruction associated with functional disability and deformity.
Three principal types of knee prostheses exist:

- **Unicompartmental knee arthroplasties**, which replace only one of the three compartments of the knee (medial, lateral, or patellofemoral), thereby preserving the remaining articular structures.
- **Total knee arthroplasties**, which replace both femoral and tibial articular surfaces and, in most cases, resurface the patella.
- **Constrained or hinged prostheses**, which are reserved for cases of major instability, severe bone loss, or revision surgery, and are designed to provide additional stability when soft tissues are insufficient.

Unicompartmental knee arthroplasties are less invasive and preserve bone stock, cruciate ligaments, and much of the native joint kinematics. They are indicated in patients with isolated compartmental osteoarthritis, intact cruciate ligaments, and correctable deformities. Their advantages include faster recovery, lower perioperative morbidity, and more natural joint motion. However, they are associated with lower long-term survival rates compared to total prostheses, and the risk of disease progression in other compartments must be considered.
Total knee arthroplasties are the most widely performed procedures worldwide. They consist of a femoral component, a tibial tray with a polyethylene spacer, and often a patellar component. Based on cruciate ligament management, designs include cruciate-retaining, posterior-stabilized, anterior-stabilized, and bicruciate-retaining implants. The prosthesis may be fixed to the bone either with polymethylmethacrylate cement or through biological fixation with porous surfaces that allow osseointegration.
Constrained prostheses, including semi-constrained condylar implants and rotating hinge designs, are used in complex primary or revision cases. These implants provide stability when collateral or cruciate ligaments are deficient but limit physiological motion and are associated with higher complication rates.
All prostheses are manufactured from metallic alloys such as cobalt–chromium or titanium, combined with high-density polyethylene inserts, and in some cases ceramics. The fixation method can be cemented or cementless, and implant survival depends on proper alignment, soft tissue balancing, and accurate surgical technique.
The articulation in total and unicompartmental knee arthroplasties is ensured by the femoral component gliding against the polyethylene insert. Depending on design, the prosthetic coupling may reproduce femoral rollback and rotational stability through specific mechanisms such as the post-cam system in posterior-stabilized implants.
Knee replacement thus encompasses a wide range of surgical solutions, from bone-preserving unicompartmental implants to complex constrained systems. The choice of prosthesis is based on the extent of articular disease, ligament competence, bone quality, and patient-specific functional demands, always balancing joint stability, mobility, and implant longevity[198–200].

HISTORICAL BACKGROUND

Attempts to improve the function of the arthritic knee began in the nineteenth century. In 1860, Verneuil suggested interposing soft tissues between the femur and the tibia, while Ferguson later

proposed reshaping the articular surfaces to use subchondral bone as a new bearing surface. Both approaches provided unsatisfactory outcomes, leading to their abandonment. In 1940, Campbell and Smith-Petersen introduced the concept of inserting a metallic component in the knee, while McKeever and MacIntosh attempted tibial hemiarthroplasty, also with poor results. The historical evolution of implants followed two main paths: surface replacement prostheses and hinged constrained prostheses. Replacement preserved collateral ligaments, whereas constrained designs facilitated alignment through intramedullary stems. Walldius proposed the first hinged prosthesis in the 1950s, but the high rate of aseptic loosening limited its use.

The true breakthrough came in the 1970s with Gunston and Freeman. Gunston introduced the first metal–polyethylene coupled prosthesis, fixed with cement and preserving ligaments. Freeman had a major influence on both technique and design, and in 1973 he established fundamental principles for successful knee replacement, including minimizing loosening, infection, and debris production, ensuring reproducibility, guaranteeing a functional range of motion, and providing rotational stability with the contribution of soft tissues.

During the same decade, new models were introduced: the bicondylar prosthesis by Ranawat, the geometric design by Coventry, and the anatomic model by Townley. Among these, the Total Condylar Prosthesis (TCP) became the foundation of modern knee arthroplasty. It required sacrificing both cruciate ligaments, used a cobalt–chromium femoral component with a flat trochlear groove, a polyethylene tibial component with a central eminence for rotational stability, and included patellar resurfacing. Insall further refined the design by introducing the post-cam mechanism, which reproduced posterior cruciate ligament function by promoting femoral rollback beyond 70° of flexion. This innovation led to the development of posterior-stabilized prostheses, which remain among the most widely used designs in contemporary knee replacement[201].

TOTAL KNEE PROSTHESES

Nowadays, the orthopedic surgeon is essentially faced with the choice between two types of implants: primary prostheses, which involve covering the distal femur and proximal tibia with metal components while only partially altering the rest of the joint and its tissues, or constrained prostheses, which provide high stability to the replaced knee through a hinge mechanism, though depriving it of one or more of its physiologically permitted degrees of freedom. In cases of osteoarthritic knees with mild deformities and good collateral ligament function, it is preferable to choose primary implants, which ensure better long-term survival, improved functional outcomes, and a lower complication rate. In cases of severe joint instability, major bone loss, or severe articular deformity, it is preferable to opt for a constrained implant to ensure adequate knee function and stability.

Indications for Total Knee Arthroplasty and Clinical-Diagnostic Evaluations

Total knee arthroplasty (TKA) represents the gold standard treatment for advanced degenerative disease of the knee joint, particularly in cases of primary osteoarthritis, post-traumatic arthritis, and secondary arthritis due to inflammatory disorders such as rheumatoid arthritis or other autoimmune arthritides. Additional indications include advanced osteonecrosis of the femoral condyles and severe joint deformities associated with malalignment, instability, or loss of function. The primary goals of the procedure are the relief of pain, restoration of alignment, improvement of mobility, and enhancement of overall quality of life.

Surgical indication requires a comprehensive evaluation combining clinical, radiographic, and functional criteria. Patients typically present with persistent knee pain, stiffness, and reduced range of motion, which significantly impair daily activities and are refractory to conservative measures such as physiotherapy, pharmacologic management, or intra-articular injections. Radiographic findings frequently demonstrate advanced joint space narrowing, subchondral sclerosis, osteophyte formation,

and deformity in the coronal or sagittal plane. Functional assessment often reveals gait impairment, quadriceps weakness, and dynamic instability that further support the indication for surgery. Absolute contraindications include active local or systemic infection and severe systemic comorbidities that preclude safe anaesthesia or surgical intervention, such as advanced cardiovascular, respiratory, or renal failure. Relative contraindications may include severe neuromuscular disorders, significant vascular insufficiency, or poor soft tissue coverage, which increase the risk of complications and compromise implant longevity. Careful patient selection is therefore critical to optimize outcomes and ensure long-term prosthetic survival[190,191].

Primary knee replacement

In recent years, the debate surrounding the design of primary knee prostheses has focused mainly on how to reproduce the anatomy of the knee: in particular, whether it is better to use implants that are as similar as possible to the native joint (anatomic implants) or others that alter its normal anatomical characteristics while restoring function more effectively (functional implants). The central issue in this debate has primarily concerned the preservation of the posterior cruciate ligament (PCL). Indeed, while the anterior cruciate ligament is often absent in severe osteoarthritic knees, the PCL usually remains intact and continues to play a key role in the rollback of the femur on the tibia during flexion. In anatomic prostheses that preserve the PCL, the insert must be as flat as possible in order to allow this rollback. In functional prostheses, also called "PCL substituting" or "Posterior Stabilized (PS)," the PCL is sacrificed during the procedure, and to allow full flexion a generally concave insert is used, which between the condyles contains a mechanism called "post-cam." This mechanism has a dual role: recreating the femoro-tibial rollback and avoiding posterior impingement during deep flexion.

Although sacrificing an intact and functional ligament may seem aggressive from a surgical standpoint, preserving the PCL makes it more difficult to achieve correct soft-tissue balance; moreover, in the event of later rupture of the PCL, instability in flexion and paradoxical anterior translation of the tibia relative to the femur may occur, a problem only partially addressed with new-generation anterior-stabilized inserts (AS). In summary, based on whether the cruciate ligaments are preserved or not, four main types of primary knee prostheses exist, generally known by widely shared acronyms: CR (Cruciate Retaining), in which the ACL is sacrificed and the PCL preserved; PS (Posterior Stabilized), in which the ACL is sacrificed and the PCL replaced with posterior stabilization; AS (Anterior Stabilized), in which the ACL is sacrificed and the PCL replaced with anterior stabilization; and BCR (Bi-Cruciate Retaining), in which both cruciate ligaments are preserved.

Today, the most commonly used primary knee prostheses worldwide are PS designs. Their concept derives from the Total Condylar Prosthesis with an important modification: the introduction of the post-cam mechanism, which allows a greater range of motion by reproducing femoral rollback. Furthermore, with implant development, many different sizes of components have been introduced, enabling adaptation of the implant to the patient's bone dimensions. The discussion on the best prosthetic design, however, remains very lively, and the literature does not report significant differences between the various types of implants: the final choice therefore depends on the overall evaluation of the patient and the preferences of the individual surgeon.

Another highly debated issue concerns the morphology of the femoral component. Until a few years ago, all implants replicated the original anatomy of the distal femur, whose sagittal radius of curvature decreases in an anteroposterior direction, shifting the relative flexion-extension axis along a kind of spiral. To reproduce these characteristics, prosthetic implants initially adopted a configuration called "J-curve," with a decreasing anteroposterior radius of curvature, thereby facilitating rollback and the achievement of full flexion.

In recent years, these designs have been criticized. It has been hypothesized that a variable radius of curvature may determine, at increasing degrees of flexion, two negative effects: first, increased stress and polyethylene wear due to the progressive reduction of the contact area between femoral and tibial components; second, decreased tension of the collateral ligaments, possibly leading to instability at intermediate degrees of flexion. These observations led to the development of single-radius prostheses. The advantages of such implants include improved stability throughout the entire range of motion, reduced polyethylene wear, and an increased lever arm of the extensor apparatus, owing to the posterior shift of the flexion-extension axis of the tibiofemoral joint produced by a single radius of curvature. Although single-radius prostheses represent the latest evolution in knee arthroplasty, it is not clear whether they provide superior outcomes compared to traditional prostheses: once again, the individual case and the surgeon's experience are of crucial importance.
A further criticism raised against traditional primary prostheses is that they do not respect the physiological kinematics of the femoral condyles, namely the posterior translation of the lateral condyle during flexion and the opposite pivot-like behaviour of the medial compartment. Consequently, implants called "medial-pivot" have been developed, characterized by a relatively static medial condyle and a highly mobile lateral condyle in the absence of a cam-post system. The use of such implants remains limited, and their superior long-term performance has yet to be demonstrated.

The two main types of constrained knee prostheses are: semi-constrained prosthesis (Constrained or CCK – Condylar Constrained Knee), which is used in cases of significant instability of the collateral ligaments (particularly severe preoperative coronal deformity, prosthetic revision procedures). This prosthetic model is characterized by a polyethylene insert with a central indentation larger than normal, which therefore completely fills the notch of the femoral component. This feature makes it possible to ensure excellent stability in the coronal plane, thus replacing the function of the collateral ligaments. The semi-constrained prosthesis offers greater stability in the coronal plane, but not in the sagittal plane, and therefore correct prosthetic positioning is essential. Considering that the implantation technique of a semi-constrained prosthesis is often similar to that of a primary prosthesis, this implant can represent a good salvage solution in the case, for example, of iatrogenic injury to the collateral ligaments during surgery.
The second type is the constrained prosthesis (Hinged), which is used in cases of complete ligamentous instability, since in such circumstances a semi-constrained implant would be subject to excessive stress and early failure due to polyethylene wear. These are completely congruent prostheses characterized by a femoral pin that connects directly to the tibial plate, allowing only the hinge motion of flexion-extension. Almost all constrained prosthetic designs have a rotating polyethylene insert ("rotating hinge prosthesis"), which helps both to dissipate stress more effectively and to preserve at least a minimal rotational capacity. In the case of a constrained implant, if the collateral ligaments are intact, they must be cut to avoid overloads at the level of the prosthetic implant.
Whichever constrained implant is chosen, it is important to remember that these are associated with a higher number of complications compared to primary prostheses. In particular, the loss of articular soft tissues (which play an important role in absorbing the energy and load stresses transmitted through the knee) means that all forces and torsional moments act on the prosthetic implant and on the bone-prosthesis interface, increasing the risk of failure due to loosening. For this reason, when using constrained or semi-constrained prostheses, it is always preferable to use intramedullary prosthetic stems, which allow a better distribution of forces on the bone[198,199,202].

Surgical approaches
Several surgical approaches have been developed for total knee arthroplasty, each with specific advantages and limitations. The most widely employed include the medial parapatellar approach, the

subvastus approach, and the midvastus approach. More recently, minimally invasive variants of these accesses have been introduced with the aim of reducing surgical trauma, facilitating early recovery, and improving post-operative outcomes.
The medial parapatellar approach, first described by von Langenbeck and later standardized by Insall, is considered the standard access for TKA. The skin incision is usually midline, extending from the superior pole of the patella to the tibial tuberosity. The arthrotomy runs along the medial border of the patella and patellar tendon, allowing excellent visualization of the femoral condyles, tibial plateau, and patella. Its main advantages include broad exposure of the joint, versatility in both primary and revision cases, and relative technical simplicity. However, it requires partial sacrifice of the medial retinaculum and may alter patellar tracking if closure is not meticulous. The patella is usually everted laterally, but this maneuver may risk ischemic damage or fracture, particularly in stiff or small patellae.
The subvastus approach exploits the intermuscular interval beneath the vastus medialis, preserving the quadriceps tendon. The incision runs along the medial border of the patella and then curves distally, with the vastus medialis elevated and retracted laterally. This approach avoids transection of the quadriceps tendon, potentially reducing post-operative pain and facilitating faster recovery of extensor function. It also preserves patellar blood supply. Its limitations lie in the reduced surgical exposure, which can make it challenging in obese patients, in severe deformities, or in revision cases. Prolonged surgical time and increased difficulty in patellar eversion are also described.
The midvastus approach represents an intermediate technique between the medial parapatellar and subvastus approaches. It involves a limited split of the vastus medialis obliquus fibers while preserving most of the quadriceps tendon. This provides better exposure than the subvastus approach while reducing quadriceps disruption compared to the standard medial parapatellar access. Clinical studies report reduced pain and quicker quadriceps recovery, though technical demands are higher and exposure in complex cases may still be limited.
Minimally invasive techniques, developed as modifications of the approaches above, aim to reduce incision length, limit disruption of the extensor mechanism, and preserve soft tissues. They are associated with improved cosmetic results and potentially faster functional recovery. Nevertheless, they require specialized instruments, present a steep learning curve, and in some cases may compromise visualization, increasing the risk of component malposition.

Each surgical approach for TKA must be chosen according to patient-specific factors, including body habitus, degree of deformity, bone quality, and whether the procedure is primary or revision. While the medial parapatellar approach remains the gold standard for its versatility and exposure, subvastus, midvastus, and minimally invasive techniques may offer advantages in selected patients, provided that accurate component positioning and joint balancing can be ensured[203].

Postoperative Assessment of a Knee Prosthesis
Postoperative evaluation of a total knee arthroplasty (TKA) must be tailored to the characteristics of the implant and the individual patient. As best practice, an initial clinical and radiographic follow-up is recommended within 20–30 days after surgery, followed by reassessments at 3–6 months, at 12 months, and subsequently every two years. Vigilance should be particularly high during the first months to identify early complications such as infection, wound dehiscence, or early instability. Later assessments are directed toward monitoring osteointegration and fixation of the components, since early aseptic loosening typically occurs within the first two years after implantation. With time, the frequency of visits may be reduced, but regular clinical and radiographic monitoring should never be completely discontinued.
The postoperative follow-up includes a thorough clinical examination and standardized anteroposterior and lateral radiographs of the operated knee. Clinically, evaluation should document the presence of

new pain, swelling, erythema, or instability, as well as range of motion, patellar tracking, and functional capacity during ambulation. Particular attention should be given to extension lag, flexion contracture, quadriceps strength, and gait abnormalities such as limping or dynamic valgus-varus instability. The examination of the surgical wound and surrounding soft tissues is also crucial to exclude local complications.
Radiographic assessment provides critical information, as several complications may initially present with radiological changes before becoming clinically evident. Postoperative images must be compared with immediate postoperative radiographs and all subsequent controls. On standard radiographs, the position and alignment of femoral and tibial components should be verified, together with the joint line restoration and limb axis correction. Any progressive shift of components greater than 2 mm or changes in their angulation are suggestive of prosthetic loosening. Radiolucent lines at the bone–cement or bone–implant interface, periosteal reactions, or focal osteolysis are early warning signs of failure.
On the tibial side, loosening is indicated by progressive subsidence, tilting of the baseplate, or widening of radiolucent lines beneath the component. On the femoral side, attention should be directed to component migration, angular changes in the sagittal plane, or radiolucent lines surrounding the condylar fixation. Cemented components should be evaluated for homogeneity of the cement mantle, while cementless implants should demonstrate progressive trabecular integration without stress shielding or bone resorption.
The patellofemoral joint requires specific attention. Maltracking, tilt, or subluxation of the patella may be associated with pain and functional impairment. Polyethylene wear is another critical aspect, usually presenting radiographically as asymmetric joint space narrowing, eccentric positioning of the patella, or periprosthetic osteolysis. In modular implants, polyethylene insert wear, or dissociation should always be considered in cases of recurrent effusion, instability, or unexpected radiographic changes.

Radiographic anomalies must always be interpreted in the clinical context, correlated with the patient's symptoms and functional status, and compared with previous imaging. When necessary, second level imaging such as CT, MRI with metal artifact reduction, or nuclear medicine studies may be employed to differentiate between septic and aseptic loosening, clarify periprosthetic osteolysis, or detect occult fractures[198,199,204,205].

COMPLICATIONS

Knee replacement is now a very common procedure characterized by a very high safety profile and excellent results; however, there is a moderately high rate of perioperative complications, both systemic and local. Complications can be classified according to site, etiology, and timing of onset.

Systemic complications

Thromboembolism: The main systemic perioperative complication of knee replacement is deep vein thrombosis which, in the absence of adequate antithromboembolic prophylaxis, affects about 50% of patients. The most frequent site of thrombosis is the veins distal to the knee, particularly the popliteal vein, while the involvement of proximal veins is less common but may extend to the iliac-femoral axis requiring surgical recanalization. Deep vein thrombosis may rarely cause massive pulmonary embolism; although the mortality risk is extremely low (<0.3%), patients should undergo antithromboembolic prophylaxis with low molecular weight heparin until recovery of normal ambulation. To reduce the risk of thromboembolism, it is necessary to accelerate the rehabilitation process by making the patient bear weight, even partially with protected load, and mobilize the operated limb on the first postoperative day. Another possible embolic complication during knee replacement is microembolism secondary to the use of bone cement to fix the implant, particularly

when stems are cemented into the tibial and femoral canals. These pulmonary microemboli can be the cause of patient death (cement embolism). During surgery it is necessary to alert the anesthetic team of the beginning of the cementation procedure. In addition, whenever possible, uncemented implants can be used.
Postoperative anemia: Patients undergoing knee replacement surgery may develop anemia. Modern surgical, anesthesiological, and pharmacological techniques have reduced the need for transfusions, which are still common after surgery. Postoperative anemia must be carefully monitored especially in cardiac patients, due to the secondary risk of ischemia, and in those undergoing anticoagulant therapies that require high-dose heparin prophylaxis, in whom anemia may occur even days after surgery. The wide joint cavity of the knee also carries an increased risk that bleeding from even small vessels may produce a large hemarthrosis requiring either reoperation for evacuation or embolization of the vessels. This treatment must be timely to avoid dangerous anemia for the patient or the formation of postoperative arthrofibrosis. To reduce risk, it is advisable in the immediate postoperative period to keep the knee flexed at 30 degrees for at least 6 hours, to use compressive dressings in the first hours after surgery, and to maintain the knee in hypothermia.[199,205]

Local complications
Vascular injuries: Rarely, during surgery, a vascular injury may occur requiring vessel repair, femoropopliteal bypass, or prosthetic replacement, most often involving the popliteal vessels and rarely the femoral ones. This vascular injury, even if treated promptly, can be the primary cause of compartment syndrome requiring fasciotomy in the days following surgery, and very rarely amputation of the limb has been reported.
Wound healing complications: The knee presents a thin envelope of soft tissues which must be intact and adequately vascularized to withstand the high stress caused by the wide range of motion. For this reason, the surgeon must pay particular attention during dissection and wound closure, as the anterior wound of the knee is mechanically stressed by flexion from the very first postoperative hours. Careful wound dressing is essential after surgery. When the wound shows mild suffering, specific dressings should be used, and flexion-extension exercises should be limited to avoid additional stress. In cases of delayed wound healing, debridement and possible replacement of the polyethylene insert may be indicated to prevent the occurrence of late periprosthetic infections. Cases of skin necrosis are very rare but represent an extremely serious complication requiring aggressive treatment, usually carried out by plastic surgeons.
Periprosthetic fractures, intraoperative and late ligament injuries: Other local complications are represented by periprosthetic fractures and patellar fractures. These fractures can occur at very different times. Intra- or perioperative fractures are often secondary to poor bone quality, such as severe osteoporosis, or surgical technique errors, such as incorrect positioning of prosthetic components. Conversely, late periprosthetic fractures are often secondary to traumatic events. Both must be treated surgically with stable fixation; in the case of late fractures, the stability of the implant must be assessed and replaced if necessary. The same approach must be adopted for collateral ligament injuries, particularly the medial collateral ligament, which is the one most frequently injured intra- and postoperatively. The resulting knee instability requires ligament reconstruction and, when this is insufficient, replacement of the prosthesis with implants intrinsically stabilized against varus-valgus stress.
Nerve complications: The nerve most frequently involved in complications is the peroneal nerve, a branch of the sciatic nerve that runs posteriorly along the thigh and curves around the fibular head, passing between the soleus and peroneus longus muscles. At the fibular neck, below the peroneus longus, it divides into a superficial and a deep branch. The deep branch continues beneath the extensor digitorum longus and sends motor fibers to the tibialis anterior, the extensor digitorum longus, the

extensor hallucis longus, and the peroneus tertius, ending distally with sensory innervation of the first interdigital space on the dorsum of the foot. The superficial branch innervates the peroneus longus and brevis muscles, giving rise distally to the medial and intermediate dorsal cutaneous nerves, which provide most of the sensory innervation of the dorsal foot, complemented laterally by the lateral dorsal cutaneous nerve, terminal branch of the sural nerve. During total knee replacement, the surgical step in which the peroneal nerve is at risk of injury is the release of the posterolateral capsule, as it lies between the popliteus tendon, the posterior fibers of the iliotibial band, and the tibial cut surface. Peroneal nerve palsy is rare, about 0.4%, but more frequent in cases of severe valgus deformities or revisions and is a concerning postoperative complication. Clinically it manifests with dysfunction of the muscles of the anterolateral compartment of the leg with foot drop and anesthesia of the dorsum of the foot. Treatment involves the use of orthoses to manage the foot drop and intensive physiotherapy of the ankle joint to avoid equinus deformity. Only rarely is complete recovery of motor and sensory function achieved. Some authors suggest a surgical decompression. Another possible nerve lesion in patients undergoing knee replacement is section of the infrapatellar branch of the saphenous nerve, which can result in hypoesthesia in its sensory distribution area. This complication, related to the surgical approach, is quite common but normally does not require treatment. Nonetheless, it is appropriate to mention it during the informed consent process.

Mechanical complications: The most frequent mechanical complications are instability, limited range of motion, loosening, and wear. Instability is a common cause of mechanical failure of knee prostheses, accounting for 10 to 20% of revision indications. It may occur in the coronal, sagittal, or both planes. Early instability may be due to malalignment of components, incorrect balancing of flexion and extension spaces, or intraoperative ligament injury. Late instability is generally due to wear of polyethylene components. Limited range of motion occurs in about 6% of cases. The most frequent cause is arthrofibrosis, that is, the presence of adhesions that prevent achieving a satisfactory ROM. This generally occurs in patients who already had a limited ROM preoperatively, in post-traumatic arthritis, or after septic arthritis. A stiff knee does not respond to physiotherapy. Possible solutions include arthroscopic or open lysis of adhesions, but in case of failure revision surgery may be required. Aseptic loosening of knee implants is a frequent complication with multifactorial origin, including malalignment, high BMI, incorrect sizing of components, polyethylene wear, and inadequate cementation. In case of loosening, infection must always be excluded. If infection is excluded, the patient is asymptomatic, and the knee is stable, close follow-up is sufficient. When the implant is unstable or painful, revision surgery is required. Wear may involve the polyethylene insert or the patellar component and is usually related to incorrect load distribution, such as malalignment or incorrect sizing of components. It causes inflammation, pain, osteolysis, and instability. The appropriate treatment must be evaluated on a case-by-case basis and may range from simple insert replacement to revision of the entire implant.

Patellar complications: The most common patellar complications are subluxation or dislocation and impingement (patellar clunk syndrome). Subluxation or dislocation is generally due to errors in femoral component rotation, with internal rotation increasing lateral soft tissue tension and patellar instability. Similarly, excessive external rotation of the tibial component increases the Q angle and contributes to patellar instability. Regarding impingement, cases have been described of fibrous nodule formation in the suprapatellar region, creating a mechanical obstacle to proper patellar tracking, known as patellar clunk syndrome.

Painful prosthesis: A certain percentage of patients undergoing total or partial knee replacement, about 1 in 300, continue to complain of pain without clinical or radiographic explanation, as the prosthesis appears well positioned and provides an excellent range of motion. Over the years, various hypotheses have been advanced as to the cause of such pain, including more severe preoperative clinical and radiographic presentation, latent infection, mild material allergy, reflex sympathetic dystrophy

characterized by burning pain, swelling, redness, and local hyperhidrosis. Management of these patients always begins with exclusion of infection, usually by joint aspiration with synovial fluid culture or by scintigraphy. If infection is found, it must be treated; if excluded, new radiographs or CT scans should be performed to search for signs of aseptic loosening, malalignment, particularly of the patella, and to exclude rare prosthetic complications. Extra-articular sources of pain, particularly hip or spine, and very rare periprosthetic tumors must also be considered in the differential diagnosis. It is important never to proceed with revision surgery without a correct diagnosis, as the outcome has been shown to remain unchanged or worsen compared to the preoperative condition. Exploratory arthroscopy may be performed to exclude interposition of soft tissues, such as a meniscal fragment[198,204–206].

Septic revision

Periprosthetic infections of the knee are a severe complication, extremely complex to manage both for their severity, sometimes systemic, and for the great effort required from the patient. Their treatment always involves a multidisciplinary approach. The incidence of periprosthetic knee infections ranges between 1 and 3%, with predisposing factors such as skin ulcers, diabetes, rheumatoid arthritis, obesity, malignant tumors in history, smoking, and HIV. Therefore, it is necessary to prevent infection by ensuring that the patient reaches surgery in the best possible systemic condition, with chronic diseases under strict control. Other preventive strategies include preoperative antibiotic prophylaxis, abundant intraoperative pulsatile lavage, and careful wound closure. For the diagnosis of periprosthetic infection, standardized criteria have been established by the Musculoskeletal Infection Society[207]. Major criteria include a sinus tract communicating with the prosthetic joint or the isolation of a pathogen from at least two separate tissue or fluid samples. Minor criteria include elevated ESR and CRP, high synovial leukocyte count, high percentage of synovial polymorphonuclear cells, presence of intra-articular pus, growth of a microorganism in a single synovial or tissue culture, and more than five neutrophils per high-power field in histological examination of periprosthetic tissue. A patient is considered infected if one of the two major criteria or four of the six minor criteria are present. In approaching periprosthetic infections, it is necessary to clarify whether the infection is superficial or deep, the time elapsed since surgery, patient risk factors such as immunodeficiency, involvement of periarticular tissues, integrity of the extensor mechanism, implant stability, and the causative microorganism. The main treatment goal is to eradicate infection, relieve pain, and preserve limb function as much as possible. The available options are antibiotic therapy, arthrotomy with debridement and insert exchange, two-stage reimplantation with an antibiotic-loaded cement spacer followed later by revision prosthesis, arthrodesis, resection prosthesis, and amputation. These options can be applied singly, in combination, or sequentially in case of failure. Management is challenging because the surgeon must choose carefully which option to employ and when. In particular, if infection is diagnosed within the first postoperative month, targeted antibiotic therapy against the responsible microorganism, always identified by culture, can be attempted along with surgical debridement, maintaining the implant and changing only the polyethylene insert. In chronic infection, beyond one month after surgery, the standard treatment is removal of the prosthesis, implantation of an antibiotic-loaded cement spacer, and later reimplantation once infection has been eradicated. In selected cases with low-virulence germs and few comorbidities, single-stage revision may be performed after extensive debridement. If infection recurs, further explantation and salvage strategies such as arthrodesis or resection arthroplasty may be required. In case of further failure, the only way to avoid systemic spread of infection is limb amputation at the thigh level[208,209].

Aseptic revision

Despite the increasing survival of knee prostheses, now exceeding 90% at 10 years, there are cases of failure requiring revision. The most frequent causes of aseptic revision are loosening, instability, wear, and periprosthetic fractures[210]. The first step is to identify the cause of failure with certainty. Careful preoperative planning is essential, considering that removal of a primary prosthesis inevitably results in bone loss and instability, obliging the surgeon to use implants with a higher degree of constraint. The goal of aseptic revision is the same as primary implantation, to achieve a stable, well-aligned limb with a painless knee providing a good range of motion. Before scheduling aseptic revision, infection must be excluded with certainty, by laboratory tests and possibly nuclear medicine imaging. The surgical approach generally uses the previous incision, possibly extended proximally to facilitate joint exposure and patellar eversion, followed by careful debridement and removal of components with bone preservation. Once components are removed, the principle remains, as in primary replacement, to balance flexion and extension spaces equally. In cases of severe bone loss, this may be difficult and sometimes bone grafts or augmented components such as wedges or cones are required[210,211].

Technological innovations: navigation and robotics

Nowadays there is increasing evidence that performing knee replacement surgery, whether total or unicompartmental, with the aid of newly available technologies, particularly navigation and robotic surgery, leads to better alignment of prosthetic components. On the other hand, it is still uncertain whether their use provides an advantage in terms of long-term prosthesis survival and improves patient satisfaction.

Navigation

Surgical navigation systems can be divided into three groups based on the method used to acquire anatomical references. There are systems that rely on CT imaging, systems that use fluoroscopy, and so-called “image-free” systems. The latter build a statistical model of the bony structures of the femur and tibia based on the calibration of certain anatomical landmarks. Image-free systems are currently the most widely used because they eliminate the additional costs and time associated with radiographic imaging. They require a series of anatomical calibrations, carried out sequentially in a predetermined order. These calibrations aim to provide the navigation system with an anatomical survey of the specific knee being examined and, from this information, to construct anatomical reference frames. Once the anatomical survey is completed, the system provides the surgeon with an interface reproducing the pre-implant geometric configuration. It is also possible to assess ligament behavior, particularly the medial and lateral collateral ligaments, by obtaining varus-valgus laxity values for different degrees of imposed knee flexion. At this point the system offers a real-time display of the sagittal and frontal views of the bone segment on which resections will be performed, along with the cutting lines estimated by the system to achieve optimal correction of knee deformities. Once the bone resections are carried out, the system requires the registration of joint kinematics before definitive implantation, using trial prosthetic components. In this phase the correct sizes of the prosthetic components and the appropriate spacing required for the polyethylene tibial insert are determined. After establishing the component sizes and verifying that all kinematic variables are physiologically correct through the acquisition of joint kinematics, the definitive components are anchored. Once implantation is completed and the joint capsule sutured, a final assessment of joint kinematics is performed[199].

Robotic surgery

Robotic systems used in surgery can be classified into four main categories: passive systems, active systems, semi-active systems, and teleoperated systems. In orthopedic prosthetic surgery most, robotic systems fall into the semi-active category, where interaction between the robot’s actions and those of

the operating surgeon is required. Robotic surgery has been shown to achieve better accuracy than traditional techniques in performing bone cuts and thus in the positioning of components in the three planes of space, but a clinical advantage for patients or a greater accuracy compared to navigation has not yet been demonstrated. Robotic surgery is characterized by the possibility of real-time assessment of prosthetic alignment through dedicated detectors, like those used in computer-assisted navigation procedures. This allows fine adjustment of bone cuts, ligament balancing, and implant positioning to achieve the planned knee kinematics.

However, knee replacement surgery performed with robotic techniques is characterized by specific disadvantages that limit its widespread use. Some robotic systems require preoperative imaging studies such as CT scans, which expose the patient to additional ionizing radiation and represent an additional cost for the healthcare system. Moreover, robotic systems are associated with high acquisition and maintenance costs for hospitals, which often cannot justify the expense of implementing robotic technology in the operating room. Finally, robotic surgery requires longer surgical times than traditional surgery, with higher operating room management costs.

In conclusion, robotic surgery represents an evolution of navigation systems that should enable greater accuracy in the positioning of prosthetic components. Nevertheless, the high cost of robotic systems limits their large-scale application, as many non-tertiary hospitals cannot justify the acquisition costs in the absence of an adequate patient volume[212].

PRINCIPLES AND TECHNIQUES OF ALIGNMENT IN TOTAL KNEE ARTHROPLASTY

The fundamental objectives of total knee arthroplasty (TKA) are the relief of pain, restoration of function, and improvement of joint stability and mobility. Achieving these outcomes requires precise control of two essential elements: soft tissue balance and spatial alignment of the prosthetic components. The long history of knee arthroplasty demonstrates how these principles have evolved from early systematic philosophies, based on average anatomical models, to the more recent personalized approaches that aim to replicate each patient's unique knee morphology and kinematics. Historically, the earliest techniques of TKA emerged in the 1970s, when the "normal" target knee was defined as one with a neutral femorotibial mechanical axis of 180° and a joint line tilted approximately 3° in varus. This assumption gave rise to the two earliest alignment philosophies: anatomical alignment and mechanical alignment. These methods, often referred to as "systematic," were highly reproducible but failed to consider the wide interindividual variability in pre-arthritic knee anatomy and biomechanics. Over time, as prosthetic designs improved and surgical instruments became more sophisticated, two distinct technical approaches were developed: the measured resection technique and the gap balancing technique. Although conceptually different, modern instrumentation has incorporated elements of both, often blurring the boundaries between them.

The measured resection technique aims to reproduce bone resections that exactly match the thickness of the prosthetic components, using anatomical landmarks to determine femoral rotation. Initially conceived for posterior cruciate ligament (PCL)–retaining prostheses, this technique has since been adapted to a wide range of implant designs. The guiding principle is that bone resections should replicate the native joint anatomy, with minimal reliance on intraoperative soft tissue releases. Among the alignment philosophies derived from this approach are anatomical alignment and kinematic alignment.

The gap balancing technique, in contrast, focuses on achieving symmetric and rectangular flexion and extension gaps, with equal tension in medial and lateral compartments. The femoral component's rotation is established by the symmetry of the flexion space, and bone cuts are adapted to the balanced state of the surrounding ligaments. Originally developed for PCL-sacrificing implants, the method is now widely applied across prosthetic designs. Mechanical alignment and functional alignment derive their principles from the gap balancing school, emphasizing soft tissue equilibrium as the primary determinant of component placement.

Anatomical alignment was the first systematic alignment strategy described. Its goal was to reproduce the average anatomical configuration of the population, with tibial resection performed at 2°–3° of varus and distal femoral resection at 2°–3° of valgus, creating a neutral mechanical axis of 180° and femoral rotation parallel to the posterior condylar line. However, despite its logical intent, this strategy yielded poor long-term results, with a high incidence of aseptic loosening and premature polyethylene wear. These failures were largely attributed to abnormal load distribution across the prosthesis and bone–implant interface, ultimately limiting the historical adoption of this method.

Mechanical alignment (MA) has been, for decades, the most widely adopted and studied alignment philosophy. It is based on systematic principles and aims to align the femoral and tibial components perpendicular to their respective mechanical axes, thereby creating a neutral 180° femorotibial mechanical axis. The femoral component is externally rotated by about 3° relative to the posterior condylar line, and the tibial cut is performed perpendicular to the tibial mechanical axis. This approach equalizes the flexion and extension gaps by releasing soft tissues, ensuring symmetrical rectangular spaces. Its main strength lies in its reproducibility and in the excellent long-term implant survival reported in registry studies. However, MA does not respect the interindividual anatomical variability of

the native knee and often fails to reproduce physiological joint line orientation. Clinically, this can result in mid-flexion instability, non-anatomical joint line elevation, patellofemoral maltracking, and functional outcomes that, despite durable implants, leave many patients dissatisfied. These limitations highlight the trade-off between long-term implant survival and patient-perceived functional performance.

In response to these limitations, and in line with rising patient expectations for higher functional performance after arthroplasty, more personalized alignment philosophies have been developed. These include kinematic alignment (KA) and functional alignment (FA), both of which are designed to respect individual variations in anatomy and kinematics rather than impose a universal "neutral" alignment.

Kinematic alignment (KA), rooted in the measured resection theory, seeks to restore the pre-arthritic native alignment of the knee by aligning prosthetic components according to the three fundamental axes that govern natural knee kinematics: the flexion–extension axis of the femur through the condylar centers, the longitudinal tibial axis, and the patellofemoral axis. In KA, distal and posterior femoral resections are made parallel to the native joint surfaces, with thicknesses exactly matching the prosthetic components. Tibial cuts are performed parallel to the pre-arthritic slope and inclination, with minor adjustments (±2°) if necessary for ligament balance. Importantly, no ligament releases are performed, and the native joint line obliquity is preserved. The philosophy is strictly bone-based, aiming to replicate the kinematic envelope of the healthy knee. However, unrestricted KA has raised concerns about restoring severe deformities without correction, which could compromise implant loading or longevity. To address this, derivative techniques have been proposed: restricted kinematic alignment (rKA), which maintains restoration of the joint line within ±3° of neutral safety margins, and inverse kinematic alignment (iKA), which reverses the order of cuts, beginning with the tibia before adjusting the femur.

Functional alignment (FA), instead, merges gap balancing principles with the personalization of KA. In FA, bone resections are "guided" by the patient's soft tissues, often with the aid of navigation or robotic technologies. The tibial cut is performed first and may deviate up to 3° from mechanical neutrality, depending on the symmetry of the extension gap. The distal and posterior femoral resections are then adjusted intraoperatively to balance flexion and extension spaces, preserving the native joint line height and obliquity. Soft tissue releases are minimized or avoided altogether. FA is thus defined as a hybrid strategy: systematic enough to ensure reproducibility, yet adaptive enough to respect patient-specific anatomy. Early clinical results suggest that FA may improve functional outcomes and patient satisfaction compared to MA, though long-term survival data are still limited.

The debate on alignment philosophies remains open. Mechanical alignment continues to represent the gold standard for reproducibility and longevity, particularly in cases of severe deformity or ligament insufficiency, whereas kinematic and functional alignment philosophies are increasingly adopted for their potential to enhance patient function and satisfaction. Current evidence suggests that no single strategy is universally superior, and the surgeon's experience, implant design, and technological adjuncts such as navigation, robotics, and patient-specific instrumentation play decisive roles.

The progressive shift from systematic to personalized alignment mirrors broader trends in orthopaedic surgery, where precision medicine seeks to tailor interventions to individual anatomical and functional characteristics. In TKA, this evolution has profound biomechanical implications: the choice of alignment philosophy not only affects joint line restoration and ligament balance but also propagates distally through the kinetic chain, influencing ankle, hindfoot, and even spinal alignment. For this reason, understanding the principles and techniques of alignment in TKA is not only crucial for optimizing implant survival and function but also for addressing the integrated biomechanics of the lower limb[9,10].

ANATOMY AND BIOMECHANICS OF THE ANKLE AND FOOT

The foot–ankle complex is the terminal segment of the lower-limb kinetic chain. It must reconcile two opposing functions: in quiet stance it distributes body weight over a broad plantar surface to ensure stability; during locomotion it becomes a deformable yet forceful lever that stores and releases elastic energy to generate propulsion. This versatility is achieved through the coordinated design of bones, joints, ligaments, retinacula, fasciae, muscles, vessels and nerves arranged in three functional regions—hindfoot, midfoot and forefoot—that act in series and in parallel.

OSSEOUS ANATOMY

The distal tibia widens to form the plafond, a rectangular articular surface concave anteroposteriorly and subtly convex mediolaterally. Medially it descends as the medial malleolus, whose anterior and posterior colliculi give attachment to components of the deltoid ligament. Laterally, the fibular notch houses the distal fibula and is bound by the syndesmosis. The fibula ends distally as the lateral malleolus, projecting farther caudally than the medial malleolus and forming the lateral buttress of the ankle mortise. Its medial facet articulates with the talus; its posterior groove guides the peroneal tendons.

The talus, interposed between leg and foot, consists of body, neck and head. The trochlear dome of the body articulates with the tibial plafond; it is wider anteriorly than posteriorly, a feature that locks the mortise in dorsiflexion. Medial and lateral facets articulate with the malleoli; inferiorly three facets (posterior, middle, anterior) articulate with the calcaneus to form the subtalar joint. The head, covered by thick hyaline cartilage, articulates with the navicular and, plantar-medially, with the spring ligament. Vascular channels enter mainly through the neck and tarsal canal; the extensive articular coverage explains the talus' susceptibility to avascular necrosis after fractures.

The calcaneus is the largest tarsal bone and the primary posterior weight-bearing structure. Superiorly it presents the posterior, middle and anterior talar facets separated by the calcaneal sulcus (completing the tarsal canal with the talar sulcus). The sustentaculum tali projects medially, supporting the talar head–neck complex and giving passage to the flexor hallucis longus. Plantarly, the calcaneal tuberosity divides into medial and lateral processes that receive the plantar fascia and intrinsic muscles; posteriorly the Achilles tendon inserts on the posterior tubercle.

The navicular forms the keystone of the medial column. Proximally it receives the talar head; distally it articulates with the three cuneiforms. Its plantar–medial tuberosity is the insertion of the tibialis posterior and a landmark in pes planus deformity. The cuboid constitutes the lateral column keystone; proximally it articulates with the calcaneus (calcaneocuboid joint), distally with the fourth and fifth metatarsals, and medially with the lateral cuneiform. A plantar groove houses the peroneus longus tendon, supported by the long plantar ligament.

The three cuneiforms (medial, intermediate, lateral) bridge the navicular to the first three metatarsals, stabilizing the transverse arch. The five metatarsals form the rays of the forefoot; the first is robust and bears medial and lateral sesamoids in the plantar plate beneath its head. Each lesser metatarsal articulates distally with a proximal phalanx at the metatarsophalangeal (MTP) joint and proximally with the tarsus at the tarsometatarsal (TMT, Lisfranc) joint. The phalanges are arranged in two (hallux) or three (lesser toes) segments, ending distally in flattened tufts for nail support[213–220].

Joints and ligaments

The tibiotalar joint is a mortise-and-tenon hinge that primarily allows dorsiflexion and plantarflexion about an oblique axis. Stability derives from bony congruity in dorsiflexion, the syndesmosis, and strong collateral ligaments. The distal tibiofibular syndesmosis comprises the anterior-inferior

tibiofibular ligament, interosseous ligament, posterior-inferior tibiofibular ligament and the transverse tibiofibular ligament; together they preserve mortise width during motion and load.
Medially, the deltoid (medial collateral) ligament fans from the medial malleolus to the talus, sustentaculum tali, navicular and spring ligament; its deep tibiotalar fibers resist valgus and external-rotation stresses. Laterally, the anterior talofibular ligament (from lateral malleolus to talar neck) restrains inversion in plantarflexion; the calcaneofibular ligament (to calcaneal lateral wall) resists inversion in neutral; and the posterior talofibular ligament stabilizes the talus in dorsiflexion and external rotation.
The subtalar joint consists of posterior, middle and anterior talocalcaneal articulations linked by the interosseous talocalcaneal ligament within the tarsal canal and sinus. It permits triplanar pronation–supination that couples with midtarsal mechanics to unlock or lock the foot.
The Chopart (midtarsal) complex includes the talonavicular and calcaneocuboid joints. The spring ligament complex (superomedial, medioplantar oblique and inferoplantar calcaneonavicular bands) forms a fibrocartilaginous sling under the talar head, essential to the medial arch. Laterally, the bifurcate ligament (calcaneonavicular and calcaneocuboid limbs) and the long and short plantar ligaments stabilize the calcaneocuboid joint and provide a pulley for the peroneus longus.
The Lisfranc (TMT) complex comprises the articulations between cuneiforms/cuboid and metatarsal bases. The strongest stabilizer is the interosseous Lisfranc ligament from the medial cuneiform to the base of the second metatarsal; dorsal and plantar ligaments complete the complex. Disturbance of this "keystone" destabilizes the medial longitudinal and transverse arches.
Metatarsophalangeal and interphalangeal joints have strong collateral ligaments and plantar plates. Beneath the first MTP joint, the medial and lateral sesamoids within the plantar plate act as a fulcrum for the flexor hallucis brevis and glide within cristae of the first metatarsal head.
The plantar fascia (aponeurosis) originates from the medial calcaneal process and expands to the toes, functioning as a windlass: dorsiflexion of the MTP joints shortens the fascia, elevates the arch and stiffens the foot at push-off. Retinacula—superior and inferior extensor, flexor (tarsal tunnel), and superior and inferior peroneal retinacula—prevent tendon bowstringing at the ankle[221–229].

MUSCLES OF THE ANKLE AND FOOT

Extrinsic compartments

The anterior compartment produces dorsiflexion and toe extension. Tibialis anterior arises from the lateral tibia and interosseous membrane; its tendon crosses medially to insert on the medial cuneiform and base of the first metatarsal, inverting the foot and supporting the medial arch. Extensor hallucis longus arises from the middle fibula and interosseous membrane, inserting on the dorsal distal phalanx of the hallux; it extends the great toe and assists dorsiflexion. Extensor digitorum longus originates from the lateral tibial condyle and fibula, dividing into four slips to the dorsal aponeuroses of toes II–V; it extends the toes and dorsiflexes the ankle. Peroneus tertius (often continuous with EDL) inserts on the base of the fifth metatarsal dorsum and contributes to dorsiflexion and eversion. All are innervated by the deep fibular (peroneal) nerve and are supplied by the anterior tibial artery.
The lateral compartment everts the foot and stabilizes the lateral column. Peroneus longus arises from the fibular head and shaft, passes behind the lateral malleolus and under the cuboid to insert on the base of the first metatarsal and medial cuneiform; by depressing the first ray it stabilizes the transverse arch and couples with tibialis posterior to support the medial arch. Peroneus brevis originates distal to the longus on the fibula and inserts on the base of the fifth metatarsal; it is a primary dynamic restraint against inversion sprain. Both are innervated by the superficial fibular nerve and receive blood from branches of the fibular and anterior tibial arteries.

The superficial posterior compartment generates plantarflexion and propulsive power. Gastrocnemius has medial and lateral heads from the posterior femoral condyles; together with the soleus (originating from the posterior tibia and fibula, including the soleal line) they form the Achilles tendon inserting on the calcaneal tuberosity. The complex acts as a powerful plantarflexor and contributes to knee flexion (gastrocnemius). Plantaris, when present, originates from the lateral supracondylar ridge and inserts variably on the calcaneus; it has minor mechanical action and a likely proprioceptive role. Innervation is via the tibial nerve; arterial supply derives from popliteal and posterior tibial branches.
The deep posterior compartment supports the medial arch and controls pronation. Tibialis posterior arises broadly from tibia, fibula and interosseous membrane; its tendon passes behind the medial malleolus to insert mainly on the navicular tuberosity with slips to cuneiforms and metatarsals, acting as a principal dynamic stabilizer of the medial longitudinal arch. Flexor digitorum longus originates from the posterior tibia and inserts on distal phalanges of toes II–V, flexing the toes and assisting plantarflexion. Flexor hallucis longus arises from the posterior fibula, courses through the sustentacular groove, and inserts on the distal phalanx of the hallux, providing powerful push-off. These muscles are innervated by the tibial nerve and supplied by the posterior tibial and fibular arteries[230–233].

Intrinsic compartments
Dorsal intrinsic muscles include the extensor digitorum brevis and extensor hallucis brevis, originating from the dorsolateral calcaneus and inserting on the extensor expansions of toes II–IV and the proximal phalanx of the hallux, respectively; both are innervated by the deep fibular nerve.
Plantar intrinsic muscles are arranged in four layers. The first layer includes abductor hallucis (from the medial calcaneal process to the medial base of the hallux proximal phalanx), flexor digitorum brevis (from the calcaneal tuberosity to the middle phalanges of toes II–V), and abductor digiti minimi (to the lateral base of the fifth proximal phalanx). The second layer contains the quadratus plantae (from calcaneus to the tendinous slip of FDL, redirecting its pull) and four lumbricals (from FDL tendons to the medial extensor expansions of toes II–V), flexing MTP and extending IP joints. The third layer comprises flexor hallucis brevis (two heads inserting via sesamoids on the base of the hallux proximal phalanx), adductor hallucis (oblique and transverse heads inserting on the lateral sesamoid), and flexor digiti minimi brevis. The fourth layer includes plantar and dorsal interossei that adduct and abduct the toes relative to the second ray and help maintain forefoot stability. Innervation is via the medial and lateral plantar nerves (terminal branches of the tibial nerve); a first branch of the lateral plantar nerve (inferior calcaneal nerve, Baxter) commonly innervates the abductor digiti minimi. Vascular supply derives from the medial and lateral plantar arteries forming the deep plantar arch with the dorsalis pedis[234–236].

BLOOD SUPPLY TO THE ANKLE AND FOOT
Blood supply to the ankle and foot include three main arteries: the popliteal artery, the anterior tibial artery and the fibular artery.
Proximally, the popliteal artery bifurcates into anterior and posterior tibial arteries; the posterior tibial gives off the fibular artery. Around the ankle, anterior and posterior malleolar networks anastomose with fibular branches. The anterior tibial artery traverses the interosseous membrane to become the dorsalis pedis at the ankle, coursing over the dorsum to give tarsal and arcuate branches and, via the deep plantar artery, to contribute to the plantar arch. The posterior tibial artery travels through the tarsal tunnel, dividing into medial and lateral plantar arteries; the latter forms the plantar arch with the deep plantar artery and gives plantar metatarsal and digital branches. The fibular artery supplies the posterolateral compartment and sends perforators to the lateral calcaneus and ankle, including calcaneal branches. Venous drainage parallels the arteries and communicates with the superficial system (great and small saphenous veins)[237–241].

NEUROANATOMY OF THE ANKLE AND FOOT

The neuroanatomy of the ankle and foot include two main nerves: The tibial nerve and the common fibular nerve.

The tibial nerve passes through the popliteal fossa and tarsal tunnel accompanied by the posterior tibial vessels. Within or distal to the tunnel it divides into medial and lateral plantar nerves. The medial plantar nerve supplies abductor hallucis, flexor hallucis brevis (medial head), flexor digitorum brevis, and the first lumbrical, and provides cutaneous sensation to the medial sole and plantar aspects of the medial three-and-a-half toes. The lateral plantar nerve innervates the remaining intrinsic plantar muscles—including interossei, adductor hallucis, quadratus plantae, and flexor digiti minimi—and supplies the lateral sole and the lateral one-and-a-half toes; its first branch (inferior calcaneal/Baxter nerve) is clinically relevant in plantar heel pain. Calcaneal branches of the tibial nerve provide heel sensation.

The common fibular nerve winds around the fibular neck and divides into the superficial fibular nerve, which supplies peroneus longus and brevis and the dorsum of the foot (except the first web space), and the deep fibular nerve, which supplies the anterior compartment and sensation to the first interdigital cleft. The sural nerve (from tibial and common fibular contributions) innervates the lateral heel and lateral foot; the saphenous nerve (from the femoral nerve) supplies the medial ankle and foot dorsum proximally. Articular branches from the tibial, deep fibular and saphenous nerves innervate the ankle and midfoot capsules, providing proprioceptive feedback essential to postural control[242–244].

JOINT PHYSIOLOGY AND FUNCTIONAL BIOMECHANICS

The functional physiology of the foot consists of its capacity to alternate between flexibility and rigidity across the gait cycle, thereby serving both weight-bearing and propulsive roles. In early stance, heel contact is accompanied by calcaneal eversion and subtalar pronation. This motion unlocks the midtarsal joints, increases the compliance of the talonavicular complex, and allows the forefoot to adapt to ground irregularities while the plantar fascia elongates. As the centre of pressure progresses anteriorly and the heel rises, the calcaneus inverts and the subtalar joint supinate, the midfoot becomes mechanically locked, and the foot transitions from a compliant adaptor to a stiff lever. Dorsiflexion of the metatarsophalangeal joints tightens the plantar fascia via the windlass mechanism, elevates the medial longitudinal arch, and facilitates efficient transmission of plantar flexor forces during push-off. Within this coordinated sequence, the medial column (talus–navicular–cuneiforms–first ray) provides shock absorption and then a robust platform for propulsion, whereas the lateral column (calcaneus–cuboid–fourth/fifth rays) functions as a stabilizing strut. Balanced co-activation of tibialis posterior and peroneus longus maintains the transverse arch and first-ray position; insufficiency of either tendon destabilizes the arches and alters proximal joint mechanics at the knee and hip.

Baropodometric studies in quiet bipedal stance indicate that approximately 60% of body weight is borne by the hindfoot and 40% by the forefoot, with meaningful variation according to foot morphology. Cavus feet typically shift load anteriorly, predisposing to metatarsalgia and stress injury of the lesser rays; planus feet favor rearfoot loading and prolonged midfoot contact, increasing strain on the plantar fascia and spring ligament. Abnormal plantar pressure profiles are strongly associated with overuse syndromes (plantar fasciitis, Achilles tendinopathy), neuropathic ulceration in diabetes, and impaired balance in the elderly.

The capacity of the foot–ankle complex to transition from a mobile adaptor to a rigid lever depends on intact joint congruity, ligamentous restraints (spring, long/short plantar, bifurcate and collateral ligaments), retinacula that prevent tendon bowstringing, and timely neuromuscular control from extrinsic and intrinsic muscles. Dysfunction of even a single link—such as subtalar joint stiffness, posterior tibial tendon insufficiency, or failure of the windlass—disrupts the sequence of pronation–

supination, compels compensations at the midfoot and forefoot, and propagates altered kinematics proximally to the knee, hip, and lumbopelvic segments. Framed in this way, the foot and ankle operate as a coupled system in which morphology, passive restraints, and muscle synergy continually modulate flexibility and stiffness to meet the competing demands of stability, shock attenuation, and propulsion[233,236,245].

RADIOGRAPHIC PARAMETERS FOR LOWER LIMB AND HINDFOOT ALIGNMENT

Accurate radiographic evaluation of lower limb and hindfoot alignment is essential for both preoperative planning and postoperative assessment in patients undergoing total knee arthroplasty (TKA). Proper understanding of these parameters enables the clinician to quantify deformities, evaluate compensatory mechanisms, and predict functional outcomes. Malalignment that persists distally despite correction at the knee level has been recognized as a potential source of residual symptoms and suboptimal satisfaction after surgery[246].

Hip–Knee–Ankle Angle (HKA)

The HKA angle is the cornerstone measurement for assessing coronal alignment of the entire lower limb. It is defined on a long-leg weight-bearing radiograph as the angle formed between a line drawn from the femoral head center to the knee center and a line from the knee center to the ankle center (the mid-point of the tibial plafond). A neutral alignment corresponds to 180° ± 3°. Angles opening medially are classified as varus (<177°), while those opening laterally are defined as valgus (>183°). From a biomechanical perspective, the HKA reflects how weight-bearing forces are transmitted along the limb. A varus HKA leads to medial compartment overload at both the knee and ankle, whereas a valgus HKA directs forces laterally. These loading asymmetries are strongly correlated with the development and progression of osteoarthritis. In the context of TKA, correction of the HKA is a central goal, but excessive modification may propagate distal changes at the ankle and hindfoot[18,247].

Lateral Distal Tibial Angle (LDTA)

The LDTA evaluates the orientation of the distal tibial articular surface in the coronal plane. It is measured as the angle between the tibial anatomical axis and the line of the tibial plafond. Normal values average 89° (physiological range 86–92°). A decreased LDTA indicates valgus orientation, whereas an increased LDTA suggests varus orientation.

The LDTA is particularly important in differentiating whether an ankle deformity arises from tibial bone morphology or from subtalar joint adaptation. For instance, varus osteoarthritis of the knee may induce compensatory valgus positioning of the calcaneus, while a pathologic LDTA suggests that the deformity originates at the tibial plafond itself. Recognizing this distinction is crucial for surgical decision-making, since correction at the knee may not resolve a deformity stemming from distal tibial malorientation[248–250].

Tibial Plafond Inclination Angle (TPIA)

The TPIA describes the inclination of the tibial plafond relative to the horizontal plane in standing radiographs. In healthy individuals, the tibial plafond inclination angle (TPIA) averages around 3–4° of medial tilt relative to the tibial axis, with a physiological range of approximately 2–6°. A medially depressed plafond corresponds to varus inclination, whereas lateral depression indicates valgus. Although subtle, changes in TPIA significantly influence ankle joint congruence and talar positioning. Alterations of the TPIA are clinically relevant after knee realignment surgery. A correction performed at the knee without considering the plafond inclination may shift load distribution at the ankle, precipitating degenerative changes. Studies suggest that abnormal TPIA values correlate with poor

postoperative satisfaction due to persistent ankle pain, especially in cases of pre-existing ankle pathology[246,250].

Talar Tilt Angle

Talar tilt measures the angular difference between the tibial plafond and the talar dome in the coronal plane. It reflects the congruence of the tibiotalar articulation and provides an indirect indicator of ligamentous integrity and load symmetry. A tilt greater than 4–5° is generally considered pathological and indicates asymmetric loading or instability, often secondary to deltoid or lateral collateral ligament insufficiency.

In the setting of TKA, correction of proximal varus deformity may unmask or accentuate talar tilt, especially when the ankle joint has adapted to longstanding malalignment. Persistent tilt, even in the absence of symptoms, should be monitored, as it may predispose to early ankle degeneration[246,250].

Hindfoot Alignment Angle

The hindfoot alignment angle assesses the relationship between the tibial axis and the calcaneal axis. It is classically evaluated using the Saltzman hindfoot alignment view, which allows measurement of the offset between the mechanical axis of the tibia and the posterior aspect of the calcaneus. This view is performed with an anteroposterior radiograph obtained with the patient standing on a platform, the X-ray beam angled 20–25° from posterior to anterior, to evaluate hindfoot and subtalar alignment under weight-bearing conditions. Physiologically, the hindfoot is in slight valgus (0°-5°), which ensures appropriate load distribution through the medial arch and facilitates shock absorption.

When compensatory mechanisms are intact, the hindfoot can adapt to knee deformities: in varus knee alignment, the calcaneus often drifts into valgus, while in valgus knee deformity, it shifts into varus. This adaptability is fundamental to maintaining global limb alignment, but its limits are defined by subtalar joint mobility and hindfoot flexibility. Persistent malalignment after TKA often reflects an exhausted compensatory capacity[251,252].

Medial and Lateral Plafond and Talus Angles

The medial and lateral plafond angles is defined as the angles between the mechanical axis of the tibia and the tangent to the medial and lateral aspects of the distal tibial articular surface, respectively. These measurements provide insight into the coronal obliquity of the distal tibial plafond and its relationship with postoperative alignment changes, particularly in terms of load redistribution along the ankle joint line.

Similarly, the medial and lateral talus angles is defined as the angles between the tibial mechanical axis and the medial or lateral border of the talar dome. These angles reflect the spatial orientation of the talus within the ankle mortise and serve as indirect indicators of talar shift or tilt secondary to proximal coronal plane correction.

The inclusion of both medial and lateral measurements allows for a more comprehensive analysis of asymmetries in ankle joint mechanics and provides valuable insights into joint congruency, compensatory mechanisms, and potential localized degeneration that may arise in response to total knee arthroplasty (TKA) realignment procedures[248,253].

Clinical Relevance

The combined assessment of HKA, LDTA, TPIA, talar tilt angle, and hindfoot alignment angle offers a comprehensive understanding of the coronal plane relationship across the entire lower limb. These measurements are not isolated: they represent interconnected elements of the kinetic chain. A surgeon performing TKA should therefore evaluate not only the knee deformity but also the capacity of the

ankle and hindfoot to adapt to proximal realignment. Failure to do so may result in unexplained ankle pain, gait abnormalities, or accelerated degeneration of the ankle and hindfoot joints[247].

ROLE OF THE SUBTALAR JOINT AS A COMPENSATORY MECHANISM

The subtalar joint, formed between the talus and calcaneus, is a complex articulation oriented along an oblique axis that traverses from posterolateral to anteromedial. Its kinematics combine inversion–eversion, abduction–adduction, and dorsiflexion–plantarflexion into a single triplanar motion. This joint is uniquely positioned to serve as the "biomechanical buffer" of the lower limb, adapting foot alignment to proximal deformities and ensuring plantigrade contact with the ground.

Physiological Role in Gait

During the early stance phase of gait, the calcaneus undergoes eversion, driving subtalar pronation. This motion unlocks the midtarsal joints, flattens the medial arch, and allows the forefoot to adapt to irregularities of the ground surface. Proprioceptive input increases due to wider plantar contact, enhancing balance.

As the body progresses into the push-off phase, the subtalar joint supinates, inverting the calcaneus and locking the midfoot. This raises the medial arch, tightens the plantar fascia through the windlass mechanism, and transforms the foot into a rigid lever capable of transmitting forces efficiently. The alternation between pronation and supination thus reflects the dual function of the foot: a flexible shock absorber and a rigid propulsive platform[254,255].

Compensation for Knee Malalignment

In the presence of knee deformities, the subtalar joint frequently assumes a compensatory role. Varus knee alignment induces medial deviation of the mechanical axis, leading the subtalar joint to pronate and the hindfoot to drift into valgus to restore vertical alignment of the limb. Conversely, valgus knee deformity is accompanied by subtalar supination, with hindfoot varus positioning that realigns the limb axis toward the midline.

This compensatory mechanism explains why many patients with severe coronal deformities of the knee remain able to walk with relatively plantigrade feet. It also highlights the importance of assessing subtalar joint mobility before TKA: if the joint is rigid due to arthritis, coalition, or chronic ligamentous insufficiency, compensation is limited, and distal malalignment persists even after knee correction[252].

Limits of Compensation

The compensatory potential of the subtalar joint is not infinite. With longstanding deformities, adaptive changes may become fixed, leading to secondary degenerative arthritis of the subtalar or tibiotalar joints. Moreover, when the deformity exceeds a certain threshold—typically beyond 15–20° of coronal deviation—subtalar motion alone is insufficient to realign the limb. In these cases, correction at the knee may paradoxically overload the ankle and provoke new symptoms[256].

Muscular and Tendinous Control

Dynamic control of subtalar mechanics is mediated by the surrounding musculature. The tibialis posterior exerts a powerful supinatory and arch-supporting action, while the peroneus longus counterbalances by maintaining lateral stability and the transverse arch. These muscles act in synergy to stabilize the medial and lateral columns of the foot. Insufficiency of tibialis posterior, as in adult-acquired flatfoot deformity, results in collapse of the medial arch and failure of the subtalar joint to supinate during push-off, with consequent alterations in knee and hip mechanics.

Clinical and Surgical Implications

Understanding subtalar compensation has direct clinical relevance for TKA. If the subtalar joint remains flexible, distal alignment often corrects spontaneously after knee realignment. If the joint is rigid, however, residual malalignment and pain may persist. For this reason, some authors advocate for preoperative hindfoot assessment and even simultaneous or staged procedures addressing hindfoot deformity in selected cases. Furthermore, radiographic assessment of subtalar orientation (via hindfoot alignment view or weight-bearing CT) is increasingly recognized as a valuable complement to knee alignment planning[252,257].

Integration in the Kinetic Chain

The subtalar joint does not operate in isolation: its compensatory motion influences midfoot, forefoot, and even proximal segments. Excessive pronation may propagate rotational changes to the tibia and femur, altering patellofemoral tracking and hip kinematics. Conversely, limited supination reduces push-off efficiency, increasing compensatory demands on the knee extensors. Thus, the subtalar joint is both a responder to proximal malalignment and a determinant of proximal joint function.

In summary, the subtalar joint functions as a dynamic regulator of lower limb alignment. Its ability to pronate or supinate in response to knee deformity preserves plantigrade stance and efficient gait. However, its compensatory potential is finite, and recognition of its role is fundamental when planning and interpreting outcomes of total knee arthroplasty[258,259].

TKA ALIGNMENT STRATEGIES AND THEIR IMPACT ON ANKLE AND HINDFOOT: A SYSTEMATIC REVIEW

Introduction

In total knee arthroplasty (TKA), several alignment techniques have been developed over the years, each with its own theoretical advantages and disadvantages based on differing philosophies and clinical implications[9].

Alignment strategies can be broadly categorized into **systematic approaches**, such as mechanical alignment (MA) and anatomical alignment (AA), and **personalized techniques**, including kinematic alignment (KA), its derivatives, and functional alignment (FA)[23,260].

Anatomical alignment aims to achieve a neutral mechanical axis of the lower limb while maintaining a joint line tilted approximately 3° in valgus relative to that axis[261]. In contrast, mechanical alignment seeks to establish a neutral axis with the joint line perpendicular to the mechanical axis[262,263]. These systematic techniques are designed to promote even load distribution across the prosthesis, thereby minimizing the risk of wear or implant loosening—potentially at the cost of individual functional optimization[264,265].

Kinematic alignment (KA) represents a patient-specific strategy aimed at restoring the pre-arthritic anatomy of the knee by resurfacing the joint and preserving the native soft-tissue envelope[266].

Functional alignment is a technique that utilizes intraoperative adjustments—such as modifying alignment, bone resections, component positioning, and, when necessary, soft tissue releases— with the aid of robotic-assisted systems. Its goal is to achieve balanced flexion-extension gaps and physiological soft-tissue tension while respecting the patient's native limb alignment[267].

In addition to these, a number of **hybrid techniques** have been proposed—such as inverse kinematic alignment (iKA) and restricted kinematic alignment (rKA)—which aim to approximate the patient's constitutional alignment as closely as possible while remaining within predefined safety margins to reduce the risk of malalignment-related complications[268,269].

While these alignment strategies have been widely investigated with regard to their effects on knee joint biomechanics, implant survival, and patient-reported outcomes, increasing attention is being directed toward their potential impact on **distal joints**, particularly the ankle and hindfoot. Alterations in knee alignment following TKA may propagate biomechanical changes throughout the lower limb, potentially affecting distal alignment and joint loading patterns.

However, to the best of our knowledge, no systematic review has yet been conducted to assess how different TKA alignment techniques influence **ankle and/or hindfoot alignment**. The objective of this review is therefore to synthesize the available evidence on this topic and provide clinicians with a comprehensive understanding of how various knee alignment strategies may impact the alignment of the ankle joint.

Scope and role of this systematic review within the thesis

This systematic review was conducted as part of the present PhD thesis to address the broad research question on how TKA alignment strategies influence ankle and hindfoot alignment. It is intended to summarize available clinical radiographic evidence, identify gaps in head-to-head comparisons between alignment philosophies (including functional/personalized strategies), and provide the rationale and hypotheses for the subsequent retrospective cohort study presented in the following chapters.

Material and Methods

A systematic review of the literature was performed with a primary search on Medline through PubMed and Cochrane Library used the following search string: ("total knee arthroplasty"[Title/Abstract] OR "knee replacement"[Title/Abstract]) AND ("ankle"[Title/Abstract] OR "hindfoot"[Title/Abstract]) AND ("alignment"[Title/Abstract] OR "biomechanics"[Title/Abstract] OR "malalignment"[Title/Abstract]). Studies were considered eligible for inclusion if they fulfilled the following criteria: they were published in English and involved patients who underwent total knee arthroplasty (TKA); they provided both preoperative and postoperative radiographic imaging, including measurements of the ankle and/or hindfoot; and they clearly specified the alignment strategy adopted during TKA—such as mechanical, anatomical, or functional alignment. Studies in which the alignment strategy was not explicitly stated but could be clearly inferred from the description of the surgical technique were also included. We considered retrospective or prospective clinical studies including randomized controlled trials, non-randomized trials, cohort studies, case–control. We do not appley any restriction on publication date. The exclusion criteria were: case report, case series and review articles; in vitro or experimental biomechanical or cadaveric studies; papers not in English. This systematic review was conducted following the PRISMA (Preferred Reporting Items for Systematic Reviews and Meta-Analyses) guidelines[270]. The selection process was conducted independently by two reviewers following the inclusion criteria. In cases of disagreement, a third senior orthopedic surgeon reviewed the article and made the final inclusion decision. An initial selection was made screening titles and abstracts. After this first phase articles were selected for full-text review. The Level of Evidence (LOE) of the studies was assigned based on the 2011 Oxford Centre for Evidence-based Medi-cine Levels of Evidence. The following data, when available, were extracted from the articles: Level of Evidence, number of patients, number of treated knees, mean age and sex of patients, mean follow-up, tka alignment, pre and postoperative X-Rays of the knee and of the ankle/hindfoot, pre and postoperative ankle functional score.

Results:
A total of 22 articles were ultimately included in this systematic review. The selection process is detailed in the PRISMA 2009 flow diagram, which outlines the identified, included, and excluded studies (Fig. PRISMA). Table 2 presents the data extracted from the selected studies. Most articles were classified as level III evidence, based on the 2011 Oxford Centre for Evidence-Based Medicine guidelines; five studies were assigned level II, while only one study reached level I, being a randomized controlled trial, and another was classified as level IV. All included studies reported preoperative and postoperative radiographic measurements of the ankle/hindfoot, along with the alignment strategy adopted for total ankle arthroplasty. Among the included studies, 16 used only mechanical alignment, 5 compared personalized alignment with mechanical alignment, and only 1 investigated personalized alignment without comparison.

Discussion
Mechanically aligned total knee arthroplasty (MA-TKA) consistently achieves substantial coronal realignment of the knee, as reflected by significant improvements in hip–knee–ankle (HKA) and femorotibial angles (FTA). This proximal correction induces measurable biomechanical adaptations along the distal kinetic chain, particularly at the ankle and hindfoot, whose responses depend on the magnitude of preoperative deformity, the presence of ankle osteoarthritis (OA), and the plane-specific adaptability of each segment.
Radiographic studies demonstrate that MA-TKA produces meaningful distal realignment. Jeong reported significant improvements in coronal parameters such as ground–talar dome angle (GD), talar tilt (TT), heel alignment (HA), and heel distance (HD), strongly correlated with HKA correction[271]. Kikuchi confirmed substantial changes in tibial plafond inclination angle (TPIA), TT, and hindfoot

alignment angle (HAA), along with medial migration of the mechanical ankle joint axis[272]. Choudhury further observed that patients with greater preoperative varus deformities (>10°) experienced the largest distal corrections[273], confirming a dose-dependent relationship between knee correction and distal adaptation. Conversely, Shichman found no significant ankle changes despite marked varus correction[274]. Most studies agree that TKA-induced realignment typically shifts the hindfoot from valgus toward neutral alignment[247,275–277].

The degree of preoperative deformity critically influences ankle and hindfoot response. Larger mTFA or HKA corrections yield greater TPI and TI improvements[278], but changes in tibiotalar tilt or talar inclination remain inconsistent, likely due to subtalar joint compensation. Jeong and Cho reported that patients with severe varus (≥10°) exhibited greater postoperative corrections at both knee and hindfoot levels, whereas milder deformities showed limited change[271,275]. Okamoto's findings suggest that hindfoot compensation is more dynamic in mild deformities, possibly due to preserved subtalar mobility and soft-tissue elasticity, while in severe cases residual deformity often persists[279].

Distal adaptation magnitude varies across planes. Kikuchi found strong correlations between ΔHKA and ΔTPIA, moderate with ΔHA, and an inverse relationship with medial ankle loading, indicating coordinated yet selective distal realignment[272]. Jeong similarly showed significant coronal but not sagittal or axial adaptations, implying strong knee–hindfoot coupling limited to the frontal plane[271]. Other authors observed postoperative mechanical decoupling between the knee and ankle, with reduced correlation between HKA and ankle tilt[280]. Shichman's data also suggest deformity-specific ankle responsiveness, with valgus knees adapting more readily than varus ones[274].

Biomechanical dissociation between ankle and hindfoot segments has been frequently reported. Okamoto found no correlation between talar or tibial inclinations and hindfoot parameters such as calcaneal pitch or naviculocuboid overlap[279], suggesting independent adaptation mechanisms. Takenaka similarly noted that postoperative correction occurred only in hindfoot valgus deformities, whereas varus hindfoot remained unchanged[276]. Clinically, this rigidity may explain persistent postoperative malalignment or pain in varus hindfoot cases.

When both ankle and hindfoot were evaluated, several studies confirmed that despite global alignment improvement, patients with ankle OA or persistent hindfoot valgus showed incomplete adaptation and more symptoms. Kikuchi found residual hindfoot valgus in OA patients despite similar HKA correction[281], and Kim reported that those with postoperative ankle pain had greater residual valgus and mechanical axis deviation, though ankle-specific parameters were unchanged[32]. These findings suggest that hindfoot alignment, more than tibiotalar geometry, influences postoperative comfort.

Preexisting ankle OA further limits compensatory capacity. OA patients exhibit more severe preoperative varus, greater baseline hindfoot valgus, and less postoperative correction[281–283]Chang also found increased postoperative ankle pain and worse WOMAC outcomes in OA patients despite comparable alignment, underscoring that structural rigidity and degenerative changes impair distal adaptability[283]. Therefore, comprehensive preoperative assessment of ankle and hindfoot alignment is essential, particularly in OA or restricted subtalar mobility.

Despite overall improvements, residual hindfoot valgus frequently persists. Kim observed that symptomatic patients retained higher hindfoot valgus angles and mechanical axis deviation than asymptomatic ones, while other ankle parameters were unchanged[32]. Mullaji similarly reported that although the tibio-calcaneal angle improved, 87% of limbs remained in valgus postoperatively, and postoperative hindfoot alignment correlated with preoperative, not knee, parameters[284]. Persistent hindfoot valgus may cause lateralized ground mechanical axis deviations, suggesting that knee realignment alone may not fully restore global limb balance.

Comparative analyses of alignment strategies reveal that while MA effectively restores global limb alignment, functional (FA), restricted kinematic (rKA), and residual varus (RV) approaches may better preserve distal joint harmony. FA achieves more precise coronal restoration with fewer outliers than

MA, likely minimizing compensatory ankle changes[285]. Li found no overall differences in ankle parameters between MA and FA[285], but Sangaletti showed that under MA, patients with larger femoral or tibial corrections exhibited greater distal changes, indicating a threshold effect[286]. Chompoosang observed that in severe varus deformities, MA produced more oblique distal tibial inclinations than FA, potentially predisposing to malalignment[287]. Kikuchi found that both MA and rKA corrected proximal deformities without substantial ankle changes, suggesting limited distal responsiveness[288]. Shichman noted that inverse kinematic alignment (IKA) improved ankle parameters only in severe deformities, whereas mild deformities remained stable[289]. Shin's comparison between MA and RV showed that tolerating mild residual varus maintained more parallel joint lines and neutral distal alignment, reducing compensatory ankle adjustments[290]. Correlation analyses confirmed that larger HKA corrections influence distal loading patterns[285], though coupling strength diminishes beyond the subtalar level[288].
Overall, these findings emphasize that while MA-TKA reliably restores mechanical axis alignment, it can impose unintended angular deviations at the ankle, particularly in rigid or severely deformed limbs. In contrast, FA and RV strategies tend to maintain coronal balance across the entire kinetic chain, potentially reducing postoperative symptoms. Individualized surgical planning—considering native limb morphology, joint flexibility, and ankle status—is therefore crucial. Preoperative long-leg, weightbearing radiographs extending from hip to calcaneus remain essential for anticipating distal biomechanical consequences and optimizing global alignment outcomes.

Implications for the present cohort study
Overall, available studies are heterogeneous in imaging protocols, measurement definitions, and alignment descriptions, and only a limited number directly compare personalized/functional strategies against conventional mechanical alignment. These gaps justify a standardized retrospective comparison using uniform long-leg weight-bearing radiographs, ankle/hindfoot measurements, and patient-reported outcomes, as presented in the next chapter.

Conclusions:
Mechanical alignment total knee arthroplasty (MA-TKA) reliably restores overall coronal limb alignment but often induces limited or unbalanced adaptations at the ankle and hindfoot, particularly in patients with severe deformities or restricted subtalar motion. These distal segments show only partial coupling with knee correction, and residual hindfoot valgus or ankle overload may persist despite accurate mechanical restoration.
In contrast, personalized alignment strategies—such as functional alignment (FA), restricted kinematic alignment (rKA), or residual varus (RV)—tend to better preserve native joint line orientation and coronal harmony along the kinetic chain, reducing compensatory ankle changes and postoperative symptoms.
Overall, individualized alignment planning that accounts for native morphology, hindfoot flexibility, and ankle condition may achieve more physiological load distribution and improved functional outcomes than the traditional MA approach. Comprehensive preoperative assessment of the entire lower-limb axis remains essential for optimal biomechanical restoration.

Limitations
This systematic review is subject to several limitations stemming from the design and methodological heterogeneity of the included studies.
The majority of included studies were retrospective in nature (Level III evidence), with only a small subset comprising prospective (Level II) or randomized controlled trials (Level I).
There was considerable variability in patient cohort size across studies. This heterogeneity reduces the

statistical power and limits the ability to generalize findings across different alignment strategies, deformity severities, or patient subgroups.
Subgroup classifications (e.g., based on varus severity, ankle osteoarthritis presence, or hindfoot alignment) were not standardized across studies, such inconsistency complicates direct comparison and limits pooled analyses.
Many studies only captured early postoperative radiographic changes, which may not reflect long-term biomechanical adaptations or symptom progression.
Although ankle or hindfoot alignment was a stated focus in most studies only three studies reported outcomes of both structures. Among the 22 studies included, the majority (16) focused exclusively on varus knees, which may limit the generalizability of the findings to valgus or neutral deformities

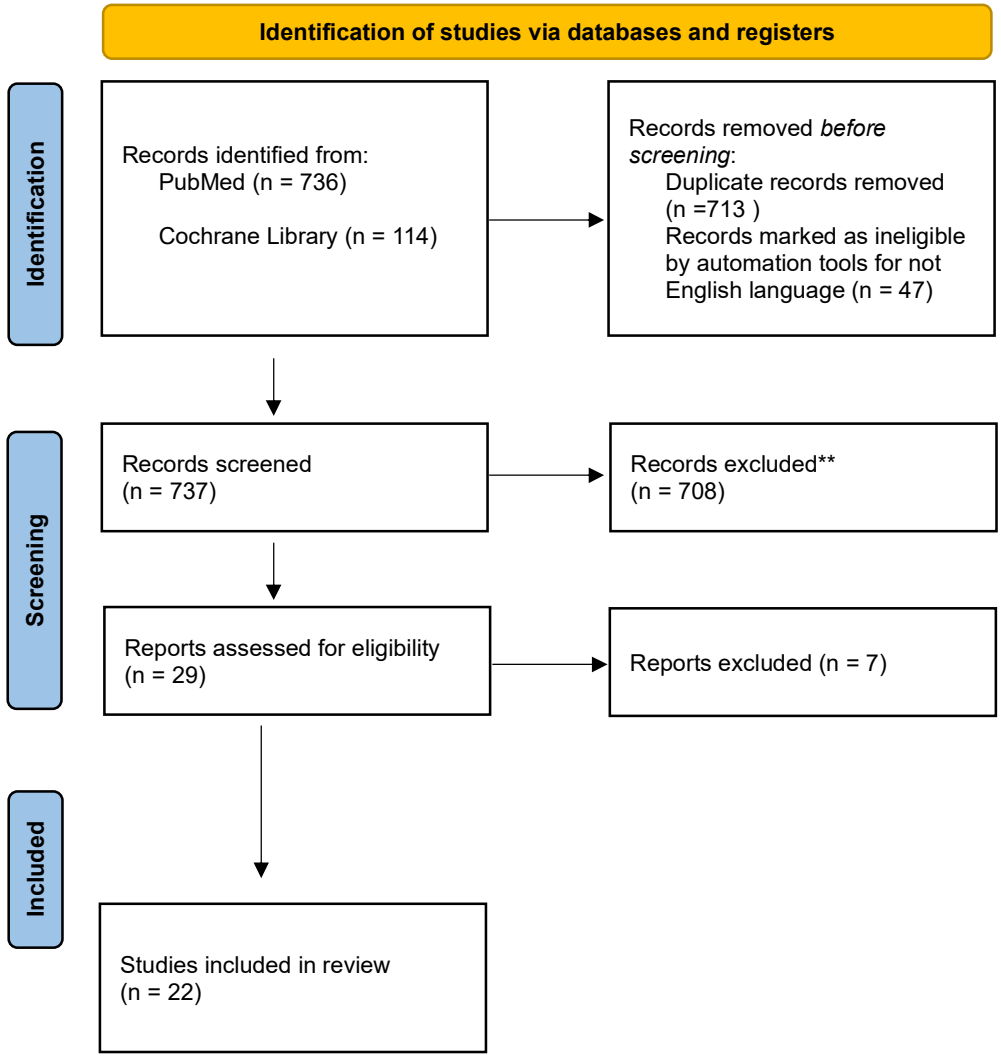

Fig 1. PRISMA flow diagram of the included studies.

TITLE	AUTHOR	YEAR	LOE	PATIENTS NUMBER	AGE	SEX	F.U.	KNEE ALIGNMENT	KNEE X-Rays PREOP.	KNEE X-RAYS POSTOP.	ANKLE X-Rays PREOP.	ANKLE X-Rays POSTOP.	PREOP. ANKLE SCORES	POSTOP. ANKLE SCORES	STATISTICALLY SIGNIFICANT RESULTS
Persistent Hindfoot Valgus Causes Lateral Deviation of Weightbearing Axis after Total Knee Arthroplasty[28] [4]	Arun Mullaji et al	2010	III	TOT(G1): 125 (165 knees); DEF <15°(G2): 121 knees; DEF ≥15°(G3): 44 knees; VAR (G4): 153knees; VAL(G5): 12knees.	66.1±9.5 (50–84)	F:M 101:24	6 weeks	MA (with navigation)	G1: HKA 170 (152–201); CMAD +34.3 (91 to +98); GMAD +31 (102 to +98). G2: HKA 171.5 (165.5–194); CMAD +28 (43 to +52.3); GMAD +25 (50 to +50). G3: HKA 164 (152–201); CMAD +53.3 (91 to +98); GMAD +49.5 (102 to +98). G4: HKA 169.5 (152–180); CMAD +35.6 (12 to +98); GMAD +32 (20 to +98). G5: HKA 187.5 (180.5–201); CMAD 59.7 (0 to 91); GMAD 73.3 (10.6 to 102).	G1: HKA 180 (170–185); CMAD 0 (17 to +28); GMAD 6 (24 to +20). G2: HKA 180 (176.5–185); CMAD 6.8 (17 to +28); GMAD 23 (24 to +20). G3: HKA 180 (177–183); CMAD 0 (8.7 to +12); GMAD 5 (15.3 to +10.6). G4: HKA 180 (176.5–185); CMAD 6.8 (17 to +28); GMAD 22.4 (24 to 20). G5: HKA 180.7 (180–183); CMAD 0 (+6 to 11); GMAD 6.9 (+5 to 16.3).	G1: TCA 188 (160–203). G2: TCA 187.5 (160–203). G3: TCA 189.7 (175–200). G4: TCA 188 (175–203). G5: TCA 186 (160–199).	G1: TCA 185.5 (173–200). G2: TCA 185.5 (173–200). G3: TCA 186.7 (178–199). G4: TCA 186 (173–200). G5: TCA 184.5 (173–198).	-	-	Preoperative hindfoot valgus alignment (TCA) decreased (p = < 0.001) after TKA (TUTTI I GRUPPI). Only preoperative hindfoot alignment influenced hind-foot alignment after TKA. The preoperative TCA correlated with (rho = 0.58; p \0.001) the postoperative TCA. We observed no correlation between preoperative HKA angle and postoperative TCA, postoperative HKA angle and postoperative TCA, and difference between pre- and postoperative HKA angle and postoperative TCA.

Hindfoot alignment at one year after total knee arthroplasty[276]	Takashi Takenaka et al	2015	III	TOT: 71 (73 knees); hindfoot valgus group (51 knees); hindfoot varus group (22 knees)	74.7± 6.3	F:M 58:15	1 year	MA	Valgus group: FTA 185.5 ± 4.5°. Varus group: FTA 183.0 ± 5.1°	Valgus group: FTA 173.9 ± 2.8°. Varus group: FTA 174.0 ± 2.7°	Hindfoot valgus group: VVA 80.5 ± 3.1. Hindfoot varus group: VVA 72.7 ± 2.6	Hindfoot valgus group: VVA 78.6 ± 3.7(3w); 77.1 ± 2.7 (1y). Hindfoot varus group: VVA 72.3 ± 3.3(3w) 73.5 ± 3.0(1y)	-	-	Prior to TKA, the mean FTA was significantly higher in the hindfoot valgus group than in the hindfoot varus group ($p = 0.04$). In the hindfoot valgus group, the mean VVA significantly declined from 80.5 ± 3.1° prior to TKA to 78.6 ± 3.7° ($p < 0.01$) 3 weeks following surgery and to 77.1 ± 2.7° ($p < 0.05$) 1 year following surgery. Nel varo NO.
Radiographic assessment of knee–ankle alignment after total knee arthroplasty for varus and valgus knee osteoarthritis[280]	Fuqiang Gao et al	2016	III	TOT: 149; unilateral valgus (G1): 24; Unilateral Varus (G2): 82; bilateral Varus (G3): 43	67.2 ± 8.7	F:M 117:32	-	MA	G1 HKA −7.8±6.7; G2 HKA 9.3±5.9 G3L HKA; 8.5±5.6 G3R HKA 8.4±5.1	G1 HKA 3.3±2.9; G2 HKA 2.4±2.8; G3L HKA 1.6±2.0; G3R HKA 3.2±2.9	G1 TTA 89.5±5.1 TAA −6.9±7.3; G2 TTA 87.9±4.8 TAA 3.6±6.7; G3L TTA 91.3 ± 4.2 TAA 3.4 ± 5.7; G3R TTA 92.0 ± 5.4 TAA 3.0 ± 6.4	G1 TTA 87.3±5.8 TAA −1.1±5.7; G2 TTA 87.5±4.4 TAA −1.4±5.0; G3L TTA 91.9 ± 3.0 TAA −0.7 ± 3.7; G3R TTA 92.1 ± 3.0 TAA 0.0 ± 4.0	-	-	Pre e post op G1 G2 e G3 HKA P value < 0,001 G2; G3L and G3R TAA pre and post operative P value < 0,001

Changes in hindfoot alignment after total knee arthroplasty in knee osteoarthritic patients with varus deformity[275]	Woo-Shin Cho et al	2016	II	TOT: 117 (195 knees); varus<10 (G1): 81 knees; varus≥10° (G2): 114 knees.	69.1±6.1	F:M 187:8	2 years	MA	Mechanical alignment angle. Overall: 10.8° (±4.8) varus; G1: 6.5 ° (±2.0) varus; G2: 13.9 ° (±3.7) varus	Mechanical alignment angle. Overall: 1.8° (±3.4) varus; G1: 0.6 ° (±3.0) varus; G2: 2.6 ° (±3.5) varus	Hindfoot alignment angle. Overall: 5.2° (±3.8) valgus; G1: 3.3° (±3.0) valgus; G2: 6.5° (±3.8) valgus.	Hindfoot alignment angle. Overall: 2.1° (±4.0) valgus (6w); 2.2° (±4.2) valgus (1y); 2.2° (±4.1) valgus (2y). G1: 1.4° (±3.5) valgus (6w); 1.4° (±3.8) valgus (1y); 1.6° (±3.8) valgus (2y). G2: 2.5° (±4.1) valgus (6w); 2.8° (±4.3) valgus (1y); 2.6° (±4.2) valgus (2y).	-	-	Hindfoot alignment angle: preop 5.2° (±3.8) valgus to postop 2.1° (±3.9) valgus p<0.001. Preoperative hindfoot alignment angle: G1 3.3° (±3.0) valgus and G2 6.5° (±3.8) valgus p<0.001. Change of hindfoot alignment: G1 1.8° (±2.5), G2 4.0° (±3.0) p<0.001.
Clinical usefulness of hindfoot assessment for total knee arthroplasty: persistent post-operative hindfoot pain and alignment in pre-existing severe knee deformity[279]	Yoshinori Okamoto et al	2016	III	TOT: 75 (80 knees); varus ≤6° (GM): 46 knees; (varus>6° (GS): 34 knees.	72.5 (58-85)	F:M 67:8	2 years	MA	M: mechanical axis 3.2 ± 4.1 (2.1–6.2); tibial inclination 9.0 ± 2.9 (6.1–12.1). S: mechanical axis 7.4 ± 4.2 (7.1–12.3); tibial inclination 11.1 ± 5.6 (5.1–16.2).	M: mechanical axis 0.4 ± 1.2 (−1.2-1.3); tibial inclination −0.2 ± 1.3 (−2.0–3.1). S: mechanical axis 1.1 ± 1.4 (−2.4-2.2); tibial inclination 2.1 ± 6.5 (−3.3–10.1).	M: talar tilt 12.1 ± 6.1 (5.8–19.1); calcaneal pitch 14.8 ± 2.2 (12.9–20.3); Naviculocuboid overlap 82.1 ± 5.3 (74.0–88.2). S: talar tilt 14.4 ± 7.1 (8.1–25.8); calcaneal pitch 15.1 ± 2.5 (10.2–20.4); Naviculocuboid overlap 88.2 ± 4.8 (75.8–90.1).	M: talar tilt 3.8 ± 3.3 (2.2–10.3); calcaneal pitch 23.4 ± 1.8 (20.2–26.4); Naviculocuboid overlap 52.3 ± 2.1 (39.8–54.2). S: talar tilt 5.2 ± 5.6 (3.2–10.3); calcaneal pitch 15.2 ± 1.4 (10.1–18.3); Naviculocuboid overlap 83.7 ± 3.1 (74.2–86.3).	M: AOFAS 50 ± 6 (48–67); pain 30 ± 3 (27–40); function 14 ± 2 (12–50); alignment 6 ± 1 (5–10). S: AOFAS 42 ± 4 (30–52); pain 22 ± 3 (20–38); function 15 ± 2 (12–46); alignment 5 ± 1 (5–10).	M: AOFAS 75 ± 3 (70–100); pain 38 ± 2 (30–40); function 29 ± 2 (24–50); alignment 8 ± 1 (5–10). S: AOFAS 47 ± 3 (42–56); pain 24 ± 2 (20–38); function 16 ± 1 (14–46); alignment 7 ± 1 (5–10).	Group M decreased naviculocuboid overlap (p = 0.0271) by 37 %, that is, the post-operative hindfoot showed a tendency to varus. In Group M, the mechanical axis exhibited a statistically significant with naviculocuboid overlap.

Following the correction of varus deformity of the knee through total knee arthroplasty, significant compensatory changes occur not only at the ankle and subtalar joint, but also at the foot[271]	Bi O Jeong et al	2017	II	331 (375 knees)	68.3 ± 7.8	F:M 308:23	6 months	MA	HKA 11.1 ± 4.9 (varus)	HKA 0.3 ± 2.5° (varus)	TT 0.4 ± 1.9 GD 6.5 ± 3.1 TAS 92.0 ± 1.5 TLS 81.8 ± 2.8 HR 0.2 ± 0.1 HA 13.5 ± 6.4° HD 11.0 ± 4.1	TT 0.1 ± 1.8 GD 0.2 ± 2.1° TAS 92.0 ± 1.3 TLS 81.3 ± 2.6 HR 0.3 ± 0.1 HA 5.8 ± 6.7 HD 5.2 ± 2.5	-	-	Pre op vs post op HKA p value < 0,001 GD p value < 0,001 HR HA HD p value < 0,001 strong negative correlation between the preop–postop variances in HKA and GD (r = 0.701, p < 0.001) A moderate correlation was observed between the preop–postop variances in HKA and the preop–postop variances in HR, HA and HD (r = 0.206, − 0.348, and − 0.418; p = 0.004, < 0.001, and < 0.001)

Radiologic Factors Affecting Ankle Pain Before and After Total Knee Arthroplasty for the Varus Osteoarthritic Knee[32]	Chang-Wan Kim et al	2018	III	TOT: 55 (65 knees); ankle pain after TKA (G1) 8pz; ankle pain before and after TKA (G2) 52pz; no ankle pain (G3) 5pz	69.3 ± 7.2 (54-80)	-	< 2 years	MA	only varus knee	Neutral alignment	G1 MA 8.4±3.2 TT 1.5±0.6 TAS 85.4±2.6 MCS 2.0±0.5 Medial tibiotalar joint space 2.4±0.8 FTGA 86.4±2.6 HAVA 5.9±4.2 G2 MA10.3±5.2 TT 1.9±1.4 TAS 86.1±3.9 MCS 2.5±1.0 Medial tibiotalar joint space 2.9±0.9 FTGA 85.6±2.5 HAVA 5.7±4.7 G3 MA 9.5±2.7 TT 2.0±0.9 TAS 84.0±4.2 MCS 2.0±0.5 Medial tibiotalar joint space 2.2±1.0 FTGA 84.6±0.5 HAVA 10.8±2.9	G1 MA 5.1±2.1 TT 1.5±0.6 TAS 84.6±3.1 MCS 2.4±1.4 Medial tibiotalar joint space 2.3±0.8 FTGA 86.6±1.2 HAVA 7.5±1.7 G2 MA 1.6±2.5 TT 1.7±1.2 TAS 84.8±5.2 MCS 2.6±1.0 Medial tibiotalar joint space 2.4±1.1 FTGA 86.5±2.1 HAVA 5.3±2.7 G3 MA 0.1±4.4 TT 2.0±0.5 TAS 86.2±1.9 MCS 2.3±0.4 Medial tibiotalar joint space 1.7±1.0 FTGA 86.4±3.0 HAVA 7.2±2.2	Group 1 VAS 1.8±2.2 AFOS 82.5±11.2 Group 2 VAS 0.1±0.5 AFOS 98.9±5.7 Group 3 VAS 2.6±0.6 AFOS 76.6±2.5	Group 1 VAS 4.6±1.6 AFOS 49.1±19.5 Group 2 VAS 0.1±0.5 AFOS 1.2±0.5(1.0to2.0) Group 3 VAS 1.2±0.5 AFOS 82.4±2.5	VAS e AFOS G1 e G2 P value < 0,01; Mechanical axis deviation angle G1 vs G2 P value = 0,001

Concomitant Ankle Osteoarthritis Is Related to Increased Ankle Pain and a Worse Clinical Outcome Following Total Knee Arthroplasty[28][3]	Chong Bum Chang et al	2018	III	TOT 56 (99 knee); ankle OA (G1): 24 knees; no ankle OA (G2)75 knees.	70±6.8 (55-83)	F:M 23:76	2 years	MA	HKA - 8.8 ±5.3 2 (varus); G1 HKA - 8.9 ±5.8 (varus); G2 HKA - 8.7 ±5.2 (varus)	HKA -1.0 ±2.5 < (varus); G1 HKA - 0.9 ±2.9 (varus); G2 HKA - 1.0 ±2.4 (varus)	Overall G-AJLO 9.4 ±5.9 medial tibitalar joint space 2.5±0.5 Medial ankle clear space 1.8±0.6 HFA -0.9 ±5.0 (varus) G1 G-AJLO 10.5 ±7.0 HFA -2.9 ±4.8 G2 G-AJLO 9.2 ±5.5 HFA - 0.2 ±4.9	Overall G-AJLO 3.4 ±3.9 medial tibitalar joint space 2.8±0.5 Medial ankle clear space 2.3±0.5 HFA -3.1 ±4.8 G1 G-AJLO 4.6 ±4.0 HFA - 3.0 ±4.7 G2 G-AJLO 3.0 ±3.8 HFA - 3.1 ±4.8	G1 ankle pain 3 G2 ankle pain 12 G1 WOMAC 40.3±8.0 G2 WOMAC 37.8±10.0	G1 ankle pain 9 (increased) G2 ankle pain 12 (stationary) G1 WOMAC 22.2±13.2 G2 WOMAC 14.2±7.9	Overall G-AJLO; medial tibitalar joint space; Medial ankle clear space; HFA pre op vs post op P value < 0,001 G1 vs G2 HFA p value < 0,001; ankle pain G1 Vs G2 p value < 0,042 WOMAC G1 Vs G2 p value < 0,002

Aggravation of Ankle Varus Incongruency Following Total Knee Replacement Correcting 10 of Genu Varum Deformity: A Radiographic Assessment[278]	Chong Bum Chang et al	2020	III	110	68.9 ± 7.2	F:M 108:2	41.1 ± 29.6	MA	mTFA: 13.7±3.4 mLDFA: 90.3±2.4 MPTA: 84.1±2.1	mTFA: 1.0±2.8 mLDFA: 91.3±2.4 MPTA: 90.5±1.9	LDTA: 88.2±4.4 TPI: 10.4±4.0 TI: 13.5±4.5 TTTA: 3.1±2.1 TMAA: 8.5±2.1	LDTA: 91.0±4.1 TPI: 3.2±3.9 TI: 7.8±4.6 TTTA: 4.7±3.0 TMAA: 0.5±1.5	-	-	TPI (P < .001) and TI (P < .001) significantly changed following TKA. TTTA showed postoperative decrease in 19 patients (17.3%), the same in 2 (1.8%), and increase in 89 (80.9%). TTTA also changed significantly following TKA (P < .001), that is, 1.4 increase in the varus incongruency of the ankle joint. TTTA showed 2.0 (SD 1.6) increase in the aggravated patients while 1.0 (SD 0.7) decrease in the improved patients. The postoperative change in TTTA was significantly correlated with that of MPTA (r 1⁄4 0.241, P 1⁄4 .011), TPI (r 1⁄4 0.261, P 1⁄4 .006),

															and TI (r 1⁄4 0.307, P 1⁄4.001), but not with that of mTFA (r 1⁄4 0.175, P 1⁄4 .068) or preoperative TTTA (r 1⁄4 0.005, P 1⁄4 .955)

Association between changes in hip-knee-ankle angle and hindfoot alignment after total knee arthroplasty for varus knee osteoarthritis[247]	Naicheng Diao et al	2021	II	108	66.31±5.55 (56-79)	F:M 89:19	3 months	MA	HKA -9.15 ± 5.54	HKA -2.37 ± 3.05	HFA 2.67 ± 3.97	HFA 0.52 ± 3.96	AOFAS 76.50± 10.89	AOFAS 90.40± 6.05	HKA from −9.15° ± 5.54 to-2.37° ± 3.05 (p <0.001). HFA from 2.67°± 3.97 to 0.52°± 3.96 (p < 0.001). AOFAS score from 76.50±10.89 to 90.40±6.05 (p<0.001)
Effect of Total Knee Arthroplasty on Coronal Alignment of the Ankle Joint[274]	Ittai Shichman et al	2022	III	TOT: 107; <10° varus/valgus correction (G1): 60; ≥10° varus correction (G2): 30; ≥10° valgus correction (G3): 17.	65±8.7 (45-88)	F:M 78:29	3 months	MA	G1 HKA 1.5±6.4 (varus); G2 HKA 20.5±5.1; G3 HKA 16.8±4.2		G1 TPIA 89.8±4.9, TIA 89.1±4.8, TT 0.7±2.4; G2 TPIA 92.2±9.2, TIA 92.4±9.4, TT 0.2±2.2; G3 TPIA 83.2±7.6, TIA 82±7.2, TT 3.2±1.6.	G1 TPIA 90.6±4.3, TIA 89.4±5.4, TT 1.2±2.2; G2 TPIA 90.0±4.7, TIA 88.7±5.6, TT 1.3±3.1; G3 TPIA 92.7±4.7, TIA 90.8±5.5, TT 1.9±2.2.	-	-	HKA change for all group P value < 0,01; TPIA in G3 p value < 0,01 (Delta 9.5 (±6.9) from valgus 83.2 (±7.6)to varus 92.7 (±4.7))

Residual varus alignment can reduce joint awareness, restore joint parallelism, and preserve the soft tissue envelope during total knee arthroplasty for varus osteoarthritis[290]	Kyun-Ho Shin et al	2022	III	TOT: 198; MA (G1): 99; RV (G2): 99	G1 72.43 ± 5.29; G2 72.41 ± 5.71	G1 F:M 91:8; G2 F:M 92:7	≧ 3 years	G1 MA; G2 RV	G1 HKA 13.56 ± 4.01 FMA 91.10 ± 2.07 TMA 84.55 ± 2.71; G2 HKA 12.88 ± 3.25 FMA 91.01 ± 1.87 TMA 84.42 ± 2.39	G1 HKA 0.37 ± 1.08 FMA 89.55 ± 1.25 TMA 89.19 ± 1.35; G2 HKA 3.14 ± 1.29 FMA 89.06 ± 0.99 TMA 87.20 ± 0.98	G1: G-Plafond -4.99±1.90; Plateua-Plafond 2.70 ± 2.02. G2: G-Plafond −5.11±1.97 Plateua-Plafond 2.69±2.15	G1: G-Plafond −0.69±1.20 Plateua-Plafond −2.65±1.56. G2: G-Plafond −0.50±1.69 Plateua-Plafond − 0.95±1.71	-	-	Postoperative G-Plateau − 3.05 ± 1.62 − 0.75 ± 1.59 P value < 0.001; Postoperative Plateau– Plafond − 2.65 ± 1.56 − 0.95 ± 1.71 P valure < 0.001
Influence of Distal Reference Point of the Tibial Mechanical Axis on the Ankle and Hind limb Alignment Change after Total Knee Arthroplasty[288]	Kenichi Kikuchi et al	2023	III	MA TKA: 50; KA TKA: 50	MA 74.8 (58–92); KA 74.9 (56–91)	MA F:M 32:18; KA F:M 40:10	6 months	MA; KA	MA: HKC -12.0±5.2; KA: HKC –9.8±3.2	MA: HKC –1.3(3.6); KA: – 0.1(2.0)	MA: DTA 0.6V1.1, TTA – 0.7±1.0, TCA 3.3±5.5; KA: DTA 0.6±0.9, TTA – 0.4±1.1, TCA 3.5±4.3	MA: DTA 0.7±1.1, TTA – 0.7±0.9, TCA 3.4±5.5; KA: DTA 0.5±1.1, TTA – 0.5±1.0, TCA 3.1±4.3	-	-	MA ΔHKC <0.001 MA Δ%HC <0.001 KA ΔHKC <0.001 KA Δ%HC <0.001 MA VS KA Pre op ΔHKC 0.02 MA VS KA Pre op Δ %HC 0.04 MA VS KA Post op ΔHKC 0.04 MA VS KA Post op Δ %HC 0.03

Increased ankle pain after total knee arthroplasty is associated with a preoperative lateralized gait and talar tilt, but not with ankle laxity or the range of motion of the subtalar joint[277]	M. Rühling et al	2023	II	varus= 45; valgus= 24	-	-	3 months	MA	VARUS: mTFA 9.25° (5.04 to 12.60); Slope 6.90° (5.26 to 9.35). VALGUS: mTFA - 9.00° (-13.10 to -6.31); Slope 6.96° (5.22 to 10.31)	VARUS: mTFA 1.39° (-0.09 to 3.62); Slope 5.84° (4.37 to 7.12). VALGUS: mTFA - 0.53° (-2.25 to 0.30); Slope 5.88° (3.70 to 6.40)	VARUS: HAVA - 3.92° (-6.53 to -2.10); TT 0.40° (-0.55 to 0.92); ADTA 83.74° (81.20 to 85.44). VALGUS: HAVA 3.75° (2.41 to 5.77); TT - 0.72° (-1.60 to 0.10); ADTA 83.39° (81.35 to 86.10)	VARUS: HAVA - 1.82° (-3.28 to 1.57); TT -0.16° (-0.99 to 0.47); ADTA 83.30° (80.64 to 85.20). VALGUS: HAVA - 2.37° (-4.79 to -1.60); TT -0.45° (-1.33 to 0.19); ADTA 84.00° (82.18 to 85.99)	median FFI =0 (sia totale che sottogruppi). VARUS: Ankle dorsiflexion 5.00 (0.00 to 10.00); Ankle plantarflexion 35.00 (30.00 to 40.00). VALGUS: Ankle dorsiflexion 5.00 5.00 (2.25 to 10.00); Ankle plantarflexion 37.50 (30.00 to 40.00)	median FFI =0 (sia totale che sottogruppi). VARUS: Ankle dorsiflexion 10.00 (0.00 to 10.00); Ankle plantarflexion 35.00 (30.00 to 40.00). VALGUS: Ankle dorsiflexion 10.00 (5.00 to 10.00); Ankle plantarflexion 35.00 (30.00 to 36.25)	VARUS: HAVA, ° -3.92 (-6.53 to -2.10) TO -1.82 (-3.28 to 1.57) P=0.001; TT TT, ° 0.40 (-0.55 to 0.92) TO -0.16 (-0.99 to 0.47) p=0.022. VALGUS: HAVA 3.75 (2.41 to 5.77) TO -2.37 (-4.79 to -1.60) p< 0.001
Total Knee Arthroplasty in Patients With Ankle Osteoarthritis Affects Contralateral Ankle Alignment and Postoperative Outcome of Total Knee Arthroplasty[282]	Tomoki Koyama et al	2024	III	64	80±8 (70-90)	F:M 53:11	X-Rays FU 6 months; clinical FU 1 year	MA	mHKA −12.2 (−16.6 to −8.3); mHKA ankle OA grade 1 −9.7 (−14.1 to −8.1); mHKA ankle OA ≧grade2 −14.2 (−17.0 to −11.0)	mHKA −1.8 (−5.1 to −0.6); mHKA ankle OA grade 1 −1.3 (−3.6 to −0.1); mHKA ankle OA ≧grade2 −2.2 (−7.4 to −0.8)	TTA 1.7 (0.7 to 2.5); TTA ankle OA grade 1 0.9 (0.4 to 1.9);TTA ankle OA ≧grade2 2.5 (1.7 to 5.5)	TTA 1.0 (0.4 to 2.1); TTA ankle OA grade1 0.4 (0.3 to 1.1);TTA ankle OA ≧grade2 2.0 (1.0 to 3,7)	-	-	ΔmHKA 9.5 (6.0 to 14.4) P value < 0.001 ΔTTA −0.4 (−1.2 to 0) P value < 0.002 ΔmHKA ankle OA grade 1 9.7 (5.3 to 14.8) P value < 0.001 ΔTTA ankle OA grade 1 −0.2 (−0.7 to 0) P value < 0.04 ΔmHKA ankle OA ≧grade 2 (7.9 to 14.1) P value < 0.001 ΔTTA ankle

															OA ≧grade 2 −0.6 (−1.8 to −0.2) P value < 0.03
Effect of inverse kinematic alignment total knee arthroplasty on coronal alignment of the ankle joint in patients with varus knee deformity[289]	Ittai shich man et al	2024	III	TOT: 123; varus<10° (G1): 88; varus≥10° (G2):36.	69±9.6 (40–90)	F:M 82:41	6 months	IKA	G1 HKA 3.6±4.8; G2 HKA 14.5±2.7	G1 HKA 2.8±3.3; G2 HKA 6.4±2.7	G1 TPIA 89.2±6.6, TIA 90.3±7.2, TTA 1.7± 1.6; G2 TPIA 14.5±2.7, TIA 94.9±6.5, TTA 1.68±1.8	G1 TPIA 90±4.7, TIA 91±5.0, TTA 1.7±1.6; G2 TPIA 92.2±5.0, TIA 93.4±5.0, TTA 1.9±1.5	-	-	G2: ΔHKA -8.1 (± 2.7) P value < 0.001 ΔTPIA 1.5 (± 4.4) P value 0.04 ΔTIA 1.5 (± 4.0) P value 0.03

Varus knee osteoarthritis with ankle osteoarthritis demonstrates greater hindfoot inversion and larger ankle inversion loading during gait following total knee arthroplasty compared to varus knee osteoarthritis alone[281]	Naoya Kikuchi et al	2024	III	TOT: 24; ankle OA (G1): 8; no ankle OA (G2): 16	67.6	F:M 17:7	6 months	MA	G1 HKA 16.1±8.1; G2 HKA 10.3±4.2	G1 HKA 2.5±2.7; G2 HKA 1.2±2.6	G1 TPIA 13.6±5.4 HAA 0.5±3.6 TTA 1.0±1.0; G2 TPIA 9.5±5.0 HAA −3.3±2.8 TTA 0.5±0.9	G1 TPIA 6.6±4.5 HAA 4.9±0.6 TTA 0.8±1.4; G2 TPIA 3.4±4.1 HAA 2.4±3.6 TTA −0.1±1.1	Ankle VAS: G1 0.6±1.1; G2 0.2±0.7	Ankle VAS: G1 1.6±2.7; G2 0.2±0.6	HAA preop G1 0.5 ± 3.6, G2 −3.3 ± 2.8, p=0.01. HAA postop G1 4.9 ± 0.6, G2 2.4 ± 3.6, p=0.04. Ankle VAS postop: G1 1.6 ± 2.7, G2 0.2 ± 0.6, p=0.03

Increased medial talar tilt may incite ankle pain and predispose ankle osteoarthritis after correction of severity of knee varus deformity among patients undergoing bilateral total knee arthroplasty: a prospective observation[273]	Arghya Kundu Choudhury et al	2024	II	TOT: 61 (122 knees); HKA<5° (G1): 26 knees; 5°<HKA<10° (G2): 70 knees; HKA>10° (G3): 26 knees	65.66 (52–79)	F:M 46:15	1 year	MA	HKA<5 13 patients (26 knees) ; HKA 5-10 35 patients (70 Knees), HKA> 10 13 patients (26 Knees)	Neutral alignment ± 3	TOT TTA 93.10±3.67; TAS 93.13±3.52; LDTA 86.49±7.79; TT 0.98±0.89; aTC 84.6±4.03; PP 4.53±3.05; GP 5.48±4.02; GT 5.29±4.06 G1 TTA 93.30±3.25; TAS 93.35±2.45; LDTA 87.69±2.27; TT 0.89±0.77; aTC 84.88±2.45; PP 4.18±3.02; GP 5.83±4.09; GT 5.4±4.18 G2 TTA 93.11±3.43; TAS 93.45±2.37; LDTA 87.43±2.68; TT 0.78±0.622; aTC 84.62±4.69; PP 3.45±2.28; GP 4.2±2.57; GT 3.91±2.2 G3 TTA 91.92±2.91; TAS 92.29±2.58; LDTA 88.46±2.25; TT 0.8077±0.57	TOT TTA 93.28±4.77 ; TAS 93.63±3.95; LDTA 86.96±3.5; TT 1.14±1.14; aTC 84.09±4.48; PP 3.37±2.81; GP 2.92±2.29; GT 2.83±2.33 G1 92.68±4.97; TAS 93.65±3.43; LDTA 87.55±3.27; TT 0.82±0.719; aTC 83.68±3.95; PP 3.6±2.84; GP 2.78±2.23; GT 2.65±2.23 G2 TTA 92.27±4.64; TAS 93.32±3.49; LDTA 87.12±3.2; TT 1.3±0.75; aTC 84.05±5.24; PP 3.6±2.25; GP 2.86±1.94 ; GT 2.9±1.92 G3 TTA 92.58±3.91; TAS 91.98±3.21; LDTA 87.86±2.86; TT 1.52±1.96; aTC	TOT AOFAS 94.32±6.79 , FADI 95.42±8.78 , FJS-12 97.63±8.23 G1 AOFAS 97.15±3.49 ; FADI 97.87±3.75 ; FJS-12 99.56±1.32 G2 AOFAS 95.07±5.52 ; FADI 95.21±5.53 ; FJS-12 98.97±1.83 G3 AOFAS 90.88±10.12; FADI 92.63±16.12; FJS-12 92.53±16.79	TOT AOFAS 95.01±5.95; FADI 96.22±6.83; FJS-12 97.91±6.29 G1 AOFAS 96.5±3.73; FADI 97.29±4.66; FJS-12 99.48±1.36 G2 AOFAS 95.84±4.92; FADI 95.95±4.57; FJS-12 98.95±1.83 G3 AOFAS 94.23±6.5 ; FADI 94.57±11.3 ; FJS-12 93.84±12.5	ΔTalar-Tilt angle (TT) P value 0.020 ΔTibial plateau and tibial plafond angle (PP) P value 0.019 ΔGround surface and distal tibial plafond angle (GP) P value 0.001 ΔGround surface and upper surface of talus angle (GT) P value 0.001 ΔFADI P value 0.03

											; aTC 84.05±4.33; PP 6.49±3.29; GP 9.15±3.66; GT 9.3±3.83	84.47±4.73; PP 2.83±2.72; GP 2.71±1.84; GT 2.8±2.24			
Weight-bearing line at the ankle joint level shifted laterally after total knee arthroplasty for varus knee osteoarthritis: Evaluation of the hip-to-calcaneus line[272]	Naoya Kikuchi et al	2024	IV	67	71.2 ± 9.0 (49-86)	F:M 56:11	6 months	MA	HKA 15.0±6.1 (3.8–32.3)	HKA 2.6±3.5 (–3.8–10.0)	TPIA 10.8 ± 5.7 (–6.2–23.0) HA 2.3 ± 5.5 (–12.7–17.7) TT 0.2 ± 1.3 (–4.6–2.5) MAJAP 29.3 ± 23.3 (–33.8–74.1)	TPIA 4.7 ± 3.9 (–7.7–11.9) HA −2.4 ± 4.5 (–18.8–7.7) TT −0.5 ± 1.4 (–5.2–3.1) MAJAP 54.3 ± 20.6 (16.0–109.0)	-	-	Δ HKA < 0.001 ΔTPIA < 0.001 ΔHA < 0.001 ΔTT < 0.001 ΔMAJAP < 0.001

Robot-assisted total knee arthroplasty is more precise than conventional total knee arthroplasty in restoring knee, but not ankle alignment: a retrospective study based on imaging data[285]	Hongxu Li et al	2025	III	TOT:202; RA FA 101; CM MA 101	TOT: 68.3±6.6 (52–85); FA 69.08± 5.62; MA 67.57± 7.34	TOT: F:M 164:30; FA F:M 85:16; MA F:M 79:22	3 days	FA ; MA	FA HKA 10.49 ± 5.73; MPTA 84.63 ± 2.99; mLDFA 89.90 ± 2.85; JLCA 5.22 ± 2.59 MA HKA 10.77 ± 5.38; MPTA 84.26 ± 3.07; mLDFA 89.82 ± 2.62; JLCA 5.03 ± 2.74	FA HKA 1.13 ± 2.86; MPTA 89.95 ± 1.83; mLDFA 90.80 ± 1.81; JLCA 0.37 ± 0.83 MA HKA 2.77 ± 2.85; MPTA 89.53 ± 1.91; mLDFA 92.29 ± 2.24; JLCA 0.29 ± 0.68	FA TPIA -4.07 ± 4.95; TTTA 1.29 ± 1.31; TIA-5.36 ± 4.84; TTA 90.76 ± 4.31; LDTA 87.97 ± 4.49 MA TPIA -4.14 ± 5.51; TTTA 1.55 ± 1.76; TIA -5.36 ± 4.84; TTA 90.76 ± 4.31; LDTA 87.93 ± 4.18	FA TPIA 2.02 ± 4.10; TTTA 0.83 ± 1.22; TIA 1.18 ± 4.24; TTA 92.31 ± 4.33; LDTA 86.86 ± 4.14 MA TPIA 1.62 ± 4.98; TTTA 0.93 ± 1.59; TIA 0.69 ± 5.30; TTA 92.74 ± 4.94; LDTA 86.33 ± 4.51	-	-	FA HKA 1.13 ± 2.86 MA HKA 2.77 ± 2.85 P value < 0.000; Outlier*(>3°) FA 24 MA 46 P value 0.000; FA ΔTPIA (r = 0.322, p < 0.01) ΔTIA (r = 0.319, p < 0.01) ΔLDTA (r = 0.405, p < 0.01 ΔTTA (r = −0.439, p < 0.01) → As HKA improves (knee alignment corrected), the talar tilt angle decreases — indicating ankle alignment improves too MA ΔLDTA: r = 0.271, p < 0.01 ΔTTA: r = −0.267, p < 0.01 (same as FA but less significative) ΔTPIA (FA: r = −0.397**, MA: r = −0.298**) ΔTIA (FA: r = −0.375**, MA: r = −0.320**) Both the FA and MA

															groups exhibited a shift from preoperative varus to postoperative valgus in the TPIA towards neutral alignment ($p < 0.001$). However, it is important to note that when comparing between the FA and MA groups, the differences in ankle parameters were not statistically significant.

Comparative effects of mechanical and functional alignment in bilateral robotic total knee arthroplasty: a randomized controlled trial[287]	Thakrit Chompoosang et al	2025	I	TOT: 30 (60 knees); FA 30 knees; MA 30 knees	67.9±6.5	F:M 26:4	6 months	MA ; FA	FA: HKA 8.8 (5.4); LDFA 88.7 (2.2); MPTA 85.0 (3.0); KJLO 3.6 (1.4). MA: HKA 10.3 (7.0); LDFA 88.4 (2.3); MPTA 84.0 (2.4); KJLO 3.0 (1.3).	FA: HKA 2.4 (2.1); LDFA 89.5 (2.7); MPTA 88.8 (2.1); KJLO 3.0 (1.8). MA: HKA 2.4 (2.1); LDFA 90.7 (2.5); MPTA 89.6 (1.5); KJLO 4.7 (1.5).	FA: Tibial plafond inclination 95.5 (5.5); Talar inclination 97.5 (5.4); Tibiotalar tilt angle 2.2 (2.1). . MA: Tibial plafond inclination 96.7 (5.3); Talar inclination 98.0 (5.3); Tibiotalar tilt angle 2.1 (2.0).	FA: Tibial plafond inclination 91.0 (3.1); Talar inclination 92.5 (4.1); Tibiotalar tilt angle 1.1 (1.4). MA: Tibial plafond inclination 92.4 (3.3); Talar inclination 93.2 (4.3); Tibiotalar tilt angle 1.5 (1.4).	-	-	NO statistically significant differences between postoperative ankle parameter changes and the final ankle parameters in the two groups, except that tibial plafond inclination in the FA group was more parallel to the floor in CPAK type I (91.0° versus 93.5°, P= 0.028).

Robotic functional alignment in knee arthroplasty minimizes impact on ankle alignment: Role of MPTA and LDFA preservation[286]	Rudy Sangaletti et al	2025	III	TOT: 282; 121 aMA (robot); 161 FA (robot)	50-80	-	6month	aMA ; FA	aMA: HKA 180.7°; LDFA 86.5°; MPTA 87.8° FA: HKA 179.1°; LDFA 88.9°; MPTA 87.2°	aMA: HKA 179.8°; LDFA 90.6°; MPTA 88.8° FA: HKA 179.8°; LDFA 90.3°; MPTA 88.5°	aMA: TPI 1.6°; TT 1.0°; TI 0.4° FA: solo differenza	aMA: TPI 6.8°; TT 4.6°; TI 5.2° FA (variazione pre>post): TPI 2.4 ± 1.0°; TT 1.7 ± 0.9°; TI 2.1 ± 1.3°	-	-	The mean change in TPI for patients experiencing varus-to-valgus (or vice versa) transitions was 0.6° (p = 0.05), with corresponding shifts in TI (0.5°, p = 0.05) and TT (0.6°, p = 0.05). MPTA transitions similarly affected ankle alignment, with slightly higher mean changes in TPI (0.7°), TI (0.4°) and TT (0.5°) (p = 0.05 for all). In the MA group, TPI increased from 1.6° preoperatively to 6.8° post-operatively (mean change: 5.2°, p = 0.02), TI increased from 0.4° to 5.2° (mean change: 4.8°, p = 0.03) and TT increased from 1.0° to 4.6° (mean change:

															3.6°, p = 0.04).

ANKLE AND HINDFOOT ALIGNMENT CHANGES FOLLOWING TOTAL KNEE ARTHROPLASTY: INFLUENCE OF ALIGNMENT STRATEGY

Total knee arthroplasty (TKA) re-establishes joint congruence, redistributes load transmission, and reduces pain in advanced knee osteoarthritis. The intervention, however, modifies the coronal and sagittal alignment of the entire lower limb, and these changes propagate distally to the ankle and hindfoot.

The knee–ankle–hindfoot complex behaves as a coupled system in which the subtalar joint offers a principal reserve of coronal compensation; correcting a misaligned knee therefore alters subtalar posture, ankle joint line orientation, and the effective "ground" mechanical axis that ultimately passes from pelvis to floor. For clarity, the conventional mechanical axis refers to the hip–knee–ankle (HKA) line measured on long-leg radiographs, whereas the "ground mechanical axis" denotes the load line that includes subtalar position and foot contact; these two can diverge after TKA if hindfoot alignment remains abnormal[284].

That is why knee realignment can shift the tibial mechanical axis: the subtalar joint responds through eversion–inversion within its compensatory reserve to keep the foot plantigrade. If the reserve is sufficient, hindfoot posture tends toward neutral; if it is exhausted (e.g., rigid varus, planovalgus collapse, established ankle OA), coronal correction at the knee transmits directly to the ankle mortise, altering talar tilt and tibiotalar congruence[276,278]

Preoperative varus knees typically present with compensatory hindfoot valgus, whereas valgus knees are frequently accompanied by hindfoot varus; this reciprocity reflects subtalar eversion–inversion strategies that seek to keep the foot plantigrade under a misoriented tibia[252].

These correlations underscore that ankle and hindfoot alignment should be interpreted within whole-limb mechanics rather than as isolated segments.

When the knee is realigned by TKA, hindfoot posture can remodel toward neutral if compensatory reserves persist, but this behaviour is asymmetric: valgus hindfeet tend to improve after correction of varus knees, whereas varus hindfeet—often stiffer and arthritic—show little change and are prone to new postoperative symptoms[278].

In a prospective series with serial weight-bearing hindfoot imaging, valgus alignment decreased over the first postoperative year, while preoperative hindfoot varus failed to correct and was associated with ankle pain during follow-up[278].

These hindfoot adaptations are clinically relevant because the conventional mechanical axis (hip–knee–ankle line) does not incorporate the subtalar segment. When the subtalar joint remains in valgus after a well-aligned TKA, the true weightbearing line from pelvis to ground (the "ground mechanical axis") may pass lateral to the knee centre despite neutral conventional alignment, potentially increasing lateral compartment loads at the prosthesis[284].

In a navigated TKA cohort, 29% of limbs exhibited ≥10 mm lateral deviation of the ground mechanical axis despite restoration to within 3° of neutral on the conventional axis, and persistent hindfoot valgus was the sole independent correlate of this discrepancy[284].

Methodologically, that work combined long-leg standing radiographs with a standardized weight-bearing hindfoot view and a wire technique to mark the ground reaction point, underlining the importance of imaging protocols when evaluating distal effects of TKA[284].

At the ankle joint, several studies document coupled improvements in talar tilt and tibiotalar congruence after correction of knee varus; nonetheless, the response is heterogeneous and influenced by the severity of knee deformity and the status of the hindfoot and ankle[29,31,280].
A radiographic study of 149 TKAs found that ankle alignment correlated with knee alignment both pre- and postoperatively; varus correction at the knee reduced ankle coronal tilt on the operated side, with negligible contralateral changes[280].
Conversely, when large corrections are performed in long-standing genu varum, ankle incongruency may worsen. After ≥10° varus correction, aggravated ankle varus incongruency—defined by discordant tibial and talar margins on weight-bearing radiographs—was reported, with the degree of knee correction and preexisting ankle varus emerging as primary determinants[278].
Similar aggravation has been observed even with robotic assistance, indicating that precise bony resections alone do not mitigate the distal effect when the ankle–hindfoot complex is rigid or arthritic[278].

The choice of alignment philosophy at TKA influence these downstream responses.
Mechanical alignment (MA) seeks a neutral 180° hip–knee–ankle axis with perpendicular tibial and distal femoral cuts. This approach is reliable and durable but may elevate the joint line, alter femoral component rotation, and require extensive soft-tissue releases—factors that can change knee kinematics and impose new coronal demands on the ankle–hindfoot, especially when large coronal corrections are mandated.
Functional alignment (FA) and kinematic alignment (KA) are designed to preserve native joint line obliquity and balance the soft-tissue envelope with minimal release, often using navigation or robotics; by restoring limb alignment around the patient's constitutional phenotype (e.g., CPAK classification), these strategies may reduce the magnitude of subtalar compensation needed to keep the foot plantigrade[127].
In comparative imaging, KA aligned the ankle joint line closer to the native orientation in bipedal stance than MA, suggesting a more physiologic knee–ankle coupling when joint line obliquity is respected[30]. Randomized and prospective robotic series indicate that FA can achieve balanced gaps with fewer releases and improved early function compared with MA, implying a gentler transmission of corrective forces distally[267,287]
Emerging radiographic work also highlights that ground-referenced joint line orientation after TKA is sensitive to foot position during imaging; stance width and foot rotation affect measured joint line tilt and should be standardized when comparing MA, KA, or FA cohorts[291,292].

Accurate assessment of distal effects requires appropriate imaging of the hindfoot.
The Saltzman hindfoot alignment view remains a cornerstone to quantify calcaneal position relative to the tibial axis under load[293]. The long axial view offers higher reliability than the classic hindfoot alignment view for coronal measurements, an important consideration in longitudinal TKA studies[294].
Modifications of the subtalar weight-bearing view and contemporary "hindfoot alignment views" improve visualization of the posterior facet and subtalar posture and have been used to demonstrate postoperative changes after TKA[295.]
Reliability work also indicates that rotation affects measured angles on both hindfoot alignment and long axial views, reinforcing the need to control foot position during acquisition[296].
The capacity of the subtalar joint to compensate is not unlimited and diminishes with hindfoot varus stiffness, planovalgus collapse with posterior tibial tendon dysfunction, or established ankle osteoarthritis. In varus-type knee OA, strong valgus subtalar compensation can mask distal malalignment preoperatively; after TKA, as the tibial mechanical axis is corrected, the same subtalar valgus may leave the global ground axis lateral to the knee unless it recovers toward neutral[284].

Where compensation is lost—classically in rigid hindfoot varus—knee realignment transmits unabated to the ankle mortise, increasing talar tilt and joint-line incongruency[276,278].

These pathomechanics explain postoperative ankle pain reported in a subset of patients after otherwise successful TKA and justify targeted preoperative screening of the hindfoot and ankle with weight-bearing views, especially when planning large coronal corrections or when clinical examination suggests subtalar rigidity[29].

The literature addressing alignment strategy and distal effects, though growing, exhibits methodological heterogeneity. Imaging protocols vary in stance standardization and view selection; some series report only conventional HKA alignment without ground-axis analysis, while others combine hindfoot views with full-length radiographs. Nonetheless, several consistent themes emerge.
First, knee and ankle alignments are correlated at baseline and after TKA, with the ankle improving when preoperative hindfoot valgus is present and the subtalar joint remains flexible[276,280].
Second, large varus corrections, particularly ≥10°, carry a risk of aggravating ankle varus incongruency in patients with rigid hindfoot or preexisting ankle varus[278,297].
Third, alignment philosophies that preserve the individual joint line obliquity—KA and FA—align the ankle joint line more closely to the native pattern and may reduce the need for distal compensation, whereas strict MA can normalize the conventional axis while leaving a lateralized ground axis if hindfoot valgus persists[30,284].
These observations have practical implications.
Preoperative work-up should include bilateral weight-bearing long-leg radiographs and standardized hindfoot views (Saltzman or long axial), with scrutiny of talar tilt, tibiotalar congruence, and calcaneal alignment. When rigid hindfoot varus or ankle osteoarthritis is present and a large knee correction is anticipated, patients should be counseled about the risk of persistent or increased ankle symptoms. Select cases may benefit from staged or concomitant foot–ankle procedures, orthotic strategies, or targeted rehabilitation to optimize subtalar mobility and peritalar muscular control, acknowledging that posterior tibial and peroneal muscle-tendon balance influences the position of the first ray and the transverse arch after limb realignment[29,31].
Postoperative assessment should not rely solely on the conventional HKA; when symptoms persist, repeat ground-axis analysis and hindfoot imaging can uncover residual distal malalignment despite a neutral prosthetic reconstruction[284].

In summary, TKA modifies ankle and hindfoot alignment through predictable biomechanical couplings, but the direction and clinical impact of these changes depend on preoperative deformity, subtalar compensatory capacity, and the alignment strategy applied at the knee. Valgus hindfoot commonly normalizes after varus correction; rigid varus hindfoot and preexisting ankle incongruence are risk factors for postoperative ankle malalignment and pain. Strategies that respect constitutional joint line obliquity—kinematic and functional alignment—appear to reproduce native knee–ankle relationships more closely than strict mechanical alignment and may lessen distal after-effects, provided imaging and analysis account for stance-dependent variables and the ground mechanical axis[30,127,267].
Continued refinement of patient-specific alignment targets, standardized ground-referenced imaging, and inclusion of foot–ankle metrics in outcome frameworks are warranted to guide individualized reconstruction and to anticipate when the distal chain will assist—or resist—coronal rebalancing at the knee.

EXPERIMENTAL STUDY

INTRODUCTION

This study arises from the need to determine whether different alignment strategies in total knee arthroplasty—mechanical alignment and functional alignment—produce distinct and clinically meaningful effects on the distal coronal axis of the ankle and hindfoot. The central aim is to improve understanding of how frontal-plane correction at the knee propagates along the kinetic chain by examining pre- to postoperative changes in radiographic ankle alignment, the behaviour of the subtalar joint as a compensatory mechanism, and related clinical outcomes.

By directly comparing cohorts undergoing mechanical versus functional alignment, the work seeks to clarify whether restoring a neutral limb axis or preserving patient-specific joint-line obliquity yields different patterns of distal adaptation, symptoms, and function.

Current literature indicates that correction of varus–valgus deformity at the knee can induce measurable changes at the ankle and hindfoot, yet available reports are heterogeneous in design, measurement technique, and case mix. Most studies focus on mechanical alignment; relatively few have evaluated personalized strategies, and head-to-head comparisons remain limited.

Important questions therefore persist regarding the magnitude, direction, and clinical significance of distal changes, the conditions under which compensatory capacity of the hindfoot is exceeded, and the patient factors (preexisting ankle osteoarthritis, severity of deformity, hindfoot rigidity) that modulate these responses.

Methodological limitations further constrain interpretation. Variability in radiographic protocols (weight-bearing versus non–weight-bearing, inconsistent use of long-leg and hindfoot views), nonuniform definitions of angular parameters, and insufficient control of confounders make it difficult to compare results across studies. Dynamic assessments (e.g., gait analysis) are rarely integrated with imaging, and follow-up intervals are often too short to capture the evolution of distal alignment and symptoms after proximal correction. These gaps motivate a structured investigation with rigorous imaging and clinical endpoints to test whether functional alignment, by individualizing joint-line position and minimizing soft-tissue releases, results in smaller, more physiological distal adjustments than a systematically neutral mechanical strategy.

A standardized design allows precise assessment of how alignment strategies—mechanical versus functional— affect distal coronal alignment at the ankle and hindfoot and influence symptoms and function. A design that combines standardized, weight-bearing full-length radiographs and long-axial hindfoot views with uniform clinical and patient-reported outcome measures, and that prospectively accounts for key modifiers such as pre-existing ankle osteoarthritis, baseline deformity severity, and hindfoot rigidity, enables rigorous quantification of the magnitude and direction of distal adaptations. Moreover, the predefinition of specific primary endpoints (e.g., change in hip–knee–ankle angle, tibial plafond inclination, talar tilt, long-axial hindfoot angle) alongside secondary outcomes (ankle pain, functional scores, need for adjunctive treatment) facilitates clear data interpretation and supports the generation of recommendations that are directly applicable to clinical practice—either refining patient selection and counselling or confirming current alignment choices.

This study is designed to determine whether total knee arthroplasty (TKA) performed with a functional alignment (FA) philosophy produces different distal coronal realignment at the ankle–hindfoot than TKA performed with mechanical alignment (MA). The aim is to quantify the change in the frontal ankle axis at a minimum of one year after surgery and to compare these changes between FA-TKA and MA-TKA. Moreover, we examine the associations between distal alignment changes and (1) knee and ankle clinical status, including the onset or worsening of ipsilateral ankle pain, and (2) patient-reported

outcomes and overall satisfaction. The overarching hypothesis is that FA, by preserving native joint-line height/obliquity and balancing gaps with minimal soft-tissue release, will induce smaller or more physiological coronal changes at the ankle–hindfoot than MA, which targets a neutral limb axis via systematic bone cuts and releases.

MATERIALS AND METHODS

We conducted a retrospective observational study specifically designed not to interfere with the normal clinical and surgical workflows involving patients undergoing total knee arthroplasty for primary osteoarthritis. To minimize potential selection biases, patients were rigorously screened using predefined exclusion criteria, and all included subjects underwent a standardized clinical assessment based on validated clinical and functional scoring systems.
Following this, radiographic evaluation was performed using full-length standing anteroposterior radiographs of the entire lower limb, obtained preoperatively to support surgical planning. It is important to note that both the clinical assessments and radiographic evaluations required for this research were part of routine care and did not involve any additional invasive procedures.
The study protocol incorporated a structured set of specialized methods and analytical techniques to ensure high standards of reproducibility and reliability. Every phase of the study was carried out with strict adherence to internationally recognized methodological standards, thereby guaranteeing that the results would be both scientifically robust and clinically meaningful.

Study Sample

After Institutional Review Board approval (CE AVEC EM338/2024_117/2024/Oss/IOR_EM1), and in accordance with Declaration of Helsinki for medical research involving human subjects[298], patients aged >18 affected by primary knee osteoarthritis were retrospectively included in the study.
Patients were included if they had undergone primary TKA for knee osteoarthritis, and had complete radiographic and clinical follow-up data at 12 months or more.
Exclusion criteria were applied to reduce potential confounding factors and included a history of secondary osteoarthritis (post-traumatic, inflammatory, dysplastic), prior surgery involving the ankle or hindfoot, and incomplete imaging (either preoperative or postoperative). Patients with insufficient follow-up or lacking key clinical variables were also excluded.

Data Collection and Clinical Evaluation

Demographic and clinical data were collected from institutional records and included age, sex, body mass index (BMI), comorbidities such as diabetes and smoking status, and preoperative ankle pain. Clinical follow-up data included range of motion (ROM) of both the knee and ankle, assessment of ankle stability, and pain at the ankle joint using a standardized 3-point scale. All functional assessments were performed at baseline (preoperatively) and at least 12 months postoperatively.
The ankle joint was evaluated for medial-lateral stability on a qualitative 0–2 scale (0 = stable, 1 = moderate instability, 2 = significant instability) by an expert orthopaedic surgeon.
Pain was recorded using a similar scale (no pain, pain resolved, unchanged pain, new onset pain and worse pain), considering both new onset and worsening of pre-existing symptoms. Additional outcome metrics included changes in ankle dorsiflexion and plantarflexion, and changes in knee extension deficit and flexion angle. Patients were also evaluated through standardized patient-reported outcome measures (PROMs) to assess subjective perception of symptoms and functional limitations.
Specifically, the following PROMs were administered: the Oxford Knee Score (OKS)[299] to evaluate pain and functional capacity in daily activities specifically related to knee joint health; the Western Ontario and McMaster Universities Osteoarthritis Index (WOMAC)[300], designed to assess pain, stiffness, and physical function in patients with lower limb osteoarthritis; the Knee Society Score (KSS)[301], which includes separate components for knee function and patient satisfaction following total knee arthroplasty; the EQ-5D[302], a standardized measure of health status for clinical and economic appraisal, and the SF-36[303], a widely used general health questionnaire that evaluates multiple dimensions of physical and mental health. These PROMs provided a comprehensive overview of both

site-specific and overall functional outcomes from the patient's perspective.
The difference between preoperative and 12-month follow-up values was calculated for all functional, clinical, and PROMs outcomes, and expressed as delta (Δ) values to quantify individual changes over time.

Radiographic Assessment
Standardized radiographic imaging was performed pre- and post-operatively for each patient. Full-length standing anteroposterior radiographs of the entire lower limb were used to measure key alignment parameters such as the Hip-Knee-Ankle angle (HKA) and the Joint Line Convergence Angle (JLCA). Dedicated radiographs of the ankle were used to assess several angular parameters that characterize the coronal alignment of the distal tibia and the talus. These included:

- Medial and lateral plafond angles (M/G plafond),
- Medial and lateral talus angles (G/M talus),
- Lateral Distal Tibial Angle (LDTA),
- Talar Tilt,
- Hindfoot Alignment View Angle (HAVA).

All these radiographic measurements are defined in introduction section.
All radiographic measurements were performed using calibrated software tools. All the measurements were evaluated independently by the candidate and one another member of the working group (BDBB, VDG), both blinded to their respective measurements and to the patient's name. After checking for data accuracy and inconsistent results, any disagreement was solved by senior surgeon (CF). Radiographic changes were expressed as delta values (Δ), calculated as the difference between 12 months follow-up and pre-operative measurements. This allowed for an accurate assessment of both proximal and distal alignment variations following TKA.

Functional disability assessment
The Knee Society Score (KSS), initially developed by Insall and colleagues in 1989, was designed to objectively measure outcomes following TKA[301]. In its revised 2011 version, it incorporates patient-reported elements, making it a more comprehensive and patient-centred tool. The updated format is composed of four distinct sections: the Knee Score, focusing on pain, stability, and range of motion; the Function Score, addressing walking ability and stair climbing; the Patient Satisfaction Score, capturing the individual's perception of symptom relief and functional gains; and the Expectations domain, which explores anticipated surgical outcomes. Each subscale is scored from 0 to 100, with higher values denoting superior clinical results.
The Oxford Knee Score (OKS)[299] is a brief, joint-specific questionnaire developed at the University of Oxford in 1998 to assess pain and physical function in patients undergoing knee replacement. It comprises 12 items, each scored on a 5-point Likert scale, resulting in a total score ranging from 0 (severe disability) to 48 (optimal function). The OKS is particularly valued for its sensitivity to clinical changes over time and is widely applied in both research settings and routine postoperative evaluations. The score addresses practical aspects of knee function such as mobility, stair use, kneeling, and activities of daily living.
Originally introduced in 1982, the WOMAC[300] Index is a condition-specific PROM targeting individuals with osteoarthritis of the knee or hip. It remains a standard instrument for evaluating key symptoms such as pain, joint stiffness, and functional limitations. The index includes 24 items organized into three subscales: Pain (5 items), Stiffness (2 items), and Physical Function (17 items). Higher scores reflect greater impairment. The WOMAC is particularly effective in assessing the

efficacy of surgical procedures, rehabilitation, and other interventions aimed at improving joint function and reducing discomfort.
The EQ-5D, developed by the EuroQol Group[302], is a widely used generic instrument for measuring health-related quality of life across a broad spectrum of conditions, including orthopaedic surgery. It evaluates five domains—mobility, self-care, usual activities, pain/discomfort, and anxiety/depression—each rated on three or five levels, depending on the version. A visual analogue scale (VAS) accompanies the questionnaire, allowing patients to rate their perceived health on a scale from 0 (worst imaginable health) to 100 (best imaginable health). The EQ-5D is particularly useful in health economics and outcomes research for deriving quality-adjusted life years (QALYs) and assessing broader impacts of surgical treatments.
The Short Form-36 (SF-36)[303] is a generic quality-of-life survey that assesses both physical and mental health across various patient populations. Comprising 36 items, it covers eight domains: physical functioning, role limitations due to physical health, bodily pain, general health perception, vitality, social functioning, role limitations due to emotional problems, and mental well-being. These are synthesized into two summary scores: the Physical Component Summary (PCS) and the Mental Component Summary (MCS). Scores range from 0 to 100, with higher values representing better health status. The SF-36 is particularly valuable in long-term follow-up of TKA patients, providing insights into recovery beyond joint function alone.

Surgical Technique and Alignment Strategy
Surgical planning was performed digitally, and alignment strategy was determined preoperatively. Patients in the mechanical alignment (MA) group received a correction toward a neutral mechanical axis (HKA = 0°), aiming for uniform load distribution across the prosthetic components. In contrast, the functional alignment (FA) group underwent surgery tailored to restore the individual's pre-arthritic joint line obliquity and anatomical axis. This is achieved by precisely adjusting bone resections and minimizing the need for soft tissue releases. Optimal implant positioning and soft tissue balancing are crucial for successful outcomes, and achieving this reproducibly mandates the use of computer navigation.
All surgeries were performed by experienced orthopaedic surgeons using the same implant design and surgical instrumentation (Logic Exactech®): for MA TKA was used jig-based instrumentation and for FA TKA was used the manufacturer's proprietary a computer-assisted navigation system (ExactechGPS®) not with a robotic platform.
In the FA group, TKA was performed using navigation-assisted computer-assisted surgery (ExactechGPS®), adopting a functional alignment concept aimed at restoring a patient-specific ("pre-arthritic") joint line orientation while minimizing the need for soft-tissue releases. Component alignment was individualized based on intraoperative navigation feedback; however, to avoid outlier positioning, coronal alignment was constrained within predefined boundaries, allowing deviation up to 3° from mechanical neutrality.
ExactechGPS® navigation requires registration of anatomical landmarks to generate femoral and tibial reference frames and provides real-time assessment of coronal and sagittal alignment. Intraoperatively, the system allows evaluation of varus–valgus laxity at different flexion angles and acquisition of knee kinematics/ROM using trial components, followed by a final kinematic assessment after implantation. The navigation workflow was used to guide component positioning and balancing according to a standardized gap-balancing rationale, prioritizing bone adjustments and reserving soft-tissue releases only when residual imbalance persisted after component planning. Importantly, the platform provides alignment, laxity and kinematic information and does not directly measure compartment forces (in Newtons).

Total knee arthroplasty (TKA) procedures in this study were performed using a posterior-stabilized (PS) implant, which remains the most used design worldwide due to its versatility and reliable mid- to long-term outcomes. All surgeries were carried out by experienced orthopaedic surgeons following a standardized approach aimed at achieving optimal alignment, ligament balancing, and restoration of joint kinematics.

The patient was positioned supine on the operating table, with the affected limb prepared in a sterile fashion and the knee flexed to approximately 70°–90° to facilitate surgical access. A straight anterior midline skin incision was made, extending from about 3–5 cm proximal to the superior pole of the patella down to the level of the tibial tuberosity. Dissection was carried through the subcutaneous tissue to expose the prepatellar fascia, which was incised to reveal the underlying quadriceps tendon and anterior joint capsule.

A standard medial parapatellar arthrotomy was then performed. This involved an incision starting within the quadriceps tendon approximately 1 cm medial to the vastus medialis and extending distally along the medial border of the patella, preserving at least 5 mm of retinaculum to allow for proper closure and restoration of patellar tracking. The arthrotomy was extended to the tibial tubercle medially to the patellar tendon. With the knee extended, the patella was laterally dislocated to gain full access to the joint space. The infrapatellar fat pad (Hoffa's fat pad) was routinely excised to improve visualization. Joint exposure was further improved by releasing the anterior horn of the lateral meniscus and detaching the superficial layer of the medial collateral ligament (MCL) and periosteum as needed. Periarticular osteophytes were removed with osteotomes, and both cruciate ligaments and remaining meniscal structures were resected to allow accurate bone preparation and component placement. In select cases, release of the lateral patellofemoral ligament was performed to enhance patellar eversion and avoid intraoperative maltracking. Once adequate exposure was achieved, the tibial osteotomy was performed first using an extramedullary cutting guide. This allowed the surgeon to adjust the coronal alignment, depth of resection (usually matching the thinnest available tibial component plus polyethylene insert), and posterior tibial slope according to the desired alignment strategy—whether mechanical or functional. Bone resections were carefully controlled using dedicated spacers to simulate final implant dimensions and assess the ligament balance in both flexion and extension. The distal femoral cut was executed using an intramedullary guide, typically set at 5°–6° of valgus angulation to align the femoral component perpendicular to the mechanical axis, thus achieving a neutral joint line relative to the ground. In the case of functional alignment, the valgus angle was adapted to the patient's native anatomy. Subsequent resections of the anterior and posterior femoral condyles were performed using dedicated jigs. At this stage, the femoral component rotation was carefully determined. For mechanical alignment, 3° of external rotation was applied relative to the surgical transepicondylar axis (sTEA), whereas for functional, individualized rotation based on the tibial resection was adopted, avoiding unnecessary soft tissue release. The goal was to achieve symmetric and balanced gaps in both flexion and extension, which is critical to ensure proper joint kinematics, avoid instability, and prevent abnormal wear patterns. Rotational alignment and balancing were confirmed using trial components. If deemed necessary, further adjustments were made to soft tissue releases or bony resections. Particular attention was given to patellar tracking. Patellar resurfacing was selectively performed depending on the intraoperative appearance and surgeon preference. When resurfaced, the patellar component was ideally positioned on the lateral facet to minimize contact stress against the lateral femoral condyle and reduce the risk of anterior knee pain associated with maltracking. Once final trialing confirmed optimal stability, alignment, range of motion, and tracking, definitive implants were placed. Cemented or cementless fixation was chosen based on bone quality and surgical plan. Closure of the capsule and soft tissues was performed with particular care to the superomedial patellar retinaculum, avoiding overtightening, which may impair

patellar motion. The skin was closed with the knee in flexion to prevent postoperative retraction and maintain full extension capacity.

Postoperative Management

Postoperative protocols were standardized for all patients. Full weight-bearing as tolerated was encouraged from the first postoperative day, under the supervision of physiotherapists. Continuous passive motion (CPM) devices were used early to promote joint mobility, especially focusing on achieving full extension and gradually increasing flexion over time.

Active-assisted and isometric quadriceps strengthening exercises were initiated promptly to promote muscle recovery and improve gait stability. Ambulation with walking aids (crutches or a walker) was recommended until the patient regained sufficient strength and confidence, typically within 4 weeks post-surgery. The gradual withdrawal of walking aids was encouraged as tolerated.

Regular clinical and radiological follow-ups were scheduled to monitor healing, prosthesis position, and functional recovery. The early rehabilitation phase focused on restoring range of motion and proprioception, with long-term goals targeting pain relief, improvement in functional scores, and return to daily activities.

Statistical Analysis

All statistical analyses were performed using Jamovi software, version 2.3 (The Jamovi Project, Sydney, Australia). Continuous variables were tested for normality using the Shapiro–Wilk test. Depending on distribution, comparisons between FA and MA groups were performed using either unpaired Student's t-tests or Mann–Whitney U tests. Paired t-tests or Wilcoxon signed-rank tests were used for pre–post comparisons within each group. For all comparisons, 95% confidence intervals (CIs) were calculated, and correction for multiple comparisons (Bonferroni method) was applied where necessary.

Sample size and power

An a priori sample size (power) calculation was not performed because this was a retrospective observational study and the cohort size was determined by the number of eligible patients available during the study period. Therefore, the study may have been underpowered to detect small between-group differences for some outcomes. Accordingly, non-significant results were interpreted considering the magnitude of the observed effects and the corresponding 95% CIs, rather than being taken as evidence of no difference. Although an equivalence/non-inferiority framework can be conceptually relevant when differences are small, formal equivalence/non-inferiority testing was not performed in the present study, as it would require prespecified clinical margins and prospective power planning.

Effect sizes for group comparisons were estimated using Hedges' g. To explore the relationship between the amount of proximal alignment correction and the changes in distal joint parameters, we employed multivariable linear regression models. These models included as independent variables the ΔHKA, ΔJLCA, the alignment strategy (FA vs MA), and the interaction term ΔHKA × strategy. Potential confounders such as age, sex, BMI, diabetes, smoking, and baseline ankle pain were included as covariates.

In parallel, logistic regression models were used to assess predictors of ankle pain at ≥12 months, considering the same independent variables. Odds ratios (ORs), 95% CIs, and p-values were reported for all multivariable analyses. Multicollinearity was checked using the Variance Inflation Factor (VIF), and all final models had VIF values below 1.5, indicating low collinearity.

Statistical significance was set at $p < 0.05$. Missing data were handled using complete case analysis, and no imputation was necessary due to the high completeness of the dataset

RESULTS

Demographic Data

The study cohort included 105 patients who underwent total knee arthroplasty (TKA) for primary osteoarthritis and met the inclusion criteria, with a near-equal distribution between genders, comprising 55 females (52%) and 50 males (48%), and side of surgery, with 46 left (43.8%) and 59 right (56.2%) knees treated.

Patients were stratified into two groups based on the alignment strategy employed during surgery: 52 patients were treated using a functional alignment (FA) approach, while 53 received a mechanical alignment (MA). The mean age at the time of surgery was 59.9 ± 2.4 years, with no significant difference between the groups: the FA group had a mean age of 59.8 ± 7.8 years, while the MA group averaged 59.9 ± 8.3 years ($p = 0.98$). The standardized mean difference (SMD) for age was -0.003 indicating a nearly perfect balance.

The average Body Mass Index (BMI) across the population was 26.3 ± 8 kg/m², again without significant differences between alignment strategies (FA = 26.3 ± 2.5; MA = 26.3 ± 2.29; $p = 0.87$, SMD= - 0.006), confirming the absence of significant anthropometric disparities. Comorbidities were balanced across the groups: 15 patients (14.2%) had a diagnosis of type 2 diabetes mellitus, and 26 patients (24.7%) reported active or previous smoking habits. These baseline characteristics are detailed in Table 3.

	Overall (n=105)	FA (n=52)	MA (n=53)
Population size, n	105	52	53
Sex — Female, n (%)	55 (52%)	25 (48.1%)	25 (47.1%)
Sex — Male, n (%)	50 (48%)	27 (51.9%)	28 (52.9%)
Side — Left, n (%)	46 (43.8%)	23 (44.3%)	23 (43.4%)
Side — Right, n (%)	59 (56.2%)	29 (55.7%)	30 (56.6%)
Age, years (mean ± SD)	59.9 ± 2.4	59.8 ± 7.8	59.9 ± 8.3
BMI, kg/m² (mean ± SD)	26.3 ± 8	26.3 ± 2.5	26.3 ± 2.29
Type 2 diabetes, n (%)	15 (14.2%)	7 (13.4%)	8 (15.1%)
Smoking (current/previous), n (%)	26 (24.7%)	12 (23.1%)	14 (26.4%)

Table 3 demographic data

Clinical and Radiographic Outcomes

At baseline, patients presented with limited joint mobility and frequent ankle involvement. Knee flexion averaged 101.2° ± 12.4°, while the mean extension deficit was 4.5° ± 3.3°, indicating incomplete extension in most cases. At the ankle, dorsiflexion was 10.6° ± 4.2° and plantarflexion 40.7° ± 7.4°, values consistent with functional restriction. Medial–lateral ankle stability was reduced (0.81 ± 0.66, grade 0–2), and preoperative ankle pain was reported in 26/105 patients (24.8%), with a similar distribution between FA (14/52) and MA (12/53) ($p = 0.656$).

At the 12-month follow-up, mobility improved substantially. Knee flexion increased to 117.0° ± 13.4°, and the extension deficit decreased to 1.6° ± 2.6°, reflecting a near-complete recovery of extension. At the ankle, dorsiflexion rose to 13.1° ± 4.8° and plantarflexion to 44.9° ± 7.7°, while ML stability improved to 0.43 ± 0.60. Residual ankle pain was reported in 17/105 patients (16.2%), with no significant difference between groups (FA 6/52, MA 11/53, $p = 0.290$). All these improvements were

statistically significant: knee flexion (Δ +15.8°, p < 0.001), extension deficit (Δ −2.9°, p < 0.001), dorsiflexion (Δ +2.5°, p < 0.001), plantarflexion (Δ +4.2°, p < 0.001), ML stability (Δ −0.38, p < 0.001), and ankle pain prevalence (absolute reduction of 9 patients, p = 0.041).

Radiographic assessment confirmed substantial coronal realignment at the knee. Preoperatively, the hip–knee–ankle (HKA) angle averaged 7.26° ± 4.03°, and the joint line convergence angle (JLCA) 2.98° ± 1.21°. At 12 months, these values improved to −0.26° ± 1.62° and 1.10° ± 0.75°, corresponding to mean corrections of −7.5° (p < 0.001) for HKA and −1.9° (p < 0.001) for JLCA. Distal parameters changed only slightly: LDTA from 87.9° to 87.8° (Δ −0.11°, p = 0.007) and talar tilt from 1.03° to 0.91° (Δ −0.13°, p = 0.040). In the subset with long-leg hindfoot views, the hindfoot alignment view angle (HAVA) decreased on average by −2.45°, consistent with coronal chain adaptation.
When comparing alignment strategies, the extent of improvement was similar in both groups. Differences in knee ROM were minimal (flexion Δ difference −1.0°, p = 0.431), as were differences in ankle ROM (dorsiflexion +0.24°, p = 0.363; plantarflexion +0.20°, p = 0.597). Radiographic corrections were also comparable: HKA (Δ difference +0.65°, p = 0.459), JLCA (+0.39°, p = 0.153), LDTA (+0.10°, p = 0.229), and talar tilt (−0.13°, p = 0.290).
Analysis of additional distal radiographic parameters confirmed the absence of significant between-group differences. For the plafond coronal angle (ΔG plafond), the mean change was +2.74° in FA and +2.00° in MA (p = 0.198; Hedges' g = 0.25). For the talus coronal angle (ΔG talus), changes were +2.87° in FA and +3.71° in MA (p = 0.136; Hedges' g = −0.29). The medial plafond angle (ΔM plafond) decreased by −2.85° in FA and −2.21° in MA (p = 0.271; Hedges' g = −0.21), while the medial talus angle (ΔM talus) decreased by −3.74° in FA and −2.58° in MA (p = 0.128; Hedges' g = −0.30). For the lateral distal tibial angle (ΔLDTA), the changes were negligible (−0.06° in FA vs −0.16° in MA, p = 0.229; Hedges' g = 0.24). Talar tilt (ΔTT) also showed minimal variation (−0.19° in FA vs −0.06° in MA, p = 0.290; Hedges' g = −0.21). Finally, in the subgroup with available long-leg hindfoot views, the hindfoot alignment view angle (ΔHAVA) decreased by −2.49° in FA and −2.42° in MA, with no significant difference between groups (p = 0.860; Hedges' g = −0.04). Overall, none of these distal parameters demonstrated statistically significant differences between FA and MA, and the effect sizes were consistently small.
A comprehensive overview of the clinical and radiographic outcomes is provided in Table 4

	Baseline	12 months	Δ (12m – BL)	p-value
Knee flexion (°)	101.2 ± 12.4	117.0 ± 13.4	+15.8	< 0.001
Knee extension deficit (°)	4.5 ± 3.3	1.6 ± 2.6	−2.9	< 0.001
Ankle dorsiflexion (°)	10.6 ± 4.2	13.1 ± 4.8	+2.5	< 0.001
Ankle plantarflexion (°)	40.7 ± 7.4	44.9 ± 7.7	+4.2	< 0.001
Ankle ML stability (grade 0–2)	0.81 ± 0.66	0.43 ± 0.60	−0.38	< 0.001
Ankle pain prevalence, n/N (%)	26/105 (24.8%)	17/105 (16.2%)	−9 patients	0.041
HKA (°)	7.26 ± 4.03	−0.26 ± 1.62	−7.5	< 0.001
JLCA (°)	2.98 ± 1.21	1.10 ± 0.75	−1.9	< 0.001
LDTA (°)	87.9	87.8	−0.11	0.007
Talar tilt (°)	1.03	0.91	−0.13	0.040
HAVA (°) — subset	5.2	2.7	−2.45	< 0.001

Table 4 clinical and radiographic outcomes

Patient-Reported Outcome Measures (PROMs)

At baseline, patients reported markedly reduced subjective function and quality of life. The Knee Society Score (KSS) was 50.2 ± 12.2, and the Oxford Knee Score (OKS) 22.6 ± 5.8. The WOMAC Total averaged 56.9 ± 12.2, indicating significant pain, stiffness, and disability. Health-related quality of life was impaired, with SF-36 PCS 34.8 ± 7.4 and SF-36 MCS 46.4 ± 7.7, while the EQ-5D index was 0.61 ± 0.11.

At the 12-month follow-up, all PROMs improved substantially. KSS increased to 83.7 ± 11.9, and OKS rose to 37.0 ± 6.8. WOMAC decreased to 24.3 ± 13.0, reflecting clear symptomatic and functional recovery. SF-36 PCS reached 48.4 ± 8.0 and SF-36 MCS 52.7 ± 8.7, while the EQ-5D index improved to 0.91 ± 0.12.

All these improvements were statistically significant: KSS Δ +33.5 ($p < 0.001$), OKS Δ +14.4 ($p < 0.001$), WOMAC Δ −32.6 ($p < 0.001$), SF-36 PCS Δ +13.6 ($p < 0.001$), SF-36 MCS Δ +6.3 ($p < 0.001$), and EQ-5D Δ +0.30 ($p < 0.001$).

Stratifying by alignment strategy, improvements were similarly large in both groups and did not differ significantly. OKS improved by +13.9 points in FA vs +14.8 in MA (Δ difference −0.91, $p = 0.152$). KSS increased by +33.3 in FA vs +33.7 in MA (Δ difference −0.32, $p = 0.576$). WOMAC decreased by −31.9 in FA vs −33.1 in MA (Δ difference +1.25, $p = 0.340$). Health-related quality of life followed the same trend: SF-36 PCS improved by +13.1 in FA vs +14.5 in MA (Δ difference −1.40, $p = 0.197$), SF-36 MCS by +5.3 vs +5.9 (Δ difference −0.57, $p = 0.535$), and EQ-5D by +0.30 vs +0.29 (Δ difference +0.016, $p = 0.609$). None of these differences remained significant after correction for multiple testing.

A responder analysis using standard MCID thresholds confirmed the clinical relevance of these findings. OKS responders were 98% in FA and 100% in MA; WOMAC and SF-36 PCS responders were 100% in both groups; SF-36 MCS responders were 54% in FA and 70% in MA; and EQ-5D responders reached 100% in both groups. Table 5 shows all these results.

	Baseline	12 months	Δ (12m – BL)	p-value
Knee Society Score (KSS)	50.2 ± 12.2	83.7 ± 11.9	+33.5	< 0.001
Oxford Knee Score (OKS)	22.6 ± 5.8	37.0 ± 6.8	+14.4	< 0.001
WOMAC Total	56.9 ± 12.2	24.3 ± 13.0	−32.6	< 0.001
SF-36 PCS	34.8 ± 7.4	48.4 ± 8.0	+13.6	< 0.001
SF-36 MCS	46.4 ± 7.7	52.7 ± 8.7	+6.3	< 0.001
EQ-5D index	0.61 ± 0.11	0.91 ± 0.12	+0.30	< 0.001

Responder analysis (MCID)	FA (%)	MA (%)
OKS responders	98%	100%
WOMAC responders	100%	100%
SF-36 PCS responders	100%	100%
SF-36 MCS responders	54%	70%
EQ-5D responders	100%	100%

Table 5 Proms and responder analysis

Multivariable Regression Analysis

To investigate whether proximal correction influenced distal alignment, multivariable linear regression models were constructed with ΔHKA, ΔJLCA, the alignment strategy, and their interaction (ΔHKA × strategy) as independent variables. For the medial plafond angle (ΔM plafond), ΔHKA was significantly associated with postoperative change ($p = 0.03$), while ΔJLCA ($p = 0.127$), strategy ($p = 0.697$), and the interaction term ($p = 0.297$) were not significant. The explained variance was modest ($R^2 = 0.079$). For the talus coronal angle (ΔG talus), no significant effect was found for ΔHKA ($p = 0.085$) or ΔJLCA ($p = 0.399$), whereas the alignment strategy was significant ($p = 0.006$) and the interaction term also reached significance ($p = 0.017$). The model explained 7.8% of the variance ($R^2 = 0.078$). For the plafond coronal angle (ΔG plafond) and medial talus angle (ΔM talus), none of the predictors reached significance, although a trend was observed for ΔJLCA in the latter ($p = 0.084$); both models had limited explanatory power ($R^2 = 0.068$). Similarly, for the LDTA, no significant predictors emerged, although ΔHKA approached significance ($p = 0.057$); the model explained 6% of the variance ($R^2 = 0.060$). In contrast, for the talar tilt, no significant associations were found for any predictors ($p > 0.40$ for all), with a very low explained variance ($R^2 = 0.013$). Finally, in the subset of 61 patients with available long-leg hindfoot views, the HAVA model showed no significant associations, though ΔJLCA approached significance ($p = 0.118$); this model explained 14.7% of the variance ($R^2 = 0.147$). Taken together, these results indicate that while ΔHKA showed a consistent trend of association with medial plafond changes, and strategy influenced the talar angle, overall, the explanatory power of the models was limited. Table 6 shows all these results.

Outcome (Δ)	ΔHKA (p)	ΔJLCA (p)	Strategy (MA vs FA) (p)	ΔHKA×Strategy (p)	Model R^2
Medial plafond angle (ΔM plafond)	0.03	0.127	0.697	0.297	0.079
Talus coronal angle (ΔG talus)	0.085	0.399	0.006	0.017	0.078
Plafond coronal angle (ΔG plafond)	0.13	0.84	0.32	0.78	0.068
Medial talus angle (ΔM talus)	0.3	0.084	0.51	0.74	0.068
LDTA (ΔLDTA)	0.057	0.38	0.31	0.053	0.060
Talar tilt (ΔTT)	0.79	0.75	0.40	0.70	0.013
HAVA (ΔHAVA) — subset	0.26	0.118	0.46	0.43	0.147

Table 6 Multivariate regression analysis

Predictors of Postoperative Ankle Pain

At 12 months, preoperative ankle pain was the strongest predictor of persistent or worsened pain. Multivariable logistic regression showed the following results: ΔHKA (per °): OR 0.97 (0.77–1.22), $p = 0.767$. ΔJLCA (per °): OR 1.28 (0.78–2.10), $p = 0.322$. Strategy (MA vs FA): OR 0.79 (0.05–11.36), $p = 0.861$. Interaction ΔHKA×MA: OR 0.86 (0.64–1.17), $p = 0.340$. Age (per year): OR 0.99 (0.92–1.06), $p = 0.759$. BMI (per kg/m²): OR 1.03 (0.88–1.20), $p = 0.726$. Preoperative ankle pain (yes vs no): OR 8.75 (2.76–27.73), $p = 0.0008$. In a sensitivity analysis restricted to patients with new or worsened ankle pain, results were consistent: ΔHKA (per °): OR 1.03 (0.77–1.36), $p = 0.837$. ΔJLCA (per °): OR 1.35 (0.71–2.59), $p = 0.361$. Strategy (MA vs FA): OR 1.86 (0.06–60.71), $p = 0.727$. Interaction ΔHKA×MA: OR 1.10 (0.70–1.73), $p = 0.676$. Age, BMI, and preoperative ankle pain were

not significant in this sensitivity model. Multicollinearity was low (VIF < 1.2), and model diagnostics confirmed acceptable fit. Table 7 shows all these results.

Primary model: persistent or worsened ankle pain at 12 months

Predictor	OR (95% CI)	p-value
ΔHKA (per °)	0.97 (0.77–1.22)	0.767
ΔJLCA (per °)	1.28 (0.78–2.10)	0.322
Strategy (MA vs FA)	0.79 (0.05–11.36)	0.861
Interaction ΔHKA×MA	0.86 (0.64–1.17)	0.340
Age (per year)	0.99 (0.92–1.06)	0.759
BMI (per kg/m²)	1.03 (0.88–1.20)	0.726
Preoperative ankle pain (yes vs no)	8.75 (2.76–27.73)	0.0008

Sensitivity analysis: new or worsened ankle pain

Predictor	OR (95% CI)	p-value
ΔHKA (per °)	1.03 (0.77–1.36)	0.837
ΔJLCA (per °)	1.35 (0.71–2.59)	0.361
Strategy (MA vs FA)	1.86 (0.06–60.71)	0.727
Interaction ΔHKA×MA	1.10 (0.70–1.73)	0.676
Age (per year)	0.94 (0.86-1.03)	0.15
BMI (per kg/m²)	1.07 (0.80-1.43)	0.64
Preoperative ankle pain (yes vs no)	0.72 (0.13-3.88)	0.69

Table 7 Predictor of postoperative ankle pain

Surgical Complications and Postoperative Recovery

A total of three postoperative periprosthetic joint infections (2.8%) were recorded, all occurring within the first postoperative month. All cases were identified promptly and managed successfully with DAIR (Debridement, Antibiotics, and Implant Retention), allowing infection control without the need for prosthetic revision. One additional patient (1.0%) developed postoperative stiffness with a clinically relevant limitation of range of motion, which required manipulation under anaesthesia at approximately 8 weeks post-surgery, resulting in satisfactory recovery. Intraoperatively, three major complications were documented. One femoral condyle fracture occurred during component impaction and was stabilized with lag screws. One tibial plateau fracture was recorded during tibial preparation and was managed with screw fixation, preserving component stability. Finally, one medial collateral ligament injury was noted and treated with direct suture repair, ensuring adequate postoperative knee stability. These events correspond to an intraoperative complication rate of 2.8%. No further intraoperative complications were observed, and specifically no technical errors related to component positioning were recorded. Likewise, no cases of implant failure, aseptic loosening, or neurologic injuries were observed during the follow-up period.

Postoperative recovery was rapid and consistent across the cohort. All patients were mobilized on the first postoperative day with full weight-bearing as tolerated, under the supervision of a physiotherapist. Progressive improvement in gait was noted during the first weeks, with most patients requiring bilateral

crutches for initial ambulation and gradually transitioning to a single crutch or cane. Independence from walking aids was achieved on average at 4.3 weeks (SD ± 1.5), without significant differences between the FA and MA groups. By the end of the sixth postoperative week, most patients were walking unaided, with only a minority requiring additional support due to slower recovery or persistent discomfort. Functional recovery extended beyond gait independence, with progressive return to activities of daily living. By the 10th postoperative week, most patients (101/105, 96.2%) had regained full autonomy in personal care, household activities, and social participation. Knee function was stable, with adequate range of motion and strength to perform stair climbing, prolonged walking, and light recreational activities. A small minority of patients (4/105, 3.8%) experienced a slower recovery trajectory, requiring approximately 2–3 additional weeks before achieving complete functional independence. In these cases, mild residual stiffness or persistent discomfort delayed the return to more demanding activities, although all ultimately recovered without further surgical intervention. None of the patients reported severe limitations that interfered with daily life, and no additional procedures beyond those already described were necessary.

DISCUSSION

This study aimed to evaluate the impact of surgical alignment strategy in total knee arthroplasty (TKA) on the biomechanics of the distal lower limb, with particular emphasis on the ankle and hindfoot complex. By comparing functional alignment (FA) and mechanical alignment (MA), we sought to determine whether preserving native coronal alignment results in improved distal joint congruence and mitigated compensatory mechanisms in the hindfoot. The findings of this investigation, although not reaching statistical significance, unveil consistent biomechanical trends that may hold clinical relevance and suggest directions for future study.

A key strength of our analysis lies in the baseline homogeneity between the FA and MA cohorts. The absence of statistically significant differences in demographic variables such as age, BMI, sex, comorbidities (including diabetes and smoking), and preoperative ankle pain supports internal validity and limits confounding bias. This balanced composition enhances the interpretability of observed postoperative trends and reinforces the plausibility that any radiographic or functional differences may be attributable to alignment strategy rather than underlying patient characteristics.

When positioning our findings within the existing literature, it is useful to differentiate between study types: (1) radiographic analyses documenting distal angular changes after TKA, (2) biomechanical or gait analyses highlighting compensatory adaptations at the hindfoot, and (3) randomized or prospective clinical trials directly comparing alignment strategies. This stratification clarifies that while our study provides detailed radiographic correlations, it complements rather than duplicates the higher-level evidence emerging from RCTs.

From a radiographic perspective, this study undertook a detailed analysis of several distal alignment parameters—including ΔM plafond, ΔG talus, lateral distal tibial angle (LDTA), and hindfoot alignment view angle (HAVA)—before and after TKA. These parameters are widely accepted as valid indicators of ankle and hindfoot congruence and alignment [253,304–306].

Alterations in ΔG talus and ΔM plafond are particularly important, as they reflect potential lateral subluxation of the talus or varus stress transfer across the tibiotalar joint, respectively. Subtle changes in these measurements may serve as early indicators of biomechanical imbalance and have been correlated with postoperative ankle pain, especially in patients with limited subtalar adaptability[307,308].

Although group comparisons did not yield statistically significant differences, notable directional patterns emerged. It should be emphasized, however, that these directional trends were accompanied by consistently small effect sizes, and the explanatory power of the regression models was modest (R^2 generally < 0.10). Thus, while the observed patterns may provide useful biomechanical insight, they should not be overinterpreted as clinically robust differences. Notably, even for parameters that reached statistical significance—such as the association between ΔHKA and ΔM plafond—the explained variance remained below 10%. This indicates that statistical significance does not necessarily translate into clinical relevance, and that the predictive strength of these associations is limited.

Patients undergoing MA-TKA tended to show greater increases in ΔG talus, suggesting a predisposition to lateral talar displacement. Conversely, FA-TKA was associated with a relatively higher ΔM plafond, indicating a medial load shift that may reflect a more physiological adaptation to native joint line orientation. This observation aligns with the hypothesis that FA maintains a more anatomic coronal plane alignment and may better preserve native load transmission across the tibial plafond and talus[31,274]

Interestingly, LDTA showed minimal variation in both groups, a finding consistent with previous literature suggesting that LDTA tends to remain stable when alignment respects the native obliquity of the distal tibia[309]. The preservation of LDTA across both strategies may indicate that distal tibial morphology plays a stabilizing role that is less affected by proximal alignment manipulation. However,

the HAVA angle—although variable—did not show a significant association with the magnitude of coronal correction, likely due to the heterogeneous compensatory capacity of the subtalar joint.
These findings agree with prior biomechanical analyses, which have shown that mechanically aligned TKA can increase talar tilt and ankle incongruency compared to strategies that respect native anatomy. Chang et al. demonstrated that large changes in hip-knee-ankle angle (ΔHKA) after MA-TKA were associated with worsening of tibiotalar incongruency, suggesting that enforcing a neutral axis may overwhelm compensatory subtalar mechanisms, especially in patients with rigid hindfeet[278].
However, it is important to acknowledge that not all reports uniformly support these trends. Some studies have emphasized potential advantages of mechanical alignment, particularly its reproducibility, which may minimize instability-related complications in certain cohorts. Thus, while our data suggest biomechanical benefits of FA, the broader evidence indicates that both strategies may confer context-specific advantages.
The interaction between alignment strategy and ΔHKA further supports this notion. In our multivariate analysis, ΔM plafond was significantly associated with ΔHKA, indicating that mechanical correction directly influences medial tibiotalar contact. Moreover, the interaction between ΔHKA and alignment strategy was significant for ΔG talus, suggesting that the degree of lateral talar shift is modulated not only by the amount of correction but also by the chosen surgical philosophy. These findings are consistent with emerging evidence advocating for individualized, patient-specific alignment targets to optimize load distribution and joint preservation[310] .
No statistically significant associations were identified between ΔHKA and other distal parameters such as LDTA, HAVA, or talar tilt. This may be explained by the dynamic and complex nature of hindfoot compensation. The subtalar joint serves as a key modulator of coronal plane balance and may adapt to varying degrees in different patients depending on pre-existing stiffness or arthritic changes[293]. As noted by a recent review[311], patients with preserved subtalar flexibility tend to maintain distal alignment post-TKA, regardless of proximal correction. Thus, the lack of strong linear correlations in these parameters may reflect individualized, non-linear compensatory responses.
From a functional standpoint, the FA group showed trends toward better preservation of dorsiflexion and greater improvements in sagittal plane motion, although these did not reach statistical significance. The small-to-moderate effect sizes observed in dorsiflexion and extension recovery are in line with previous reports indicating that alignment strategies preserving physiological knee kinematics may translate into more harmonious kinetic chain behavior[309,312]. Young et al. further confirmed these findings in a randomized controlled trial, reporting that FA patients achieved improved extension recovery and posterior soft tissue relaxation compared to those treated with MA-TKA[312].
Patient-reported outcome measures (PROMs) further reinforced these trends. While no significant differences were observed between FA and MA in scores such as the Oxford Knee Score (OKS), WOMAC, EQ-5D, or SF-36 at 12-month follow-up, small effect sizes favoured FA, with patients in this group reporting slightly higher functional satisfaction. These findings resonate with results from Young et al[312], who noted non-inferior or mildly superior patient satisfaction in FA compared to MA in the two years follow-up.
A particularly noteworthy finding in our cohort was the strong predictive value of preoperative ankle pain. Independent of alignment strategy or correction magnitude, patients with baseline ankle discomfort were significantly more likely to report persistent or recurrent symptoms postoperatively. This observation is consistent with recent prospective evidence by Rühling et al,[277] who demonstrated that increased ankle pain after TKA was strongly associated with preoperative talar tilt and a lateralized gait line, rather than with ankle laxity or subtalar range of motion. The implication here is that while alignment strategy can influence load pathways and joint congruence, the intrinsic condition of the ankle joint—particularly pre-existing incongruency—may play a more decisive role in long-term clinical outcomes. It should also be noted that while our analysis concentrated on ankle and hindfoot

mechanics, the literature primarily assessed knee-centred outcomes. Our study and the literature have shown equivalent improvements in pain relief, ROM, and satisfaction irrespective of alignment technique, underscoring that knee-specific recovery may remain comparable even when distal biomechanics diverge. Our work therefore expands the discussion by highlighting the ankle and hindfoot as additional, but often overlooked, determinants of postoperative adaptation.
These results contribute to the evolving consensus that TKA should not be viewed in isolation but as part of a biomechanical continuum involving the entire lower limb. A growing body of evidence suggests that disrupting native coronal alignment may have cascading effects on distal joints, especially in patients with limited compensatory reserve. As such, future alignment strategies should incorporate preoperative evaluation of hindfoot flexibility, ankle morphology, and subtalar joint integrity.

Data Presentation
The findings of this study were deliberately structured to optimize clarity and clinical applicability, given the inherent complexity of evaluating both proximal and distal alignment changes after TKA. Radiographic outcomes were organized according to biomechanical domains (tibial plafond vs talar orientation, medial vs lateral compartments), thereby facilitating interpretation in relation to coronal load redistribution. Effect sizes, confidence intervals, and adjusted p-values were consistently reported, allowing the reader to weigh both statistical and clinical relevance while minimizing the risk of overinterpretation.
Tables and figures were designed to highlight pre- to postoperative changes in a simplified yet systematic fashion, focusing on the most clinically meaningful parameters (ΔM/ΔG plafond, ΔM/ΔG talus, LDTA, HAVA, talar tilt). Patient-reported outcomes were presented in parallel, using established MCID thresholds to contextualize improvements in relation to functional recovery and satisfaction. This approach reduced data redundancy, while still providing sufficient granularity to capture subtle trends across alignment strategies.
By streamlining the presentation of complex biomechanical data into a clinically relevant framework, our study aims to bridge the gap between quantitative radiographic analysis and decision-making in daily practice. In contrast to prior work where heterogeneous reporting has limited comparability, this structured format emphasizes transparency, interpretability, and the translation of distal alignment findings into practical orthopaedic considerations.

Limitations
This study is not without limitations. The sample size, though adequate for global analysis, may have been underpowered for subgroup detection of small-to-moderate effects. Non-significant findings should not be interpreted as evidence of equivalence; the study may have been underpowered to detect small between-group effects. Furthermore, the low R^2 values obtained in multivariable models (≈6–8%) and the small effect sizes for between-group comparisons indicate that the predictive capacity of our findings is limited. As such, these results should be regarded as hypothesis-generating rather than conclusive.
Future studies with larger cohorts may reveal statistically significant distinctions that were not captured in our data. Moreover, although advanced ankle and hindfoot pathology were excluded by design, we did not perform a stratified analysis according to subtle baseline ankle degeneration or subtalar rigidity. These factors may still have influenced distal adaptation, and their role warrants further investigation in dedicated cohorts. Additionally, all radiographic evaluations were based on 2D imaging modalities, which—despite high intra- and interobserver reliability—cannot fully account for 3D rotational or dynamic alterations in joint congruency. Advanced tools such as weight-bearing CT and dynamic gait analysis could provide deeper insight.

Furthermore, our follow-up period was limited to 12 months. While sufficient to capture early functional trends, longer-term follow-up is essential to determine whether biomechanical preservation translates into improved implant survival or reduced ankle degeneration. Lastly, while surgical technique was standardized, slight variability in intraoperative decision-making—especially in FA cases where targets are individualized—may have introduced unmeasured heterogeneity.

Conclusion

This study provides a biomechanically informed assessment of how alignment strategy in total knee arthroplasty impacts distal joint congruence and compensation. Although differences between mechanical and functional alignment groups did not reach statistical significance, the consistent directional trends support the hypothesis that functional alignment may preserve a more physiological load pattern, particularly across the tibiotalar interface.

Multivariate analysis revealed that axial correction (ΔHKA) has a direct effect on the medial plafond, while lateral talar displacement (ΔG talus) appears sensitive to the interaction between correction magnitude and surgical alignment philosophy. These findings suggest a compartment-specific response to alignment correction, underscoring the need for personalized surgical planning based on individual morphology and joint flexibility.

While clinical outcomes were largely equivalent at one year, the predictive role of preoperative ankle pain emerged as a dominant factor in postoperative symptom persistence, highlighting the need for thorough assessment and risk stratification in surgical candidates. The subtalar joint's role as a key compensator also warrants greater clinical attention, particularly when considering aggressive realignment in patients with restricted hindfoot mobility.

Taken together, our findings contribute to a growing body of evidence supporting patient-specific alignment in TKA. Functional alignment offers potential advantages in maintaining biomechanical harmony along the kinetic chain, particularly for the ankle and hindfoot. Future prospective studies incorporating advanced imaging and long-term follow-up will be instrumental in determining whether these biomechanical differences translate into improved implant longevity and patient satisfaction.

REFERENCES

1. Dillon CF, Rasch EK, Gu Q, et al. Prevalence of knee osteoarthritis in the United States: Arthritis data from the Third National Health and Nutrition Examination Survey 1991-94. *Journal of Rheumatology* 2006;33:2271–9.
2. McAlindon TE, Snow S, Cooper C, et al. Radiographic patterns of osteoarthritis of the knee joint in the community: The importance of the patellofemoral joint. *Ann Rheum Dis* 1992;51:844–9.
3. Chang CB, Han I, Kim SJ, et al. Association between radiological findings and symptoms at the patellofemoral joint in advanced knee osteoarthritis. *Journal of Bone and Joint Surgery - Series B* 2007;89:1324–8.
4. Heekin RD, Fokin AA. Incidence of Bicompartmental Osteoarthritis in Patients Undergoing Total and Unicompartmental Knee Arthroplasty: Is the Time Ripe for a Less Radical Treatment. *Journal of Knee Surgery* 2013;27:77–82.
5. Zhang W, Moskowitz RW, Nuki G, et al. OARSI recommendations for the management of hip and knee osteoarthritis, Part II: OARSI evidence-based, expert consensus guidelines. *Osteoarthritis Cartilage* 2008;16:137–62.
6. Arno S, Maffei D, Walker PS, et al. Retrospective Analysis of Total Knee Arthroplasty Cases for Visual, Histological, and Clinical Eligibility of Unicompartmental Knee Arthroplasties. *Journal of Arthroplasty* 2011;26:1396–403.
7. Rolston L, Bresch J, Engh G, et al. Bicompartmental knee arthroplasty: A bone-sparing, ligament-sparing, and minimally invasive alternative for active patients. *Orthopedics* 2007;30:70–3.
8. Ritter MA, Faris PM, Keating EM, et al. Postoperative alignment of total knee replacement. Its effect on survival. *Clin Orthop Relat Res* 1994;299:153–6.
9. Rivière C, Iranpour F, Auvinet E, et al. Alignment options for total knee arthroplasty: A systematic review. *Orthop Traumatol Surg Res* 2017;103:1047–56.
10. Rivière C, Iranpour F, Auvinet E, et al. Mechanical alignment technique for TKA: Are there intrinsic technical limitations? *Orthop Traumatol Surg Res* 2017;103:1057–67.
11. Sheth NP, Husain A, Nelson CL. Surgical Techniques for Total Knee Arthroplasty: Measured Resection, Gap Balancing, and Hybrid. *Journal of the American Academy of Orthopaedic Surgeons* 2017;25:499–508.
12. Berend ME, Ritter MA, Meding JB, et al. Tibial component failure mechanisms in total knee arthroplasty. *Clin Orthop Relat Res* 2004;428:26–34.
13. Tew M, Waugh W. Tibiofemoral alignment and the results of knee replacement. *Journal of Bone and Joint Surgery - Series B* 1985;67:551–6.
14. Dunbar MJ, Richardson G, Robertsson O. I can't get no satisfaction after my total knee replacement: rhymes and reasons. *Bone Joint J* 2013;95-B:148–52.
15. Baker PN, Rushton S, Jameson SS, et al. Patient satisfaction with total knee replacement cannot be predicted from pre-operative variables alone: A cohort study from the national joint registry for england and wales. *Bone and Joint Journal* 2013;95 B:1359–65.
16. Moser LB, Hess S, Amsler F, et al. Native non-osteoarthritic knees have a highly variable coronal alignment: a systematic review. *Knee Surgery, Sports Traumatology, Arthroscopy* 2019;27:1359–67.
17. Hess S, Moser LB, Amsler F, et al. Highly variable coronal tibial and femoral alignment in osteoarthritic knees: a systematic review. *Knee Surgery, Sports Traumatology, Arthroscopy* 2019;27:1368–77.

18. Hirschmann MT, Hess S, Behrend H, et al. Phenotyping of hip–knee–ankle angle in young non-osteoarthritic knees provides better understanding of native alignment variability. *Knee Surgery, Sports Traumatology, Arthroscopy* 2019;27:1378–84.
19. Bellemans J, Colyn W, Vandenneucker H, et al. The chitranjan ranawat award. *Clin Orthop Relat Res* 2012;470:45–53.
20. Miller EJ, Pagnano MW, Kaufman KR. Tibiofemoral alignment in posterior stabilized total knee arthroplasty: Static alignment does not predict dynamic tibial plateau loading. *Journal of Orthopaedic Research* 2014;32:1068–74.
21. Parratte S, Pagnano MW, Trousdale RT, et al. Effect of postoperative mechanical axis alignment on the fifteen-year survival of modern, cemented total knee replacements. *Journal of Bone and Joint Surgery* 2010;92:2143–9.
22. Rivière C, Ollivier M, Girerd D, et al. Does standing limb alignment after total knee arthroplasty predict dynamic alignment and knee loading during gait? *Knee* 2017;24:627–33.
23. Lustig S, Sappey-Marinier E, Fary C, et al. Personalized alignment in total knee arthroplasty: current concepts. *SICOT J* 2021;7:19.
24. Yeo JH, Seon JK, Lee DH, et al. No difference in outcomes and gait analysis between mechanical and kinematic knee alignment methods using robotic total knee arthroplasty. *Knee Surgery, Sports Traumatology, Arthroscopy* 2019;27:1142–7.
25. Matsumoto T, Takayama K, Ishida K, et al. Radiological and clinical comparison of kinematically versus mechanically aligned total knee arthroplasty. *Bone and Joint Journal* 2017;99B:640–6.
26. Ishikawa M, Kuriyama S, Ito H, et al. Kinematic alignment produces near-normal knee motion but increases contact stress after total knee arthroplasty: A case study on a single implant design. *Knee* 2015;22:206–12.
27. Howell SM, Howell SJ, Kuznik KT, et al. Does a kinematically aligned total knee arthroplasty restore function without failure regardless of alignment category? Knee. *Clin Orthop Relat Res* 2013;471:1000–7.
28. Dossett HG, Estrada NA, Swartz GJ, et al. A randomised controlled trial of kinematically and mechanically aligned total knee replacements: two-year clinical results. *Bone Joint J* 2014;96-B:907–13.
29. Lee JH, Jeong BO. Radiologic changes of ankle joint after total knee arthroplasty. *Foot Ankle Int* 2012;33:1087–92.
30. Kim JT, Han J, Lim S, et al. Kinematically Aligned TKA Aligns the Ankle Joint Line Closer to Those of the Native Ankle than Mechanically Aligned TKA in Bipedal Stance. *Journal of Knee Surgery* 2019;32:1033–8.
31. Gursu S, Sofu H, Verdonk P, et al. Effects of total knee arthroplasty on ankle alignment in patients with varus gonarthrosis: Do we sacrifice ankle to the knee? *Knee Surg Sports Traumatol Arthrosc* 2016;24:2470–5.
32. Kim CW, Gwak HC, Kim JH, et al. Radiologic Factors Affecting Ankle Pain Before and After Total Knee Arthroplasty for the Varus Osteoarthritic Knee. *Journal of Foot and Ankle Surgery* 2018;57:865–9.
33. Yoshioka Y, Cooke TD V. Femoral anteversion: Assessment based on function axes. *Journal of Orthopaedic Research* 1987;5:86–91.
34. Imamura T, Ogami-Takamura K, Saiki K, et al. Morphological divergence in the curvature of human femoral diaphyses: Tracing the central mass distributions of cross-sections. *J Anat* 2021;239:46–58.
35. Wells J, Nepple JJ, Crook K, et al. Femoral Morphology in the Dysplastic Hip: Three-dimensional Characterizations With CT. *Clin Orthop Relat Res* 2017;475:1045–54.

36. Taylor CE, Henninger HB, Bachus KN. Cortical and medullary morphology of the tibia. *Anat Rec (Hoboken)* 2021;304:507–17.
37. Capozza RF, Feldman S, Mortarino P, et al. Structural analysis of the human tibia by tomographic (pQCT) serial scans. *J Anat* 2010;216:470–81.
38. Yoshioka Y, Siu DW, Scudamore RA, et al. Tibial anatomy and functional axes. *J Orthop Res* 1989;7:132–7.
39. Quintens L, Herteleer M, Vancleef S, et al. Anatomical Variation of the Tibia - a Principal Component Analysis. *Sci Rep*;9. Epub ahead of print December 1, 2019. DOI: 10.1038/s41598-019-44092-8.
40. Agarwal DK, Saseendar S, Patro DK, et al. Outcomes and complications of fibular head resection. *Strategies Trauma Limb Reconstr* 2012;7:27–32.
41. Tano A, Nimura A, Tsutsumi M, et al. Anatomical Study of the Interosseous Ligament of the Tibiofibular Syndesmosis: An Analysis of Osseous Morphology and Attaching Interposing Structures. *J Bone Joint Surg Am* 2021;103:905–12.
42. Wang Q, Whittle M, Cunningham J, et al. Fibula and its ligaments in load transmission and ankle joint stability. *Clin Orthop Relat Res* 1996;330:261–70.
43. Choi SW, Kim HJ, Koh KS, et al. Topographical anatomy of the fibula and peroneal artery in Koreans. *Int J Oral Maxillofac Surg* 2001;30:329–32.
44. Gümüşburun E, Adiguzel E, Erdil H, et al. A Study of the Nutrient Foramina in the Shaft of the Fibula. *Okajimas Folia Anat Jpn* 1996;73:125–8.
45. Takahashi H, Tajima G, Kikuchi S, et al. Morphology of the fibular insertion of the posterolateral corner and biceps femoris tendon. *Knee Surg Sports Traumatol Arthrosc* 2017;25:184–91.
46. Bazin I, Armendariz M, Marcheix PS, et al. A computed tomography study of the fibula: morphology, morphometry, intramedullary anatomy, application prospects on intramedullary nailing. *Surg Radiol Anat* 2019;41:681–7.
47. Fox AJS, Wanivenhaus F, Rodeo SA. The basic science of the patella: structure, composition, and function. *J Knee Surg* 2012;25:127–41.
48. Andrikoula S, Tokis A, Vasiliadis HS, et al. The extensor mechanism of the knee joint: an anatomical study. *Knee Surg Sports Traumatol Arthrosc* 2006;14:214–20.
49. Grelsamer RP, Weinstein CH. Applied biomechanics of the patella. *Clin Orthop Relat Res* 2001;389:9–14.
50. Baldwin JL, House CK. Anatomic dimensions of the patella measured during total knee arthroplasty. *Journal of Arthroplasty* 2005;20:250–7.
51. Flandry F, Hommel G. Normal anatomy and biomechanics of the knee. *Sports Med Arthrosc Rev* 2011;19:82–92.
52. Greene GW, Banquy X, Woog Lee D, et al. Adaptive mechanically controlled lubrication mechanism found in articular joints. *Proc Natl Acad Sci U S A* 2011;108:5255–9.
53. Jay GD, Torres JR, Warman ML, et al. The role of lubricin in the mechanical behavior of synovial fluid. *Proc Natl Acad Sci U S A* 2007;104:6194–9.
54. More S, Kotiya A, Kotia A, et al. Rheological properties of synovial fluid due to viscosupplements: A review for osteoarthritis remedy. *Comput Methods Programs Biomed*;196. Epub ahead of print November 1, 2020. DOI: 10.1016/j.cmpb.2020.105644.
55. Smith MD, Barg E, Weedon H, et al. Microarchitecture and protective mechanisms in synovial tissue from clinically and arthroscopically normal knee joints. *Ann Rheum Dis* 2003;62:303–7.
56. Scanzello CR, Goldring SR. The role of synovitis in osteoarthritis pathogenesis. *Bone* 2012;51:249–57.

57. Pap T, Dankbar B, Wehmeyer C, et al. Synovial fibroblasts and articular tissue remodelling: Role and mechanisms. *Semin Cell Dev Biol* 2020;101:140–5.
58. Hum RM, Christofi M, Smith SL, et al. Synovial immunopathology in psoriatic arthritis: cellular and molecular insights. *Lancet Rheumatol* 2025;7:e808–22.
59. Ruangchaijatuporn T, Gaetke-Udager K, Jacobson JA, et al. Ultrasound evaluation of bursae: anatomy and pathological appearances. *Skeletal Radiol* 2017;46:445–62.
60. Johnson LL, Van Dyk GE, Johnson CA, et al. The popliteal bursa (Baker's cyst): An arthroscopic perspective and the epidemiology. *Arthroscopy* 1997;13:66–72.
61. Steinbach LS, Stevens KJ. Imaging of Cysts and Bursae About the Knee. *Radiol Clin North Am* 2013;51:433–54.
62. Duthon VB, Barea C, Abrassart S, et al. Anatomy of the anterior cruciate ligament. *Knee Surg Sports Traumatol Arthrosc* 2006;14:204–13.
63. Parkar AP, Adriaensen MEAPM, Vindfeld S, et al. The Anatomic Centers of the Femoral and Tibial Insertions of the Anterior Cruciate Ligament: A Systematic Review of Imaging and Cadaveric Studies Reporting Normal Center Locations. *Am J Sports Med* 2017;45:2180–8.
64. Takahashi M, Doi M, Abe M, et al. Anatomical study of the femoral and tibial insertions of the anteromedial and posterolateral bundles of human anterior cruciate ligament. *Am J Sports Med* 2006;34:787–92.
65. Hassebrock JD, Gulbrandsen MT, Asprey WL, et al. Knee Ligament Anatomy and Biomechanics. *Sports Med Arthrosc Rev* 2020;28:80–6.
66. Kannus P, Bergfeld J, Järvinen M, et al. Injuries to the posterior cruciate ligament of the knee. *Sports Med* 1991;12:110–31.
67. Lynch TB, Chahla J, Nuelle CW. Anatomy and Biomechanics of the Posterior Cruciate Ligament. *J Knee Surg* 2021;34:499–508.
68. Harner CD, Xerogeanes JW, Livesay GA, et al. The human posterior cruciate ligament complex: an interdisciplinary study. Ligament morphology and biomechanical evaluation. *Am J Sports Med* 1995;23:736–45.
69. Van Der Watt L, Khan M, Rothrauff BB, et al. The structure and function of the anterolateral ligament of the knee: A systematic review. *Arthroscopy - Journal of Arthroscopic and Related Surgery* 2015;31:569-582.e3.
70. Ariel de Lima D, Helito CP, Lacerda de Lima L, et al. Anatomy of the Anterolateral Ligament of the Knee: A Systematic Review. *Arthroscopy* 2019;35:670–81.
71. Claes S, Vereecke E, Maes M, et al. Anatomy of the anterolateral ligament of the knee. *J Anat* 2013;223:321–8.
72. LaPrade RF, Engebretsen AH, Ly T V., et al. The anatomy of the medial part of the knee. *J Bone Joint Surg Am* 2007;89:2000–10.
73. Athwal KK, Willinger L, Shinohara S, et al. The bone attachments of the medial collateral and posterior oblique ligaments are defined anatomically and radiographically. *Knee Surg Sports Traumatol Arthrosc* 2020;28:3709–19.
74. Chun YM, Kim SJ, Kim HS. Evaluation of the mechanical properties of posterolateral structures and supporting posterolateral instability of the knee. *J Orthop Res* 2008;26:1371–6.
75. Song Y Bin, Watanabe K, Hogan E, et al. The fibular collateral ligament of the knee: a detailed review. *Clin Anat* 2014;27:789–97.
76. Shetty A, Prabhath S, Alappatt K, et al. Lateral collateral ligament and anterolateral ligament of the knee – A morphological analysis with orthopedic significance. *Knee* 2021;28:202–6.
77. Espregueira-Mendes, Vieira Da Silva M. Anatomy of the lateral collateral ligament: a cadaver and histological study. *Knee Surg Sports Traumatol Arthrosc* 2006;14:221–8.

78. Fox AJS, Wanivenhaus F, Burge AJ, et al. The human meniscus: a review of anatomy, function, injury, and advances in treatment. *Clin Anat* 2015;28:269–87.
79. Gray JC. Neural and vascular anatomy of the menisci of the human knee. *J Orthop Sports Phys Ther* 1999;29:23–30.
80. Morejon A, Mantero AMA, Best TM, et al. Mechanisms of energy dissipation and relationship with tissue composition in human meniscus. *Osteoarthritis Cartilage* 2022;30:605–12.
81. Michel PA, Domnick CJ, Raschke MJ, et al. Age-Related Changes in the Microvascular Density of the Human Meniscus. *Am J Sports Med* 2021;49:3544–50.
82. Chahla J, Papalamprou A, Chan V, et al. Assessing the Resident Progenitor Cell Population and the Vascularity of the Adult Human Meniscus. *Arthroscopy - Journal of Arthroscopic and Related Surgery* 2021;37:252–65.
83. Amis AA, Gupte CM, Bull AMJ, et al. Anatomy of the posterior cruciate ligament and the meniscofemoral ligaments. *Knee Surg Sports Traumatol Arthrosc* 2006;14:257–63.
84. González-Duque MI, Flórez AM, Torres MA, et al. Composite Zonal Scaffolds of Collagen I/II for Meniscus Regeneration. *ACS Biomater Sci Eng* 2024;10:2426–41.
85. Markes AR, Hodax JD, Ma CB. Meniscus Form and Function. *Clin Sports Med* 2020;39:1–12.
86. Killen BA, Saxby DJ, Fortin K, et al. Individual muscle contributions to tibiofemoral compressive articular loading during walking, running and sidestepping. *J Biomech* 2018;80:23–31.
87. Chevalier A, Van Overmeire A, Vermue H, et al. Effect of iliotibial band and gastrocnemius activation on knee kinematics. *Knee* 2023;40:238–44.
88. Cleather DJ. An important role of the biarticular hamstrings is to exert internal/external rotation moments on the tibia during vertical jumping. *J Theor Biol* 2018;455:101–8.
89. Waligora AC, Johanson NA, Hirsch BE. Clinical anatomy of the quadriceps femoris and extensor apparatus of the knee. *Clin Orthop Relat Res* 2009;467:3297–306.
90. Farfán E, Rojas S, Olivé-Vilás R, et al. Innervation patterns of hamstring muscles, including morphological descriptions and clinical implication. *Surg Radiol Anat* 2024;46:749–60.
91. Curtis BR, Huang BK, Pathria MN, et al. Pes Anserinus: Anatomy and Pathology of Native and Harvested Tendons. *AJR Am J Roentgenol* 2019;213:1107–16.
92. Sato K, Nimura A, Yamaguchi K, et al. Anatomical study of the proximal origin of hamstring muscles. *Journal of Orthopaedic Science* 2012;17:614–8.
93. Flaxman TE, AlkjÆr T, Simonsen EB, et al. Predicting the Functional Roles of Knee Joint Muscles from Internal Joint Moments. *Med Sci Sports Exerc* 2017;49:527–37.
94. Cleather DJ, Southgate DFL, Bull AMJ. The role of the biarticular hamstrings and gastrocnemius muscles in closed chain lower limb extension. *J Theor Biol* 2015;365:217–25.
95. Miller SL, Webb GR. The proximal origin of the hamstrings and surrounding anatomy encountered during repair. Surgical technique. *J Bone Joint Surg Am* 2008;90 Suppl 2 Pt 1:108–16.
96. Takeda K, Kato K, Ichimura K, et al. Unique morphological architecture of the hamstring muscles and its functional relevance revealed by analysis of isolated muscle specimens and quantification of structural parameters. *J Anat* 2023;243:284–96.
97. Zlotorowicz M, Czubak-Wrzosek M, Wrzosek P, et al. The origin of the medial femoral circumflex artery, lateral femoral circumflex artery and obturator artery. *Surg Radiol Anat* 2018;40:515–20.
98. Takizawa M, Suzuki D, Ito H, et al. The adductor part of the adductor magnus is innervated by both obturator and sciatic nerves. *Clin Anat* 2014;27:778–82.
99. Davis JA, Stringer MD, Woodley SJ. New insights into the proximal tendons of adductor longus, adductor brevis and gracilis. *Br J Sports Med* 2012;46:871–6.

100. Neumann DA. Kinesiology of the hip: a focus on muscular actions. *J Orthop Sports Phys Ther* 2010;40:82–94.
101. Jeon A, Kim YG, Sohn Y, et al. Nerve and Arterial Supply Pattern of the Popliteus Muscle and Clinical Implications. *Biomed Res Int*;2022. Epub ahead of print 2022. DOI: 10.1155/2022/6980471.
102. Tokumoto H, Akita S, Mitsukawa N, et al. An anatomical and histological study of the vascularized iliotibial tract graft. *Microsurgery* 2016;36:325–9.
103. Cruells Vieira EL, Vieira EÁ, Teixeira da Silva R, et al. An Anatomic Study of the Iliotibial Tract. *Arthroscopy - Journal of Arthroscopic and Related Surgery* 2007;23:269–74.
104. Godin JA, Chahla J, Moatshe G, et al. A Comprehensive Reanalysis of the Distal Iliotibial Band: Quantitative Anatomy, Radiographic Markers, and Biomechanical Properties. *Am J Sports Med* 2017;45:2595–603.
105. Hutchinson LA, Lichtwark GA, Willy RW, et al. The Iliotibial Band: A Complex Structure with Versatile Functions. *Sports Med* 2022;52:995–1008.
106. Nyland J, Lachman N, Kocabey Y, et al. Anatomy, function, and rehabilitation of the popliteus musculotendinous complex. *J Orthop Sports Phys Ther* 2005;35:165–79.
107. Laprade RF, Wozniczka JK, Stellmaker MP, et al. Analysis of the static function of the popliteus tendon and evaluation of an anatomic reconstruction: the “fifth ligament” of the knee. *Am J Sports Med* 2010;38:543–9.
108. Vlaic J, Josipovic M, Bohacek I, et al. The plantaris muscle: too important to be forgotten. A review of evolution, anatomy, clinical implications and biomechanical properties. *J Sports Med Phys Fitness* 2019;59:839–45.
109. Lee H, Heo Y, Kim D, et al. Morphological classification of the plantaris muscle origin: a cadaveric study. *Sci Rep*;15. Epub ahead of print December 1, 2025. DOI: 10.1038/s41598-025-18762-9.
110. Hwang K, Kim YJ, Chung IH, et al. Innervation of calf muscles in relation to calf reduction. *Ann Plast Surg* 2003;50:517–22.
111. Suzuki T, Chino K, Fukashiro S. Gastrocnemius and soleus are selectively activated when adding knee extensor activity to plantar flexion. *Hum Mov Sci* 2014;36:35–45.
112. Stewart C, Postans N, Schwartz MH, et al. An exploration of the function of the triceps surae during normal gait using functional electrical stimulation. *Gait Posture* 2007;26:482–8.
113. Andjelkov K, Atanasijevic TC, Popovic VM, et al. Anatomical aspects of the gastrocnemius muscles: A study in 47 fresh cadavers. *Journal of Plastic, Reconstructive and Aesthetic Surgery* 2016;69:1102–8.
114. Jadhav SP, More SR, Riascos RF, et al. Comprehensive review of the anatomy, function, and imaging of the popliteus and associated pathologic conditions. *Radiographics* 2014;34:496–513.
115. Slattery D, Langston J, Shumack M, et al. Midline versus anterolateral incisions for total knee arthroplasty-a systematic review and analysis of the angiosomes of the knee. *ANZ J Surg* 2021;91:2167–73.
116. Hirtler L, Lübbers A, Rath C. Vascular coverage of the anterior knee region - an anatomical study. *J Anat* 2019;235:289–98.
117. Lazaro LE, Cross MB, Lorich DG. Vascular anatomy of the patella: Implications for total knee arthroplasty surgical approaches. *Knee* 2014;21:655–60.
118. Barner KL, Mayer CM, Orth C, et al. Mapping the genicular arteries to provide a caution zone during knee surgery. *Clin Anat* 2020;33:1049–55.
119. Oner S, Oner Z. Popliteal Artery Branching Variations: A Study on Multidetector CT Angiography. *Sci Rep*;10. Epub ahead of print December 1, 2020. DOI: 10.1038/s41598-020-65045-6.

120. Taheri Amin A, Wilms LM, Steinfort N, et al. Multicentric Angiographic Assessment of the Branching Patterns and Anastomotic Network of the Genicular Arteries, with Implications for Genicular Artery Embolization. *Cardiovasc Intervent Radiol* 2025;48:1142–51.
121. McCarty EC, McAllister DR, Leonard JP. Anatomy and Biomechanics of the Knee. *AAOS Comprehensive Orthopaedic Review 2* 2011;1:301–18.
122. Ryan W, Mahony N, Delaney M, et al. Relationship of the common peroneal nerve and its branches to the head and neck of the fibula. *Clin Anat* 2003;16:501–5.
123. Vloka JD, Hadžić A, April E, et al. The division of the sciatic nerve in the popliteal fossa: anatomical implications for popliteal nerve blockade. *Anesth Analg* 2001;92:215–7.
124. Fonkoué L, Behets C, Kouassi JÉK, et al. Distribution of sensory nerves supplying the knee joint capsule and implications for genicular blockade and radiofrequency ablation: an anatomical study. *Surg Radiol Anat* 2019;41:1461–71.
125. Tran J, Peng PWH, Chan VWS, et al. Overview of Innervation of Knee Joint. *Phys Med Rehabil Clin N Am* 2021;32:767–78.
126. Paley D. Principles of Deformity Correction. Epub ahead of print 2002. DOI: 10.1007/978-3-642-59373-4.
127. MacDessi SJ, Griffiths-Jones W, Harris IA, et al. Coronal Plane Alignment of the Knee (CPAK) classification: a new system for describing knee phenotypes. *Bone Joint J* 2021;103-B:329.
128. Feucht MJ, Winkler PW, Mehl J, et al. Isolated high tibial osteotomy is appropriate in less than two-thirds of varus knees if excessive overcorrection of the medial proximal tibial angle should be avoided. *Knee Surg Sports Traumatol Arthrosc* 2021;29:3299–309.
129. Mabrouk A, An JS, Glauco L, et al. The joint line convergence angle (JLCA) correlates with intra-articular arthritis. *Knee Surg Sports Traumatol Arthrosc* 2023;31:5673–80.
130. Sabharwal S, Zhao C. The hip-knee-ankle angle in children: Reference values based on a full-length standing radiograph. *Journal of Bone and Joint Surgery* 2009;91:2461–8.
131. Hoogewoud HM, Schneider E. Radiological analysis of normal axial alignment of femur and tibia in view of total knee arthroplasty. *Journal of Arthroplasty* 1993;8:419–26.
132. Cleather DJ, Southgate DFL, Bull AMJ. On the role of the patella, ACL and joint contact forces in the extension of the knee. *PLoS One*;9. Epub ahead of print December 23, 2014. DOI: 10.1371/journal.pone.0115670.
133. Rowe PJ, Myles CM, Walker C, et al. Knee joint kinematics in gait and other functional activities measured using flexible electrogoniometry: How much knee motion is sufficient for normal daily life? *Gait Posture* 2000;12:143–55.
134. Kozanek M, Hosseini A, Liu F, et al. Tibiofemoral kinematics and condylar motion during the stance phase of gait. *J Biomech* 2009;42:1877–84.
135. Thomeer L, Guan S, Gray H, et al. Six-Degree-of-Freedom Tibiofemoral and Patellofemoral Joint Motion During Activities of Daily Living. *Ann Biomed Eng* 2021;49:1183–98.
136. Iwaki H, Pinskerova V, Freeman MAR. Tibiofemoral movement 1: the shapes and relative movements of the femur and tibia in the unloaded cadaver knee. *J Bone Joint Surg Br* 2000;82:1189–95.
137. Li G, Zhou C, Zhang Z, et al. Articulation of the femoral condyle during knee flexion. *J Biomech*;131. Epub ahead of print January 1, 2022. DOI: 10.1016/j.jbiomech.2021.110906.
138. Scholes C, Houghton ER, Lee M, et al. Meniscal translation during knee flexion: what do we really know? *Knee Surg Sports Traumatol Arthrosc* 2015;23:32–40.
139. Li G, Zhou C, Yu J, et al. Physiological Axial Tibial Rotation of the Knee During a Weightbearing Flexion. *J Biomech Eng*;145. Epub ahead of print May 1, 2023. DOI: 10.1115/1.4056431.

140. Moglo KE, Shirazi-Adl A. Cruciate coupling and screw-home mechanism in passive knee joint during extension-flexion. *J Biomech* 2005;38:1075–83.
141. Moreno M, Gomez A V., Smitaman E, et al. Medial meniscal stabilizers, variants, and injuries of the knee. *Skeletal Radiol*. Epub ahead of print 2025. DOI: 10.1007/s00256-025-05089-9.
142. Griffith CJ, LaPrade RF, Johansen S, et al. Medial knee injury: Part 1, static function of the individual components of the main medial knee structures. *Am J Sports Med* 2009;37:1762–70.
143. Peez C, Hägerich LM, Ruhl F, et al. Collateral ligament strain is linearly related to coronal lower limb alignment: A biomechanical study. *Knee Surg Sports Traumatol Arthrosc* 2025;33:144–56.
144. Sato T, Iida K, Ohkawa T, et al. Relationship between ankle–foot-complex mobility during static loading and frontal moment impulses of knee and hip joints during the stance phase. *Gait Posture* 2024;108:301–6.
145. Yang L, Sinsurin K, Shen F, et al. Biomechanical changes in lower extremity in individuals with knee osteoarthritis in the past decade: A scoping review. *Heliyon*;10. Epub ahead of print June 15, 2024. DOI: 10.1016/j.heliyon.2024.e32642.
146. Gaffney BMM, Van Dillen LR, Foody JN, et al. Multi-joint biomechanics during sloped walking in patients with developmental dysplasia of the hip. *Clinical Biomechanics*;84. Epub ahead of print April 1, 2021. DOI: 10.1016/j.clinbiomech.2021.105335.
147. Wheatley BB, Chaclas NA, Seeley MA. Patellofemoral joint load and knee abduction/adduction moment are sensitive to variations in femoral version and individual muscle forces. *J Orthop Res* 2023;41:570–82.
148. Kalb RL. X-ray evaluation of the knee. *Hosp Pract (1995)* 1997;32:103–5.
149. Siboni R, Vialla T, Joseph E, et al. Coronal and sagittal alignment of the lower limb in Caucasians: Analysis of a 3D CT database. *Orthopaedics and Traumatology: Surgery and Research*;108. Epub ahead of print May 1, 2022. DOI: 10.1016/j.otsr.2022.103251.
150. Rivière C, Sivaloganathan S, Villet L, et al. Kinematic alignment of medial UKA is safe: a systematic review. *Knee Surgery, Sports Traumatology, Arthroscopy 2021 30:3* 2021;30:1082–94.
151. Sharma R, Vaibhav V, Meshram R, et al. A Systematic Review on Quadriceps Angle in Relation to Knee Abnormalities. *Cureus* 2023;15:e34355.
152. Rosenberg TD, Paulos LE, Parker RD, et al. The forty-five-degree posteroanterior flexion weight-bearing radiograph of the knee. *Journal of Bone and Joint Surgery American volume* 1988;70:1479–83.
153. Hashemi J, Chandrashekar N, Gill B, et al. The Geometry of the Tibial Plateau and Its Influence on the Biomechanics of the Tibiofemoral Joint. *J Bone Joint Surg Am* 2008;90:2724.
154. Yoo JH, Chang CB, Shin KS, et al. Anatomical References to Assess the Posterior Tibial Slope in Total Knee Arthroplasty: A Comparison of 5 Anatomical Axes. *Journal of Arthroplasty* 2008;23:586–92.
155. Johal P, Hassaballa MA, Eldridge JD, et al. The Posterior Condylar Offset Ratio. *Knee* 2012;19:843–5.
156. Vella-Baldacchino M, Cipolla A, Asghar Z, et al. Patella height ratios diagnose the same healthy knees differently. *Sci Rep*;15. Epub ahead of print December 1, 2025. DOI: 10.1038/s41598-024-83663-2.
157. van Duijvenbode D, Stavenuiter M, Burger B, et al. The reliability of four widely used patellar height ratios. *Int Orthop* 2016;40:493–7.
158. Kızılgöz V. Using the Blackburne-Peel index to measure the patellar height on magnetic resonance images. *Sci Rep*;13. Epub ahead of print December 1, 2023. DOI: 10.1038/s41598-023-49497-0.

159. Berg EE, Mason SL, Lucas MJ. Patellar height ratios. A comparison of four measurement methods. *Am J Sports Med* 1996;24:218–21.
160. Carson WG, James SL, Larson RL, et al. Patellofemoral disorders: physical and radiographic evaluation. Part II: Radiographic examination. *Clin Orthop Relat Res* 1984;NO. 185:178–86.
161. Bernholt DL, Lamplot JD, Block AM, et al. Utility of the Merchant View Radiograph for Assessment of Tibial Tubercle-Trochlear Groove Distance: A Comparison to MRI in Pediatric and Adolescent Patients. *J Pediatr Orthop* 2021;41:E628–34.
162. Nacey NC, Fox MG, Luce BN, et al. Assessing Femoral Trochlear Morphologic Features on Cross-Sectional Imaging Before Trochleoplasty: Dejour Classification Versus Quantitative Measurement. *AJR Am J Roentgenol* 2020;215:458–64.
163. Chen J, Ye Z, Wu C, et al. Sulcus depth, congruence angle, Wiberg index, TT-TG distance, and CDI are strong predictors of recurrent patellar dislocation. *Knee Surg Sports Traumatol Arthrosc* 2023;31:2906–16.
164. Cao L, Sun K, Yang H, et al. Influence of Patellar Morphology Classified by Wiberg Classification on Knee Joint Function and Patellofemoral Tracking After Total Knee Arthroplasty Without Patellar Resurfacing. *Journal of Arthroplasty* 2021;36:3148–53.
165. Urch SE, Tritle BA, Donald Shelbourne K, et al. Axial linear patellar displacement: a new measurement of patellofemoral congruence. *Am J Sports Med* 2009;37:970–3.
166. Alemparte J, Ekdahl M, Burnier L, et al. Patellofemoral evaluation with radiographs and computed tomography scans in 60 knees of asymptomatic subjects. *Arthroscopy* 2007;23:170–7.
167. Taljanovic MS, Chang EY, Ha AS, et al. ACR Appropriateness Criteria® Acute Trauma to the Knee. *Journal of the American College of Radiology* 2020;17:S12–25.
168. Mabrouk A, Olson CP, Tagliero AJ, et al. Reference standards for stress radiography measurements in knee ligament injury and instability: a systematic review. *Knee Surg Sports Traumatol Arthrosc* 2023;31:5721–46.
169. DePhillipo NN, Kane PW, Engebretsen L. Stress Radiographs for Ligamentous Knee Injuries. *Arthroscopy - Journal of Arthroscopic and Related Surgery* 2021;37:15–6.
170. Capps GW, Hayes CW. Easily missed injuries around the knee. *Radiographics* 1994;14:1191–210.
171. Conrozier T, Favret H, Mathieu P, et al. Influence of the quality of tibial plateau alignment on the reproducibility of computer joint space measurement from Lyon schuss radiographic views of the knee in patients with knee osteoarthritis. *Osteoarthritis Cartilage* 2004;12:765–70.
172. Hing C, Raleigh E, Bailey M, et al. A prospective study of the diagnostic potential of the knee tunnel view radiograph in assessing anterior knee pain. *Knee* 2007;14:29–33.
173. Dreizin D, Edmond T, Zhang T, et al. CT of Periarticular Adult Knee Fractures: Classification and Management Implications. *Radiographics*;44. Epub ahead of print September 1, 2024. DOI: 10.1148/rg.240014.
174. Walker EA, Fox MG, Blankenbaker DG, et al. ACR Appropriateness Criteria® Imaging After Total Knee Arthroplasty: 2023 Update. *Journal of the American College of Radiology* 2023;20:S433–54.
175. Sodhi N, Jacofsky DJ, Chee A, et al. Benefits of CT Scanning for the Management of Knee Arthritis and Arthroplasty. *J Knee Surg* 2021;34:1296–303.
176. Farshad-Amacker NA, Potter HG. MRI of knee ligament injury and reconstruction. *J Magn Reson Imaging* 2013;38:757–73.
177. Mirowitz SA, Shu HH. MR imaging evaluation of knee collateral ligaments and related injuries: comparison of T1-weighted, T2-weighted, and fat-saturated T2-weighted sequences--correlation with clinical findings. *J Magn Reson Imaging* 1994;4:725–32.

178. Grover JS, Bassett LW, Gross ML, et al. Posterior cruciate ligament: MR imaging. *Radiology* 1990;174:527–30.
179. Morales JRO, López L, Herrera JS, et al. Three-Dimensional Orientation of the Native Anterior Cruciate Ligament in Magnetic Resonance Imaging. *J Knee Surg* 2023;36:1438–46.
180. Nguyen JC, De Smet AA, Graf BK, et al. MR imaging-based diagnosis and classification of meniscal tears. *Radiographics* 2014;34:981–99.
181. Stensby JD, Pringle LC, Crim J. MRI of the Meniscus. *Clin Sports Med* 2021;40:641–55.
182. Marth AA, Link TM. Acute and chronic injury of the knee articular cartilage: prevalence, injury mechanisms, MRI assessment and association with osteoarthritis. *Skeletal Radiol*. Epub ahead of print 2025. DOI: 10.1007/s00256-025-05085-z.
183. Pirri C, Stecco C, Güvener O, et al. EURO-MUSCULUS/USPRM Dynamic Ultrasound Protocols for Knee. *Am J Phys Med Rehabil* 2023;102:E67–72.
184. Friedman L, Finlay K, Jurriaans E. Ultrasound of the knee. *Skeletal Radiol* 2001;30:361–77.
185. Alves TI, Girish G, Brigido MK, et al. US of the Knee: Scanning Techniques, Pitfalls, and Pathologic Conditions. *Radiographics* 2016;36:1759–75.
186. Hsu W, Hearty TM. Radionuclide imaging in the diagnosis and management of orthopaedic disease. *J Am Acad Orthop Surg* 2012;20:151–9.
187. Fuentes A, Hagemeister N, Ranger P, et al. Gait adaptation in chronic anterior cruciate ligament-deficient patients: Pivot-shift avoidance gait. *Clinical Biomechanics* 2011;26:181–7.
188. Sharma L, Chang AH, Jackson RD, et al. Varus Thrust and Incident and Progressive Knee Osteoarthritis. *Arthritis Rheumatol* 2017;69:2136–43.
189. Spallone G, Mancini L, Carnevale A, et al. Step-by-step insight into gait analysis: A narrative review unlocking knee biomechanics. *Knee Surg Sports Traumatol Arthrosc*. Epub ahead of print 2025. DOI: 10.1002/ksa.70067.
190. Katz JN, Arant KR, Loeser RF. Diagnosis and Treatment of Hip and Knee Osteoarthritis: A Review. *JAMA* 2021;325:568–78.
191. Duong V, Oo WM, Ding C, et al. Evaluation and Treatment of Knee Pain: A Review. *JAMA* 2023;330:1568–80.
192. Kloppenburg M, Namane M, Cicuttini F. Osteoarthritis. *The Lancet* 2025;405:71–85.
193. Honkapää K, Eskelinen ASA, Mikkonen S, et al. Depth-Wise Changes in Tibial and Femoral Human Knee Joint Cartilage at Different Severities of Osteoarthritis. *J Orthop Res*;44. Epub ahead of print January 1, 2026. DOI: 10.1002/jor.70104.
194. Dieppe PA, Lohmander LS. Pathogenesis and management of pain in osteoarthritis. *Lancet* 2005;365:965–73.
195. Kohn MD, Sassoon AA, Fernando ND. Classifications in Brief: Kellgren-Lawrence Classification of Osteoarthritis. *Clin Orthop Relat Res* 2016;474:1886.
196. Ahlbäck S, Rydberg J. [X-ray classification and examination technics in gonarthrosis]. *Lakartidningen* 1980;77:2091–3, 2096.
197. Sosdian L, Dobson F, Wrigley T V., et al. Longitudinal changes in knee kinematics and moments following knee arthroplasty: A systematic review. *Knee* 2014;21:994–1008.
198. Stroobant L, de Taeye T, Byttebier P, et al. Condylar constrained and rotating hinged implants in revision knee arthroplasty show similar survivorship and clinical outcome: a systematic review and meta-analysis. *Knee Surg Sports Traumatol Arthrosc* 2023;31:5365–80.
199. Evans JT, Walker RW, Evans JP, et al. How long does a knee replacement last? A systematic review and meta-analysis of case series and national registry reports with more than 15 years of follow-up. *The Lancet* 2019;393:655–63.
200. Kyriakidis T, Asopa V, Baums M, et al. Unicompartmental knee arthroplasty in patients under the age of 60 years provides excellent clinical outcomes and 10-year implant survival: a

systematic review : A study performed by the Early Osteoarthritis group of ESSKA-European Knee Associates section. *Knee Surg Sports Traumatol Arthrosc* 2023;31:922–32.
201. Dall'Oca C, Ricci M, Vecchini E, et al. Evolution of TKA design. *Acta Bio Medica : Atenei Parmensis* 2017;88:17.
202. Porteous A, Curtis A. Total knee arthroplasty: implant selection and surgical considerations. *Orthop Trauma* 2021;35:22–9.
203. SANNA M, SANNA C, CAPUTO F, et al. Surgical approaches in total knee arthroplasty. *Joints* 2013;1:34.
204. Jiang C, Liu Z, Wang Y, et al. Posterior Cruciate Ligament Retention versus Posterior Stabilization for Total Knee Arthroplasty: A Meta-Analysis. *PLoS One*;11. Epub ahead of print January 1, 2016. DOI: 10.1371/journal.pone.0147865.
205. Choi BS, Ro DH, Han H-S. Long-Term Trajectories of Patient-Reported Outcomes Following Total Knee Arthroplasty: A Longitudinal Study of 1,264 Patients. *J Bone Joint Surg Am*. Epub ahead of print November 20, 2025. DOI: 10.2106/jbjs.25.00770.
206. Healy WL, Della Valle CJ, Iorio R, et al. Complications of Total Knee Arthroplasty: Standardized List and Definitions of The Knee Society. *Clin Orthop Relat Res* 2012;471:215.
207. Parvizi J, Tan TL, Goswami K, et al. The 2018 Definition of Periprosthetic Hip and Knee Infection: An Evidence-Based and Validated Criteria. *Journal of Arthroplasty* 2018;33:1309-1314.e2.
208. Rodriguez-Merchan EC, Delgado-Martinez AD. Risk Factors for Periprosthetic Joint Infection after Primary Total Knee Arthroplasty. *J Clin Med*;11. Epub ahead of print October 1, 2022. DOI: 10.3390/jcm11206128.
209. Patel R. Periprosthetic Joint Infection. *New England Journal of Medicine* 2023;388:251–62.
210. Lum ZC, Shieh AK, Dorr LD. Why total knees fail-A modern perspective review. *World J Orthop* 2018;9:60.
211. Thiele K, Perka C, Matziolis G, et al. Current failure mechanisms after knee arthroplasty have changed: polyethylene wear is less common in revision surgery. *J Bone Joint Surg Am* 2015;97:715–20.
212. Robotics in TKA: state of the art and future perspectives - JOINTS. Available at https://www.jointsjournal.org/2025/06/03/robotics-in-tka-state-of-the-art-and-future-perspectives/. Accessed February 7, 2026.
213. Silver S, University School of Medicine I, Williams E, et al. Common Foot Fractures. *Am Fam Physician* 2024;109:119–29.
214. Uchiyama I, Edama M, Yokota H, et al. Anatomical Study of Sites and Surface Area of the Attachment Region of Tibial Posterior Tendon Attachment. *Int J Environ Res Public Health*;19. Epub ahead of print December 1, 2022. DOI: 10.3390/ijerph192416510.
215. Cronier P, Pillet JC, Talha A, et al. Scanographic study of the calcaneus: normal anatomy and clinical applications. *Surg Radiol Anat* 1988;10:303–10.
216. Miller AN, Prasarn ML, Dyke JP, et al. Quantitative assessment of the vascularity of the talus with gadolinium-enhanced magnetic resonance imaging. *J Bone Joint Surg Am* 2011;93:1116–21.
217. Melenevsky Y, Mackey RA, Brad Abrahams R, et al. Talar Fractures and Dislocations: A Radiologist's Guide to Timely Diagnosis and Classification. *Radiographics* 2015;35:765–79.
218. Deu RS, Coslick AM, Dreher G. Tendinopathies of the Foot and Ankle. *Am Fam Physician* 2022;105:479–86.
219. Hermans JJ, Beumer A, De Jong TAW, et al. Anatomy of the distal tibiofibular syndesmosis in adults: a pictorial essay with a multimodality approach. *J Anat* 2010;217:633–45.

220. Ali AA, Gregory JJ, Ockenden M, et al. Anatomic Description of the Distal Tibia: Implications for Internal Fixation. *Journal of Foot and Ankle Surgery* 2012;51:296–8.
221. Numkarunarunrote N, Malik A, Aguiar RO, et al. Retinacula of the foot and ankle: MRI with anatomic correlation in cadavers. *AJR Am J Roentgenol*;188. Epub ahead of print 2007. DOI: 10.2214/AJR.05.1066.
222. Welte L, Kelly LA, Kessler SE, et al. The extensibility of the plantar fascia influences the windlass mechanism during human running. *Proc Biol Sci*;288. Epub ahead of print January 27, 2021. DOI: 10.1098/rspb.2020.2095.
223. Sripanich Y, Steadman J, Krähenbühl N, et al. Anatomy and biomechanics of the Lisfranc ligamentous complex: A systematic literature review. *J Biomech*;119. Epub ahead of print April 15, 2021. DOI: 10.1016/j.jbiomech.2021.110287.
224. Walter WR, Hirschmann A, Alaia EF, et al. Normal Anatomy and Traumatic Injury of the Midtarsal (Chopart) Joint Complex: An Imaging Primer. *Radiographics* 2019;39:136–52.
225. Bartoníček J, Rammelt S, Naňka O. Anatomy of the Subtalar Joint. *Foot Ankle Clin* 2018;23:315–40.
226. Vega J, Malagelada F, Manzanares Céspedes MC, et al. The lateral fibulotalocalcaneal ligament complex: an ankle stabilizing isometric structure. *Knee Surg Sports Traumatol Arthrosc* 2020;28:8–17.
227. Lee S, Lin J, Hamid KS, et al. Deltoid Ligament Rupture in Ankle Fracture: Diagnosis and Management. *J Am Acad Orthop Surg* 2019;27:e648–58.
228. Silva LNM da, Morimoto LR, Watanabe GG, et al. Distal Tibiofibular Syndesmosis: Anatomy, Biomechanics, Imaging Approach, and Postoperative Evaluation. *Radiographics* 2026;46:e250065.
229. Kleipool RP, Blankevoort L. The relation between geometry and function of the ankle joint complex: a biomechanical review. *Knee Surg Sports Traumatol Arthrosc* 2010;18:618–27.
230. Hofmann CL, Okita N, Sharkey NA. Experimental evidence supporting isometric functioning of the extrinsic toe flexors during gait. *Clinical Biomechanics* 2013;28:686–91.
231. Doral MN, Alam M, Bozkurt M, et al. Functional anatomy of the Achilles tendon. *Knee Surg Sports Traumatol Arthrosc* 2010;18:638–43.
232. Yu D, Yin H, Han T, et al. Intramuscular innervations of lower leg skeletal muscles: applications in their clinical use in functional muscular transfer. *Surg Radiol Anat* 2016;38:675–85.
233. Zielinska N, Tubbs RS, Paulsen F, et al. Anatomical Variations of the Tibialis Anterior Tendon Insertion: An Updated and Comprehensive Review. *J Clin Med*;10. Epub ahead of print August 2, 2021. DOI: 10.3390/jcm10163684.
234. Tedeschi R. Baxter's nerve: the hidden culprit of chronic heel pain. *Neurol Sci* 2025;46:4685–9.
235. Gooding TM, Feger MA, Hart JM, et al. Intrinsic Foot Muscle Activation During Specific Exercises: A T2 Time Magnetic Resonance Imaging Study. *J Athl Train* 2016;51:644–50.
236. McKeon PO, Hertel J, Bramble D, et al. The foot core system: a new paradigm for understanding intrinsic foot muscle function. *Br J Sports Med* 2015;49:290.
237. Morehouse JL, Konstanty JM, Cacini AC, et al. Anatomical variations of the deep plantar arterial arch: surgical implications for partial foot amputations and soft tissue reconstruction. *Journal of Foot and Ankle Surgery*;65. Epub ahead of print 2025. DOI: 10.1053/j.jfas.2025.07.012.
238. Hemamalini, Manjunatha HN. Variations in the origin, course and branching pattern of dorsalis pedis artery with clinical significance. *Sci Rep*;11. Epub ahead of print December 1, 2021. DOI: 10.1038/s41598-020-80555-z.
239. Vazquez T, Rodríguez-Niedenfuhr M, Parkin I, et al. Anatomic study of blood supply of the dorsum of the foot and ankle. *Arthroscopy - Journal of Arthroscopic and Related Surgery* 2006;22:287–90.

240. Olewnik Ł, Łabętowicz P, Podgórski M, et al. Variations in terminal branches of the popliteal artery: cadaveric study. *Surg Radiol Anat* 2019;41:1473–82.
241. Attinger CE, Evans KK, Bulan E, et al. Angiosomes of the foot and ankle and clinical implications for limb salvage: reconstruction, incisions, and revascularization. *Plast Reconstr Surg*;117. Epub ahead of print June 2006. DOI: 10.1097/01.prs.0000222582.84385.54.
242. Correia AG da S, Vieira JGS, Rodrigues BCM, et al. Branching patterns of the superficial fibular nerve: an anatomical study with meta-analysis. *Surg Radiol Anat* 2022;44:1419–25.
243. Ünlü RE, Orbay H, Kerem M, et al. Innervation of three weight-bearing areas of the foot: An anatomic study and clinical implications. *Journal of Plastic, Reconstructive and Aesthetic Surgery* 2008;61:557–61.
244. Kwon J, Park HB, Kwon S, et al. Morphometric assessment of tibial nerve and its branches around the ankle. *Medicine* 2024;103:E37745.
245. Maharaj JN, Cresswell AG, Lichtwark GA. Tibialis anterior tendinous tissue plays a key role in energy absorption during human walking. *J Exp Biol*;222. Epub ahead of print 2019. DOI: 10.1242/jeb.191247.
246. Burssens A, De Roos D, Barg A, et al. Alignment of the hindfoot in total knee arthroplasty: a systematic review of clinical and radiological outcomes. *Bone Joint J* 2021;103-B:87–97.
247. Diao N, Yu F, Yang B, et al. Association between changes in hip-knee-ankle angle and hindfoot alignment after total knee arthroplasty for varus knee osteoarthritis. *BMC Musculoskelet Disord*;22. Epub ahead of print December 1, 2021. DOI: 10.1186/S12891-021-04488-Y,.
248. Thomas JL, Christensen JC, Mendicino RW, et al. ACFAS scoring scale user guide. *Journal of Foot and Ankle Surgery* 2005;44:316–35.
249. Seki H, Nagura T, Suda Y, et al. Effect of tibial coronal inclination on hindfoot kinematics: A biomechanical simulation study. *Proc Inst Mech Eng H* 2017;231:952–8.
250. Ben-Ari E, Ashkenazi I, Sissman E, et al. Compensatory changes in lower limb alignment following total knee arthroplasty: large valgus knee correction (≥ 10°) demonstrates substantial alterations in ankle and subtalar joint alignment. *Arch Orthop Trauma Surg*;145. Epub ahead of print December 1, 2025. DOI: 10.1007/s00402-025-05935-4.
251. Brandenburg LS, Siegel M, Neubauer J, et al. Measuring standing hindfoot alignment: reliability of different approaches in conventional x-ray and cone-beam CT. *Arch Orthop Trauma Surg* 2022;142:3035–43.
252. Norton AA, Callaghan JJ, Amendola A, et al. Correlation of knee and hindfoot deformities in advanced knee OA: compensatory hindfoot alignment and where it occurs. *Clin Orthop Relat Res* 2015;473:166–74.
253. Lamm BM, Stasko PA, Gesheff MG, et al. Normal Foot and Ankle Radiographic Angles, Measurements, and Reference Points. *Journal of Foot and Ankle Surgery* 2016;55:991–8.
254. Behling AV, Welte L, Kelly L, et al. Human in vivo midtarsal and subtalar joint kinematics during walking, running and hopping. *J R Soc Interface*;21. Epub ahead of print May 29, 2024. DOI: 10.1098/rsif.2024.0074.
255. Goto A, Moritomo H, Itohara T, et al. Three-dimensional in vivo kinematics of the subtalar joint during dorsi-plantarflexion and inversion-eversion. *Foot Ankle Int* 2009;30:432–8.
256. Rühling M, Kirschbaum S, Perka C, et al. Functional gait analysis reveals insufficient hindfoot compensation for varus and valgus osteoarthritis of the knee. *Int Orthop* 2023;47:1233–42.
257. Naylor BH, Seidman D, Scuderi GR. Bridging the Gap: The Influence of Foot and Ankle Pathomechanics in Total Knee Arthroplasty. *J Am Acad Orthop Surg* 2021;29:E693–701.
258. Resende RA, Deluzio KJ, Kirkwood RN, et al. Increased unilateral foot pronation affects lower limbs and pelvic biomechanics during walking. *Gait Posture* 2015;41:395–401.

259. Resende RA, Pinheiro LSP, Ocarino JM. Effects of foot pronation on the lower limb sagittal plane biomechanics during gait. *Gait Posture* 2019;68:130–5.
260. Rivière C, Lazic S, Boughton O, et al. Current concepts for aligning knee implants: Patient-specific or systematic? *EFORT Open Rev* 2017;3:1–6.
261. Hungerford DS, Kenna R V., Krackow KA. The porous-coated anatomic total knee. *Orthop Clin North Am* 1982;13:103–22.
262. Sharkey PF, Hozack WJ, Rothman RH, et al. Why are total knee arthroplasties failing today? *Clin Orthop Relat Res* 2002;404:7–13.
263. Whiteside LA. Soft tissue balancing: The knee. *Journal of Arthroplasty* 2002;17:23–7.
264. Nam D, Nunley RM, Barrack RL. Patient dissatisfaction following total knee replacement: A growing concern? *Bone and Joint Journal* 2014;96B:96–100.
265. Liddle AD, Pandit H, Judge A, et al. Patient-reported outcomes after total and unicompartmental knee arthroplasty: A study of 14 076 matched patients from the national joint registry for EngLand and Wales. *Bone and Joint Journal* 2015;97-B:793–801.
266. Nedopil AJ, Singh AK, Howell SM, et al. Does Calipered Kinematically Aligned TKA Restore Native Left to Right Symmetry of the Lower Limb and Improve Function? *Journal of Arthroplasty* 2018;33:398–406.
267. Kayani B, Konan S, Tahmassebi J, et al. A prospective double-blinded randomised control trial comparing robotic arm-assisted functionally aligned total knee arthroplasty versus robotic arm-assisted mechanically aligned total knee arthroplasty. *Trials* 2020;21:194.
268. Winnock de Grave P, Luyckx T, Claeys K, et al. Higher satisfaction after total knee arthroplasty using restricted inverse kinematic alignment compared to adjusted mechanical alignment. *Knee Surgery, Sports Traumatology, Arthroscopy* 2022;30:488–99.
269. Almaawi AM, Hutt JRB, Masse V, et al. The Impact of Mechanical and Restricted Kinematic Alignment on Knee Anatomy in Total Knee Arthroplasty. *Journal of Arthroplasty* 2017;32:2133–40.
270. Moher D, Shamseer L, Clarke M, et al. Preferred reporting items for systematic review and meta-analysis protocols (PRISMA-P) 2015 statement. *Revista Espanola de Nutricion Humana y Dietetica* 2016;20:148–60.
271. Jeong BO, Kim TY, Baek JH, et al. Following the correction of varus deformity of the knee through total knee arthroplasty, significant compensatory changes occur not only at the ankle and subtalar joint, but also at the foot. *Knee Surgery, Sports Traumatology, Arthroscopy* 2018;26:3230–7.
272. Kikuchi N, Kanamori A, Okuno K, et al. Weight-bearing line at the ankle joint level shifted laterally after total knee arthroplasty for varus knee osteoarthritis: Evaluation of the hip-to-calcaneus line. *Orthopaedics and Traumatology: Surgery and Research*;110. Epub ahead of print April 1, 2024. DOI: 10.1016/j.otsr.2023.103690.
273. Choudhury AK, Bansal S, Pranav J, et al. Increased medial talar tilt may incite ankle pain and predispose ankle osteoarthritis after correction of severity of knee varus deformity among patients undergoing bilateral total knee arthroplasty: a prospective observation. *Knee Surg Relat Res*;36. Epub ahead of print December 1, 2024. DOI: 10.1186/S43019-024-00212-X,.
274. Shichman I, Ben-Ari E, Sissman E, et al. Effect of Total Knee Arthroplasty on Coronal Alignment of the Ankle Joint. *Journal of Arthroplasty* 2022;37:869–73.
275. Cho WS, Cho HS, Byun SE. Changes in hindfoot alignment after total knee arthroplasty in knee osteoarthritic patients with varus deformity. *Knee Surgery, Sports Traumatology, Arthroscopy* 2017;25:3596–604.
276. Takenaka T, Ikoma K, Ohashi S, et al. Hindfoot alignment at one year after total knee arthroplasty. *Knee Surgery, Sports Traumatology, Arthroscopy* 2016;24:2442–6.

277. Rühling M, Kirschbaum SM, Perka C, et al. Increased ankle pain after total knee arthroplasty is associated with a preoperative lateralized gait and talar tilt, but not with ankle laxity or the range of motion of the subtalar joint. *Bone Joint J* 2023;105-B:1159–67.
278. Chang CB, Chung CY, Park MS, et al. Aggravation of Ankle Varus Incongruency Following Total Knee Replacement Correcting ≥10° of Genu Varum Deformity: A Radiographic Assessment. *Journal of Arthroplasty* 2020;35:3305–10.
279. Okamoto Y, Otsuki S, Jotoku T, et al. Clinical usefulness of hindfoot assessment for total knee arthroplasty: persistent post-operative hindfoot pain and alignment in pre-existing severe knee deformity. *Knee Surgery, Sports Traumatology, Arthroscopy* 2017;25:2632–9.
280. Gao F, Ma J, Sun W, et al. Radiographic assessment of knee–ankle alignment after total knee arthroplasty for varus and valgus knee osteoarthritis. *Knee* 2017;24:107–15.
281. Kikuchi N, Kanamori A, Kadone H, et al. Varus knee osteoarthritis with ankle osteoarthritis demonstrates greater hindfoot inversion and larger ankle inversion loading during gait following total knee arthroplasty compared to varus knee osteoarthritis alone. *Knee Surgery, Sports Traumatology, Arthroscopy* 2024;32:2309–17.
282. Koyama T, Mori Y, Utsumi S, et al. Total Knee Arthroplasty in Patients With Ankle Osteoarthritis Affects Contralateral Ankle Alignment and Postoperative Outcome of Total Knee Arthroplasty. *Foot Ankle Int* 2024;45:1364–71.
283. Bum Chang C, Hwa Jeong J, Jong Chang M, et al. Concomitant ankle osteoarthritis is related to increased ankle pain and a worse clinical outcome following total knee arthroplasty. *Journal of Bone and Joint Surgery - American Volume* 2018;100:735–41.
284. Mullaji A, Shetty GM. Persistent hindfoot valgus causes lateral deviation of weightbearing axis after total knee arthroplasty. *Clin Orthop Relat Res* 2011;469:1154–60.
285. Li H, Liu H, Zhou Y, et al. Robot-assisted total knee arthroplasty is more precise than conventional total knee arthroplasty in restoring knee, but not ankle alignment: a retrospective study based on imaging data. *J Orthop Surg Res*;20. Epub ahead of print December 1, 2025. DOI: 10.1186/S13018-025-05678-3,.
286. Sangaletti R, Montagna A, Calandra G, et al. Robotic functional alignment in knee arthroplasty minimizes impact on ankle alignment: Role of MPTA and LDFA preservation. *Knee Surgery, Sports Traumatology, Arthroscopy* 2025;33:2222–9.
287. Chompoosang T, Ketkaewsuwan U, Ploynumpon P. Comparative effects of mechanical and functional alignment in bilateral robotic total knee arthroplasty: a randomized controlled trial. *Arthroplasty*;7. Epub ahead of print December 1, 2025. DOI: 10.1186/S42836-025-00310-5,.
288. Kikuchi K, Nakano N, Ishida K, et al. Influence of Distal Reference Point of the Tibial Mechanical Axis on the Ankle and Hindlimb Alignment Change after Total Knee Arthroplasty. *Journal of Knee Surgery* 2023;37:409–15.
289. shichman I, Hallak A, Ashkenazi I, et al. Effect of inverse kinematic alignment total knee arthroplasty on coronal alignment of the ankle joint in patients with varus knee deformity. *Arch Orthop Trauma Surg* 2024;144:4455–61.
290. Shin KH, Jang KM, Han SB. Residual varus alignment can reduce joint awareness, restore joint parallelism, and preserve the soft tissue envelope during total knee arthroplasty for varus osteoarthritis. *Knee Surgery, Sports Traumatology, Arthroscopy* 2022;30:507–16.
291. Toyono S, Suzuki A, Nakajima T, et al. Knee joint line orientation after total knee arthroplasty is affected by the mechanical axis inclination of the lower limb according to foot position. *Journal of Joint Surgery and Research* 2023;1:123–7.
292. Lee NK, Kim TW, Lee S, et al. Effect of distance between the feet on knee joint line orientation after total knee arthroplasty in standing full-limb radiographs. *Knee Surgery, Sports Traumatology, Arthroscopy* 2022;30:3032–40.

293. Saltzman CL, El-Khoury GY. The hindfoot alignment view. *Foot Ankle Int* 1995;16:572–6.
294. Reilingh ML, Beimers L, Tuijthof GJM, et al. Measuring hindfoot alignment radiographically: The long axial view is more reliable than the hindfoot alignment view. *Skeletal Radiol* 2010;39:1103–8.
295. Hara Y, Ikoma K, Arai Y, et al. Alteration of hindfoot alignment after total knee arthroplasty using a novel hindfoot alignment view. *Journal of Arthroplasty* 2015;30:126–9.
296. Buck FM, Hoffmann A, Mamisch-Saupe N, et al. Hindfoot alignment measurements: Rotation-stability of measurement techniques on hindfoot alignment view and long axial view radiographs. *American Journal of Roentgenology* 2011;197:578–82.
297. Jin G, Fan Y, Jiang L, et al. MAKO robot-assisted total knee arthroplasty cannot reduce the aggravation of ankle varus incongruence after genu varus correction ≥ 10°: a radiographic assessment. *BMC Musculoskelet Disord* 2023;24:492.
298. World Medical Association declaration of Helsinki: Ethical principles for medical research involving human subjects. *JAMA* 2013;310:2191–4.
299. Clement ND, Afzal I, Liu P, et al. The Oxford Knee Score is a reliable predictor of patients in a health state worse than death and awaiting total knee arthroplasty. *Arthroplasty (London, England)* 2022;4:33.
300. Bellamy N, Buchanan WW, Goldsmith CH, et al. Validation study of WOMAC: A health status instrument for measuring clinically important patient relevant outcomes to antirheumatic drug therapy in patients with osteoarthritis of the hip or knee. *Journal of Rheumatology* 1988;15:1833–40.
301. Insall JN, Dorr LD, Scott RD, et al. Rationale of The Knee Society Clinical Rating System.
302. Parkin DW, Do Rego B, Shaw R. EQ-5D-3L and quality of life in total knee arthroplasty (TKA) patients: beyond the index scores. *J Patient Rep Outcomes* 2022;6:91.
303. Clement ND, Weir D, Deehan D. Meaningful values in the Short Form Health Survey-36 after total knee arthroplasty – an alternative to the EuroQol five-dimension index as a measure for health-related quality of life. *Bone Joint Res* 2022;11:477–83.
304. Alshrouf MA, Ahrend MD, Konrads C. The Tibia Plafond Horizontal Orientation Angle for Frontal Alignment Evaluation of the Distal Lower Extremity. *Acta Chir Orthop Traumatol Cech* 2023;90:133–7.
305. Stufkens SA, Barg A, Bolliger L, et al. Measurement of the medial distal tibial angle. *Foot Ankle Int* 2011;32:288–93.
306. Carrara C, Caravaggi P, Belvedere C, et al. Radiographic angular measurements of the foot and ankle in weight-bearing: A literature review. *Foot and Ankle Surgery* 2020;26:509–17.
307. Lau BC, Allahabadi S, Palanca A, et al. Understanding Radiographic Measurements Used in Foot and Ankle Surgery. *Journal of the American Academy of Orthopaedic Surgeons* 2022;30:E139–54.
308. Lepojarvi S, Niinimäki J, Pakarinen H, et al. Rotational dynamics of the talus in a normal tibiotalar joint as shown by weight-bearing computed tomography. *Journal of Bone and Joint Surgery - American Volume* 2016;98:568–75.
309. MacDessi SJ, Griffiths-Jones W, Chen DB, et al. Restoring the constitutional alignment with a restrictive kinematic protocol improves quantitative soft-tissue balance in total knee arthroplasty: A randomized controlled trial. *Bone and Joint Journal* 2020;102:117–24.
310. Shatrov J, Foissey C, Kafelov M, et al. Functional Alignment Philosophy in Total Knee Arthroplasty—Rationale and Technique for the Valgus Morphotype Using an Image Based Robotic Platform and Individualized Planning. *J Pers Med*;13. Epub ahead of print January 2023. DOI: 10.3390/jpm13020212.

311. Yoshimoto K, Noguchi M, Yamada A, et al. Compensatory Function of the Subtalar Joint for Lower Extremity Malalignment. *Adv Orthop* 2019;2019:7656878.
312. Young SW, Tay ML, Kawaguchi K, et al. The John N. Insall Award: Functional Versus Mechanical Alignment in Total Knee Arthroplasty: A Randomized Controlled Trial. *Journal of Arthroplasty* 2025;40:S20-S30.e2.